AN ABSTRACT OF THE THESIS OF

Tzu-Yang Hsien for the degree of Doctor of Philosophy in Chemical Engineering presented on April 29, 1996. Title: Removal of Cadmium Ions by Porous Chitosan Beads: Effects of Acylation & Crosslinking on Material Properties and Adsorption Isotherms

Abstract approved: _____

Gregory L. Rorrer

Chitosan is nature's most abundant biopolymer next to cellulose and a selective adsorbent for heavy metal ions. However, the chitosan raw material needs to be modified for use in low pH environments. To address this need, chemically modified porous chitosan beads were synthesized. Two chemical modifications of chitosan were considered, including partial N-acylation of 7 % of the amine groups with C_9 hydrocarbon side chains before bead casting, and glutaric dialdehyde crosslinking of chitosan chains after bead formation but before freeze drying.

N-acylation, crosslinking, and freeze drying steps must be combined to minimize acid solubility and maximize the internal surface area of the chitosan beads. Chemical modifications of acylation and crosslinking improved the material properties of the chitosan beads for use in waste water treatment applications, but did not improve the adsorption capacity for cadmium ions. Freeze drying without crosslinking increased the internal surface area to 44.2 m^2/g. Acylation improved the cadmium adsorption capacity from 169 mg Cd^{+2}/g to 216 mg Cd^{+2}/g but only at high cadmium concentrations exceeding

also reduced the cadmium adsorption capacity. An extent of crosslinking equal to 0.81 mole GA/total mole -NH_2 increased the internal surface area from 44.2 m^2/g to 223.6 m^2/g and rendered the bead insoluble in acid solution, but reduced the cadmium adsorption capacity to 83 mg Cd^{+2}/g.

A diffusion-limited modified shrinking core model was developed to describe the formation of the crosslinked layer within the gel bead. The effective diffusivity for glutaric dialdehyde in the gel beads was estimated to be $4.11 \pm 0.082 \bullet 10^{-8}$ (1s) cm^2/s.

The adsorbent can be regenerated by dilute acid treatment, and 100 % cadmium recovery from the chitosan beads was feasible at pH less than 3.0. Decreasing the equilibrium pH increased the percentage of cadmium desorbed according to an S-shaped profile, consistent with the ion-exchange mechanism. A Langmuir-Freundlich model proposed that the desorption process is accomplished by displacing adsorbed cadmium ions with hydrogen ions.

Removal of Cadmium Ions by Porous Chitosan Beads: Effects of Acylation & Crosslinking on Material Properties and Adsorption Isotherms

by

Tzu-Yang Hsien

A THESIS

submitted to

Oregon State University

in partial fulfillment of

the requirements for the

degree of

Doctor of Philosophy

Completed April 29, 1996

Commencement June 1996

Doctor of Philosophy dissertation of Tzu-Yang Hsien presented on April 29, 1996

APPROVED:

Redacted for Privacy

Major Professor, representing Chemical Engineering

Redacted for Privacy

Chair of Department of Chemical Engineering

Redacted for Privacy

Dean of Graduate School

I understand that my dissertation will become part of the permanent collection of Oregon State University libraries. My signature below authorizes release of my dissertation to any reader upon request.

Redacted for Privacy

Tzu-Yang Hsien, Author

ACKNOWLEDGMENTS

The preparation of this thesis could not have been successful without the constant help and support of many people. I am especially grateful to my major professor Dr. Gregory Rorrer who has supported and encouraged me to go beyond my limits. I would also like to thank my committee members: Drs. Baham, Frederick, Klein, Koretsky, Semprini. Their time and assistance are gratefully acknowledged.

I gratefully acknowledge support by the U.S. Environmental Protection Agency through the Exploratory Research Grants Program (Grant #818626-01-0) in the form of a graduate research assistantship. I also thank Vansen Chemical Company for the donation of flaked chitosan.

Lastly, I would like to acknowledge the endless support and love from my parents, Yu-In and Chen-Ho. A great genuine love has also come from my wife and daughter, Dr. Yu-Ling Liu and Angela, who encouraged the efforts and shared in all pain and fun during these past years.

TABLE OF CONTENTS

	Page
CHAPTER 1 INTRODUCTION	1
1.1 Background and Motivation	1
1.2 Rationale	2
1.3 Research Goals and Objectives	9
CHAPTER 2 EFFECTS OF ACYLATION AND CROSSLINKING ON THE MATERIAL PROPERTIES AND CADMIUM ION ADSORPTION CAPACITY OF POROUS CHITOSAN BEADS	12
2.1 Introduction	13
2.2 Materials and Methods	19
2.2.1 Chemicals	19
2.2.2 Bead Synthesis	19
2.2.3 Physical Properties	22
2.2.4 Adsorption Isotherms	24
2.3 Results and Discussion	26
2.3.1 Physical Properties of Porous Chitosan Beads	26
2.3.2 Cadmium Ion Adsorption Isotherms	32
2.4 Summary and Conclusions	42

TABLE OF CONTENTS, CONTINUED

	Page
CHAPTER 3 GLUTARIC DIALDEHYDE CROSSLINKING MECHANISM AND ITS EFFECT ON CADMIUM ADSORPTION CAPACITY FOR CHITOSAN BEADS	44
3.1 Introduction	45
3.2 Materials and Methods	45
3.2.1 Gel Bead Synthesis	45
3.2.2 Crosslinking	46
3.2.3 Adsorption Capacity	48
3.2.4 EDAX Sample Preparation	49
3.2.5 Modified Shrinking Core Model for Diffusivity Estimation	50
3.3 Results	56
3.3.1 Crosslinking Kinetics	56
3.3.2 Effect of Initial Glutaric Dialdehyde Concentration on the Extent of Crosslinking	58
3.3.3 Cadmium Adsorption Isotherms	63
3.3.4 Saturation Cadmium Adsorption Capacity vs. Extent of Crosslinking	65
3.3.5 EDAX Profiles for Adsorbed Cadmium	67
3.4 Discussion	70
3.4.1 Crosslinking Mechanism	70
3.4.2 Effect of Crosslinking on Cadmium Adsorption Capacity	77

TABLE OF CONTENTS, CONTINUED

	Page
CHAPTER 4 DESORPTION OF CADMIUM FROM CHITOSAN BEADS	85
4.1 Introduction	86
4.2 Materials and Methods	86
4.2.1 Chitosan Bead Synthesis	86
4.2.2 Single Stage Desorption	87
4.2.3 Multiple Stage Desorption	90
4.2.4 pH and Cadmium Ion Concentration Measurements	91
4.3 Results and Discussion	93
4.3.1 Kinetics of Adsorption and Desorption	93
4.3.2 Optimum pH and Hydrogen Ion Consumption	96
4.3.3 Exchange Between Cadmium Ions and Hydrogen Ions	102
CHAPTER 5 SUMMARY AND CONCLUSIONS	110
BIBLIOGRAPHY	116
APPENDICES	121

LIST OF FIGURES

FIGURE		Page
1. 1	Chemical structure of chitosan.	3
1. 2	N-acylation of chitosan.	6
1. 3	Crosslinking of chitosan.	7
2. 1	Chemical structures. (a) Chitosan.	14
2. 1	(b) N-acylation of chitosan. (c) Crosslinking of chitosan.	16
2. 2	Flowchart for synthesis of N-acylated, crosslinked chitosan beads.	18
2. 3	Crushing strength test apparatus.	23
2. 4	Effect of glutaric dialdehyde concentration in the crosslinking bath on internal surface area and acid solubility for N-acylated chitosan beads.	29
2. 5	Effect of glutaric dialdehyde concentration in the crosslinking bath on the crushing strength of N-acylated chitosan beads.	30
2. 6	Effect of background $NaNO_3$ concentration on the cadmium adsorption isotherm for nonacylated, crosslinked chitosan beads.	33
2. 7	Effect of crosslinking on the cadmium ion adsorption isotherm for nonacylated chitosan beads.	35
2. 8	Effect of crosslinking on the cadmium ion adsorption isotherm for nonacylated chitosan powder.	37
2. 9	Effect of glutaric dialdehyde concentration in the crosslinking bath on the cadmium ion adsorption isotherm for N-acylated chitosan beads.	38
2. 10	Low concentration adsorption isotherms (4-80 mg Cd^{+2}/L).	40

LIST OF FIGURES, CONTINUED

FIGURE		Page
3. 1	(a) X_T and pH profiles for 3 mm 7 % N-acylated gel beads at C_{A0} = 0.75 g/100 mL. (b) X_T vs. T for 3 mm chitosan gel beads at C_{A0} = 0.75 g/100 mL.	57
3. 2	(a) X_T and pH profiles for 3 mm 7 % N-acylated gel beads at C_{A0} = 2.5 g/100 mL. (b) X_T vs. T for 3 mm chitosan gel beads at C_{A0} = 2.5 g/100 mL.	59
3. 3	Effect of mixing speed on the overall extent of crosslinking for 3 mm 7 % N-acylated gel beads at C_{A0} = 2.5 g/100 mL.	60
3. 4	X_R and X_T vs. C_{A0} at t = 48 hours. (a) 3 mm 7 % acylated gel beads. (b) 3 mm chitosan gel beads.	61
3. 5	Cadmium adsorption isotherms for 7 % N-acylated chitosan gel beads and freeze-dried beads crosslinked with C_{Ao} = 0.75 g GA/100 mL.	64
3. 6	Qe vs. X_R at saturation for (a) 7 % 3 mm N-acylated and (b) nonacylated chitosan gel beads.	66
3. 7	Representative EDAX images for 3 mm crosslinked chitosan beads with cadmium (C_o = 1026 mg Cd/L). (a) line. (b) mapping.	68
3. 7	(c) Mapping image for 3 mm uncrosslinked chitosan beads	69
3. 8	Molecular structures. (a) glutaric dialdehyde polymer. (b) crosslinked glutaric dialdehyde polymer.	72
3. 9	Modified shrinking core model plot for 7 % N-acylated chitosan gel beads crosslinked at C_{Ao} = 2.5 g GA/100 mL.	74

LIST OF FIGURES, CONTINUED

FIGURE		Page
3. 10	Predicted $X_{T,model}$ vs. Time for (a) C_{Ao} = 0.75 g GA/100mL. and (b) C_{Ao} = 2.5 g GA/100mL.	76
3. 11	Chelation scheme of Cd^{+2} in crosslinked chitosan.	80
3. 12	The change of the thickness of the cadmium un-saturation zone (r_M) and the uncrosslinked zone (r_c) versus X_T for N-acylated gel beads.	84
4.1	Spinning basket reactor.	88
4.2	(a) cadmium ion concentration versus time (b) hydrogen ion capacity and the pH change in the cadmium solution in the spinning basket reactor for a single stage adsorption/desorption experiment.	95
4.3	The hydrogen ion consumption and pH versus time for cadmium-free water saturation experiment.	97
4.4	The percentage of cadmium desorbed versus desorption time for different amounts of hydrogen ion initially charged to the vessel.	99
4.5	The experimental and predicted percentage of cadmium desorbed versus equilibrium pH for shake flask experiments.	100
4.6	The titration curve for crosslinked chitosan beads.	102
4.7	The competitive ion exchange scheme.	103

LIST OF TABLES

TABLE		Page
2. 1	Crosslinking bath parameters for synthesis of N-acylated, crosslinked chitosan beads	22
2. 2	Summary of conditions for adsorption isotherm measurements	25
2. 3	Summary of physical properties for selected chitosan adsorbent preparations	28
2. 4	Freundlich parameters for low-concentration Cd^{+2} isotherm data	41
3. 1	Initial pH value and GA/-NH_2 ratio in the crosslinking bath	48
3. 2	Residual glutaric dialdehyde concentration after soaking crosslinked chitosan gel beads in water (C_{A0} = 2.5 g GA/100 mL)	62
4.1	The adsorption/desorption parameters for spinning basket reactor experiments	87
4.2	The adsorption/desorption parameters for shake flask experiments	90
4.3	Stability of the adsorbed cadmium ion in distilled water at pH 6.0	94
4.4	The effect of pH adjustment on the % of cadmium desorbed (D) for the multiple stage desorption experiment	98

LIST OF APPENDICES

	Page
Appendix A Procedures	122
A-1 Preparation of 7 % N-Acylation Chitosan	122
A-2 Gel Bead Casting	123
A-3 Crosslinking Experiments	123
A-4 Glutaric Dialdehyde Analysis in Crosslinking Bath by Gas Chromatography	124
A-5 Gravimetric Analysis of Crosslinking Chitosan	133
A-6 Homogeneous Crosslinking of Chitosan	134
A-7 Bead Characterization Measurements	135
A-8 Cadmium Ion Adsorption Capacity	142
A-9 EDAX Sample Preparation	151
A-10 Single Stage Adsorption/Desorption Experiments	151
A-11 Equilibrium Desorption Measurements	153
Appendix B Calculation for Crosslinking Study	154
B-1 Calculations for D_0	154
B-2 Results of Statistical Analysis for Calculation of D_c	155
B-3 Computer Program	157
B-4 Reaction Control for Crosslinking Study	160
Appendix C Effect of Cadmium Loading on BET Surface Area and Pore Size Distribution	163

LIST OF APPENDIX FIGURES

FIGURE		Page
A.1	The first calibration curve for glutaric dialdehyde	131
A.2	The second calibration curve for glutaric dialdehyde	132
A.3	The first calibration curve for cobalt	149
A.4	The first calibration curve for cadmium	149
A.5	The second calibration curve for cobalt	150
A.6	The second calibration curve for cadmium	150
B.1	The extent of crosslinking versus crosslinking time for N-acylated chitosan gel beads crosslinked with 0.75 wt % GA	162
C.1	The pore size distribution for 1 mm chitosan beads before and after cadmium adsorption	177
C.2	The pore size distribution for 3 mm chitosan beads before and after cadmium adsorption	178
C.3	The pore size distribution for crosslinked and uncrosslinked 3mm chitosan beads	179

LIST OF APPENDIX TABLES

TABLE		Page
A-1	The first set of calibration data for GC analysis	129
A-2	The second set of calibration data for GC analysis	130
A-3	The first set of calibration data for IC analysis	148
A-4	The second set of calibration data for IC analysis	148
B-1	The results of statistical analysis for calculation of D_c	155
B-2	Numerical implementation of crosslinked model	156
C-1	The BET surafec area comparisons for 1mm crosslinked, 3 mm uncrosslinked, and crosslinked chitosan beads before and after cadmium loading	163
C-2	The BJH adsorption pore distribution for crosslinked 3 mm beads	164
C-3	The BJH desorption pore distribution report for 3 mm crosslinked chitosan beads	165
C-4	The control experiment of BJH desorption pore distribution for 3 mm crosslinked chitosan beads	166
C-5	The control experiment of BJH adsorption pore distribution for 3 mm crosslinked chitosan beads	167
C-6	The BJH desorption pore distribution report for 3 mm cadmium-loaded crosslinked chitosan beads	168
C-7	The BJH adsorption pore distribution report for 3 mm cadmium-loaded crosslinked chitosan beads	169
C-8	The BJH desorption pore distribution report for 3 mm uncrosslinked chitosan beads	170

LIST OF APPENDIX TABLES, CONTINUED

TABLE		Page
C-9	The BJH desorption pore distribution report for 1 mm crosslinked chitosan beads	171
C-10	The BJH adsorption pore distribution report for 1 mm crosslinked chitosan beads	172
C-11	The control experiment of BJH desorption pore distribution report for 1 mm crosslinked chitosan beads	173
C-12	The control experiment of BJH adsorption pore distribution report for 1 mm crosslinked chitosan beads	174
C-13	The BJH desorption pore distribution report for 1 mm cadmium -loaded crosslinked chitosan beads	175
C-14	The BJH adsorption pore distribution report for 1 mm cadmium -loaded crosslinked chitosan beads	176

NOMENCLATURE

$C(t)$ cadmium ion concentration in the vessel at different adsorption or desorption times, mg Cd/L

C_A concentration of glutaric dialdehyde at position r ($r_c < r < R$) within the crosslinked zone of the gel bead in chapter 3, mole/cm^3

C_A concentration of glutaric dialdehyde in the crosslinking bath in Chapter 4, mole/cm^3

C_{AS} concentration of glutaric dialdehyde at the surface of the gel bead ($r = R$) in Chapter 3, mole/cm^3

C_a concentration of HNO_3 added into the spinning basket reactor before desorption, mole H^+/L

C_{ae} equilibrium hydrogen ion concentration in the cadmium solution, mole/L

C_e equilibrium cadmium ion concentration in the vessel, mole /L

C_o initial concentration of Cd^{+2}, mg Cd^{+2}/L

C_f final concentration of Cd^{+2} at equilibration, mg Cd^{+2}/L

C_{min} lowest cadmium concentration along the adsorption or desorption process, mg Cd/L

$C_{min,i}$ lowest cadmium concentration along the adsorption or desorption process at a specific desorption stage, mg Cd/L

$C_{0,i}$ initial cadmium concentration in the spinning basket reactor at specific desorption stage " i " , mg Cd/L

D percentage of cadmium desorbed at a given desorption time, %

D_{Ae} effective diffusion coefficient of glutaric dialdehyde within the crosslinked zone of the gel bead, cm^2/sec

K measure of the adsorption capacity or binding strength

NOMENCLATURE, CONTINUED

K_a' equilibrium constant for the neutralization reaction, $(mole/L)^{-1}$

K_{cd} equilibrium constant for chelation, $(mole/L)^{-1/2}$

$M_{w,Cd^{+2}}$ molecular weight of the cadmium ions, g/mole

m_b mass of freeze-dried beads in chapter 2 , g

m_b total mass of the gel beads within the crosslinking bath in chapter 3, g

m_b mass of chitosan beads in the spinning basket reactor impeller assembly in Chapter 4 , g

n number of desorption stage in Chapter 4

$1/n$ measure of adsorption intensity

pH_t pH value at different adsorption or desorption times

Q cadmium adsorption capacity on the chitosan beads, mg Cd/g-chitosan

Q_f adsorption capacity of Cd^{+2} on the bead in Chapter 2, mg Cd^{+2}/g-adsorbent

Q_f final cadmium adsorption capacity on the chitosan beads in Chapter 4, mg Cd^{+2}/g chitosan

$Q(H^+)$ accumulated hydrogen ion adsorption capacity in the present stage, mg Cd/g-chitosan

$q_{Cd,f}$ final cadmium adsorption capacity before the desorption process in Chapter 2, mmole Cd^{+2}/g chitosan

q_{Cd} equilibrium cadmium ion capacity of the crosslinked chitosan beads in Chapter 4, mmole Cd^{+2}/g chitosan

Q_M theoretical maximum capacity of chitosan, 6.2 mmole active sites/g chitosan

$\overline{Q}_1$ theoretical maximum loading of the cadmium ion in the crosslinked zone, mg Cd^{+2}/g

NOMENCLATURE, CONTINUED

$\overline{Q}_2$ theoretical maximum loading of the cadmium ion in the uncrosslinked zone, mg Cd^{+2}/g

q_H equilibrium hydrogen ion capacity of the crosslinked chitosan beads, mmole H^+/g chitosan

R radius of the gel bead, cm

r radial position within the gel bead, cm

r_C radial position within the gel bead defining the boundary between the outer crosslinked zone and the inner unreacted core zone, cm

r_M cadmium un-saturation zone, cm

t time of crosslinking

V volume of solution in Chapter 3, L

V current cadmium solution volume loaded in the spinning basket reactor vessel in Chapter 4 , L

V_a acid volume added into the spinning basket reactor, L

V_c volume of glutaric dialdehyde solution in the crosslinking bath in Chapter 2, cm^3

V_t volume of solution in the spinning basket reactor at a given time, L

x_B weight fraction of chitosan in the gel bead, g chitosan/g of gel bead

extent of crosslinking, moles of crosslink/total moles of $-NH_2$ groups

X_T moles of glutaric dialdehyde consumed by the gel bead/total moles of $-NH_2$ groups within the gel bead

X_R moles of glutaric dialdehyde crosslinked per total mole of $-NH_2$ groups within the gel bead

Y_B total moles of amine groups/g of chitosan

NOMENCLATURE, CONTINUED

β moles of glutaric dialdehyde consumed to form a crosslink/moles of $-NH_2$ crosslinked

ρ_b overall density of the gel bead, g/cm^3

ν chelation coordination number for cadmium, 2 moles active sites/mole Cd^{+2}

$\Delta Q_i\,(H^+)$ hydrogen ion adsorption capacity for chitosan beads at the *i*th desorption stage mg H/g-chitosan

Removal of Cadmium Ions by Porous Chitosan Beads: Effects of Acylation & Crosslinking on Material Properties and Adsorption Isotherms

CHAPTER 1

INTRODUCTION

1.1 Background and Motivation

Cadmium pollution of the environment has become a serious problem due to the increasing consumption of cadmium by industry in the past 20 years. Cadmium is introduced into the environment from the effluence of electroplating industry, and in solid and aqueous discharges from mining operations.

Increased environmental awareness has resulted in the promulgation of more stringent legislation in several countries for water quality. For example, in Italy and the United States, the maximum permitted concentrations of heavy metals such as cadmium, lead, chromium, and nickel ions are 5, 50, 50, and 50 μg/l respectively (Rozzlle, 1987; Yoo, 1987). Recently, the International Union of Pure and Applied Chemistry (IUPAC) pointed out the relationship between cadmium toxicity and its effects on human kidneys and lungs. Well known human diseases, which results from exposure to cadmium, are itai-itai disease and renal dysfunction in Japan, Belgium, and China.

The removal of toxic cadmium from aqueous waste streams poses significant technical challenges. The common treatment processes for removal of cadmium ions from aqueous streams include chemical precipitation, ion-exchange, reverse osmosis, and solvent extraction (Lankford and Torrens, 1988). However, these processes are limited

due to incomplete metal removal, high reagent or energy requirements, and generation of toxic sludge or other waste products that require disposal (Trujlllo et al., 1991). These disadvantages are encountered even at parts per million (ppm) levels.

1.2 Rationale

The development of new adsorbents for removing cadmium ions from dilute aqueous waste streams has been recognized as a research priority because of inefficiency of existing adsorbents at low concentration of cadmium solution (King et al., 1987). An exciting new adsorbent material for cadmium ion is chitosan. Chitosan, which is derived from the deacetylation of chitin, is the nature's most abundant biopolymer next to cellulose (Sandford et al., 1987). Chitosan is a cationic polymer containing of 2-amino-2-deoxy-D-glucose (Fig 1.1) which serves as a chelation site for the transition metal ions. However, alkali metal ions are not adsorbed by chitosan. Chitosan is soluble in both mineral and organic acids and has the ability to selectively bind trace amounts of group III transition metal ions in the presence of high concentrations of other metal ions. Consequently chitosan has been studied for waste water treatment applications since the 1960's. However, since chitosan is nonporous and soluble in acid solution, it has found limited use in waste water treatment processes. Therefore, it is appropriate to develop new technologies to convert chitosan to a form suitable for use in aggressive chemical environments within packed-bed processes.

In this work, new processes for the synthesis of highly porous chitosan beads will be developed. The physical properties of the chitosan beads, including crushing strength, internal surface area, and solubility, will be evaluated. The adsorption isotherms for

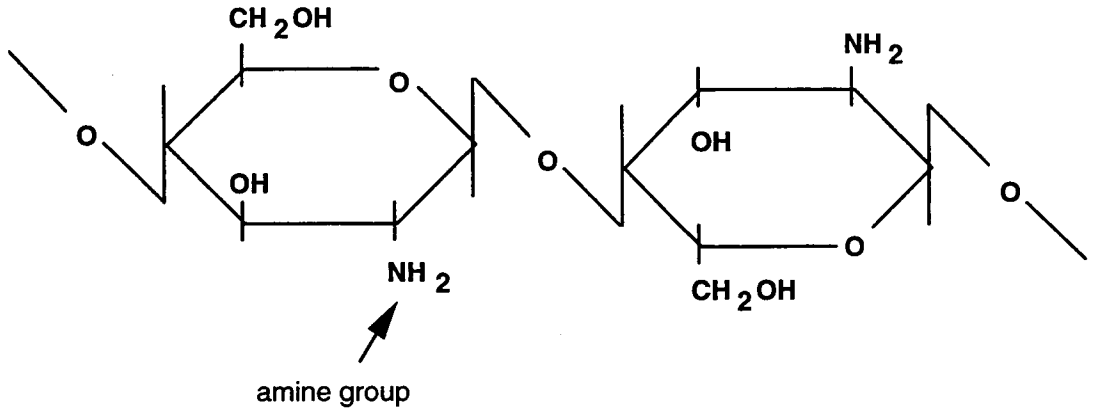

Figure 1.1 Chemical structure of chitosan

cadmium ions on the chitosan beads will also be measured and correlated to material properties. The regeneration of chitosan beads after cadmium adsorption will also be studied to further assess their potential for practical use.

The adsorption of heavy metals ions onto chitosan flakes or powder are well documented. Muzzarelli et al. (1969) used a packed column of 100-200 mesh chitosan to study the removal several transition metal ions from sea water. Muzzarelli (1971) claimed that chitosan powder collected trace metals (zinc, cerium, lead, nickel, cobalt, silver, and cadmium) from water by chelation accompanied by co-precipitation.

Muzzarelli et al. (1970) also demonstrated that very large artificial concentrations of Na^{+} (0.66 M) or Mg^{+2} (0.42 M) in nitrate solutions had no effect on the adsorption capacity for most transition metal ions. However, Jha et al. (1988) claimed that the presence of 5 mM calcium did reduce the adsorption of Cd^{+2} onto chitosan powder.

Maruca (1982) determined the adsorption isotherms for chromium onto various sizes of chitosan flakes and showed an increase in adsorption capacity with a decrease in flake size. The same observation was presented by Jha et al. (1988) for the adsorption of Cd^{+2} (1-10 ppm) onto 0.037-0.328 mm chitosan powder. These works suggested that the adsorption capacity was a function of accessible surface area of the adsorbent.

In order to increase the concentration of exposed active sites within chitosan so that the adsorption capacity and transport rate of metal ions into the particle can be enhanced, porous chitosan beads need to be developed. Nishimura et al. (1986) prepared porous chitin beads (0.54-1.0 mm) from 80 % deacetylated chitin for use as a drug carrier. The application of chitosan microbeads (10 μm) for the chelation of heavy metal ions (Zn^{+2}, Cd^{+2}, Fe^{+3}, and Mn^{+2}) was presented by Seo et al. (1988). However, the details on the preparation of chitosan beads and cadmium adsorption isotherm data onto the chitosan beads are not well documented by these previous studies.

Magnetic chitosan particles can be prepared by the addition of magnetite to chitosan solution. Yen et al. (1981) claimed that spherical chitosan micelles (100Å -1000 μm) can be easily produced by coating chitosan on ferrous chloride or ferric chloride.

Recently Rorrer, Way, and Hsien (1993) described the synthesis of 1 mm and 3 mm porous, magnetic, chitosan beads for cadmium ion separation from aqueous solutions. Complete adsorption isotherms over a large range of cadmium ion

concentrations (2-1700 ppm) onto the chitosan beads were obtained. However, the physical properties of the chitosan beads, including internal surface area, crushing strength, and solubility, were not well described. The effects of alkali and alkaline earth metal ions on the chitosan beads for transition metal ion capacity were also not evaluated.

The adsorption isotherms for transition metal ions on chitosan flake and powder have been well studied. Masri et al. (1974) reported the adsorption capacities on 20-mesh chitosan flakes for 15 different heavy metal ions such as Cr^{+3} (0.024 g Cr/g chitosan), Cd^{+2} (0.31 g Cd/g chitosan), Hg^{+2} (1.1 g Hg/g chitosan), and Cu^{+2} (1.98 g Cu/g chitosan). Yang et al. (1984) provided the adsorption isotherms of Cu^{+2}, Zn^{+2}, Cr^{+3}, and Cd^{+2} on chitosan powder, and the isotherm data was fitted to the Langmuir equation. The adsorption isotherms and kinetics for cadmium ions onto various sizes of chitosan powder at a low cadmium concentrations were studied by Jha et al. (1988), and the isotherm data was fit to the Freundlich equation. Additional adsorption isotherms for chromium onto chitosan powder were studied by Udaybhaskar et al. (1990), and the data was compared with three different isotherm models (Lagergren's, Langmuir, and Freundlich). However, adsorption isotherm models were not considered in our previous studies for adsorption of cadmium ions on porous chitosan beads. Thus, this present study will find a suitable adsorption isotherm model for the adsorption of cadmium ions onto chitosan beads, particularly at low cadmium ion concentrations.

Chemical modifications of chitosan, including the addition of hydrocarbon side chains through partial N-acylation will be considered. The chemical derivatization of chitosan by N-acylation (Fig 1.2) can disrupt the bonding network between chitosan chains. This may expose more amine chelation sites to metal ions and enhance the

adsorption capacity. In a previous study, the adsorption capacity of copper (II) on chitosan improved remarkably by the acylation of a small fraction of the amine groups with nonanoyl chloride (Kurita et al., 1988). The effects of partial acylation on the

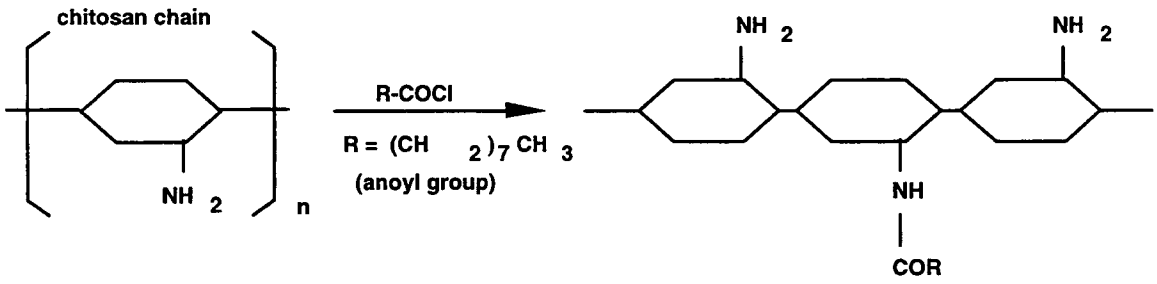

Figure 1. 2 N-acylation of chitosan

physical properties of N-acylated chitosan beads, including internal surface area, crushing strength, and solubility, are not known. Thus, in this study the physical properties on partially N-acylated chitosan beads will be compared with the physical properties of nonacylated chitosan beads. The effect of partial N-acylation chitosan on the cadmium ion adsorption capacity will also be evaluated.

The solubility of chitosan can be reduced by chemical crosslinking with glutaric dialdehyde (Fig 1.3) to help the material cope with acidic environments. Masri et al. (1978) crosslinked chitosan powder directly with an aqueous solution of glutaric dialdehyde to allow its use in acidic media. The transition metal ion adsorption capacity of chitosan powder decreased as the result of crosslinking. Koyama et al. (1986) claimed

that the homogeneous crosslinking of chitosan with a aldehyde/amine group ratio of 1.0 increased the space between chitosan chains and also increased copper (II) adsorption capacity. Seo et al. (1988) also pointed out that the relative surface area of chitosan

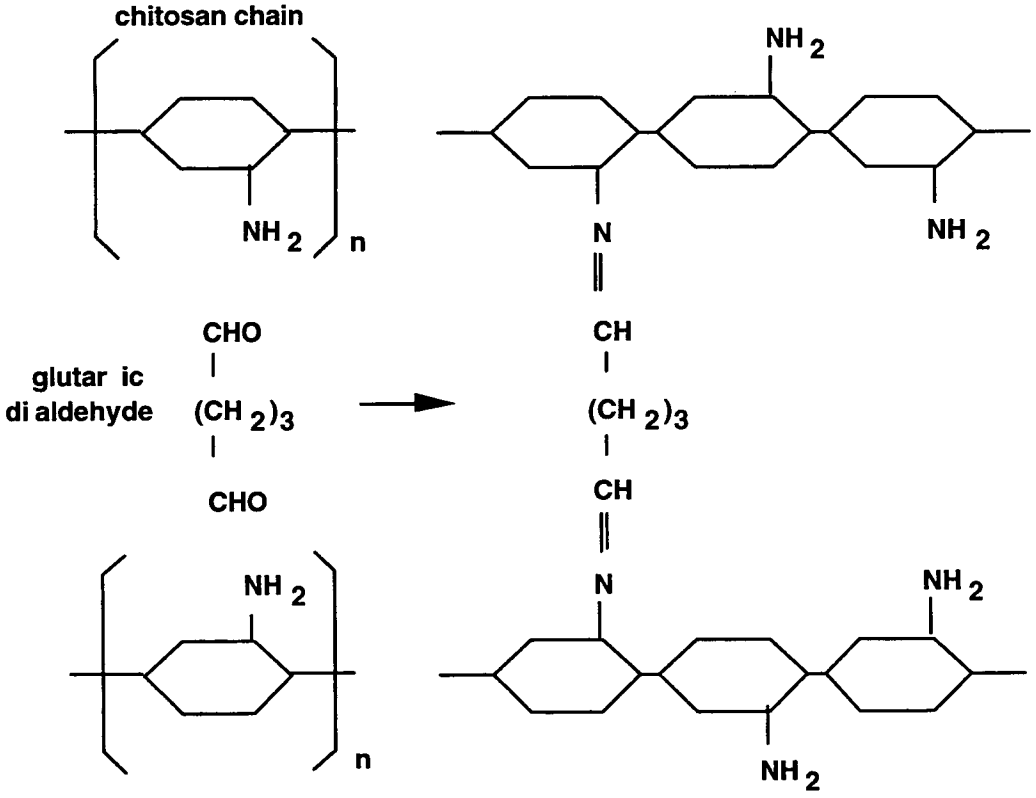

Figure 1. 3 Crosslinking of chitosan

micelles could be increased by partial crosslinking. The effects of several variables on the gelling behavior of the chitosan/glutaric dialdehyde system has been studied by Roberts et al. (1989). However, the effects of partial crosslinking on the material

properties and adsorption capacity of nonacylated and partial N-acylated chitosan beads have not been considered by previous works. In order to enhance the porosity within the biopolymer matrix, a mechanism for crosslinking of the gelled chitosan bead will be proposed by this study.

Chitosan is a cationic polymer which can displace adsorbed metal ions by hydrogen ions in a low pH environment. Muzzarelli et al. (1974) pointed that a packed column of mercury-adsorbed chitosan could be regenerated by flushing the bed with a 10 mM potassium iodide solution or other eluting agents. Randall et al. (1979) regenerated chitosan powder in a packed column by flushing the bed with a 0.2 N NH_4Cl solution. Nickel removal efficiencies were as high as 97 %. The pH effect on the desorption process for regeneration of cadmium-adsorbed chitosan powder was first considered by Jha et al. (1988). An economic comparison of two different processes to recycle chitosan after the adsorption process was provided by Coughlin et al. (1990). Thus, it is valuable to define the optimum regeneration parameters for chitosan beads. The recycle efficiency of the cadmium-adsorbed chitosan beads will also be considered by this study.

An important parameter for regeneration of cadmium ions from chitosan beads is to define an optimum pH range, the titration curve, to ensure the complete cadmium ions desorption. Yoshida et al. (1994) developed a titration curve for adsorption of hydrogen ions on polyaminated chitosan beads.

1.3 Research Goals and Objectives

The overall goals of this research are to 1) to prepare highly porous nonacylated and partially N-acylated chitosan beads, and then 2) evaluate these beads for removal of cadmium ions from dilute waste water. These preparation of the chitosan beads involves three major steps. Specifically, acidic chitosan solution is cast into spherical gel beads. Porous chitosan beads are formed through the processes of crosslinking to strengthen the internal matrices, and freeze drying to remove water without collapsing of the internal structure. Parameters for the synthesis process of the beads, including the casting solution conditions, crosslinking conditions, and drying methods will also be defined to maximize the cadmium ion adsorption capacity of nonacylated and partially N-acylated chitosan beads. The adsorption of cadmium ions onto the beads are carried out in a well-mixed batch contactor, and the cadmium ion concentrations is analyzed by ion chromatography.

The hydrogen ion consumption and optimum pH range for the regeneration of chitosan beads after cadmium adsorption will be studied. Specifically, the desorption process after cadmium adsorption will be carried out in a spinning-basket reactor with online pH measurement to determine the effect of pH and H^+ consumption on cadmium desorption and bead regeneration efficiency.

In summary, the proposed research has five specific objectives:

1. To synthesize partial N-acylated chitosan beads and optimize the bead synthesis processes, particularly, the crosslinking process;
2. To characterize and compare the material properties of nonacylated and N-acylated

chitosan beads including internal surface area, acid solubility, and crushing strength;

3. To predict the extent of crosslinking within the chitosan bead as a function of time and crosslinking agent concentration;
4. To measure and correlate the cadmium ion adsorption isotherms for each chitosan bead preparation to the material properties;
5. To determine the feasible pH range and H^+ consumption for regeneration of cadmium adsorbed chitosan beads.

In Chapter 2, the combined effects of N-acylation and crosslinking on the material properties including internal surface area, solubility in acid solution, and crushing strength of porous chitosan beads were explored. The subsequent effects on the adsorption capacity for the toxic heavy metal cadmium were measured. Adsorption isotherms for cadmium ions on each adsorbent preparation were obtained over a broad range of Cd^{+2} concentration (5 to 1500 mg/L) in order to gain insights on how material properties affect the heavy metal ion adsorption. In Chapter 3, the crosslinking kinetics were characterized, and the overall extent of crosslinking (X_T) was correlated to the saturation cadmium ion adsorption capacity. The possible roles of crosslinking time, initial glutaric dialdehyde concentration, pH, and glutaric dialdehyde polymer (PGA) formation on the crosslinking process were examined. These insights are used to help validate the modified shrinking core model for crosslinking process. Finally, the adsorption and desorption kinetics for single stage adsorption desorption experiments were determined in a spinning basket reactor. The hydrogen ion capacity of the chitosan beads and the pH of the cadmium solution in the vessel were also measured as a function of time. Additionally, an equilibrium model for the desorption process was presented in

Chapter 4 in order to describe the competitive relationships associated with displacing adsorbed cadmium ions with hydrogen ions.

CHAPTER 2

EFFECTS OF ACYLATION ON THE MATERIAL PROPERTIES AND CADMIUM IONS ADSORPTION CAPACITY OF POROUS CHITOSAN BEADS

Tzu-Yang Hsien and Gregory L. Rorrer*

Department of Chemical Engineering
Oregon State University
Corvallis, Oregon 97331

(tel) 503-737-3370, (fax) 503-737-4600

* corresponding author

Published in *Separation Science and Technology*

2.1 Introduction

Biopolymers are a promising new class of adsorbents for heavy metal ion separations from aqueous process waste streams (Volesky, 1987). Many biopolymers are inexpensive, environmentally benign, and exhibit selective binding for transition metal ions over other ionic species. Of particular interest is chitosan, a linear polysaccharide based on the glucosamine unit (Figure 2.1a). Chitosan is obtained from the deacetylation of chitin, a major component of the shells of crustacean organisms and the second most abundant biopolymer in nature next to cellulose (Muzzarelle, 1973 and 1977). Inter-chain hydrogen bonding between hydroxyl groups on the chitin biopolymer chain make the material para-crystalline and nonporous. The amine group on each glucosamine unit within the chitosan biopolymer chain serves as a selective binding site for group III transition metal ions, and the β-1,4 glycosidic linkage between the glucosamine units resists chemical degradation or short-term biological degradation.

The adsorption of heavy metal ions on chitosan is well documented (Masri et al., 1974, Yang and Zall, 1984, and MaKay et al., 1989). Rorrer et al. (1993) summarized previous work on adsorption isotherm and adsorption kinetic measurements. Previous studies also attempted to define the selectivity series for adsorption of group III transition metal ions on chitosan or chitosan derivatives (Inoue et al., 1988, Delben and Muzzarelli, 1989, and Kawamura, 1993). Coughlin et al. (1990) demonstrated metal recovery and adsorbent regeneration by washing metal-adsorbed chitosan with acid and base solutions respectively.

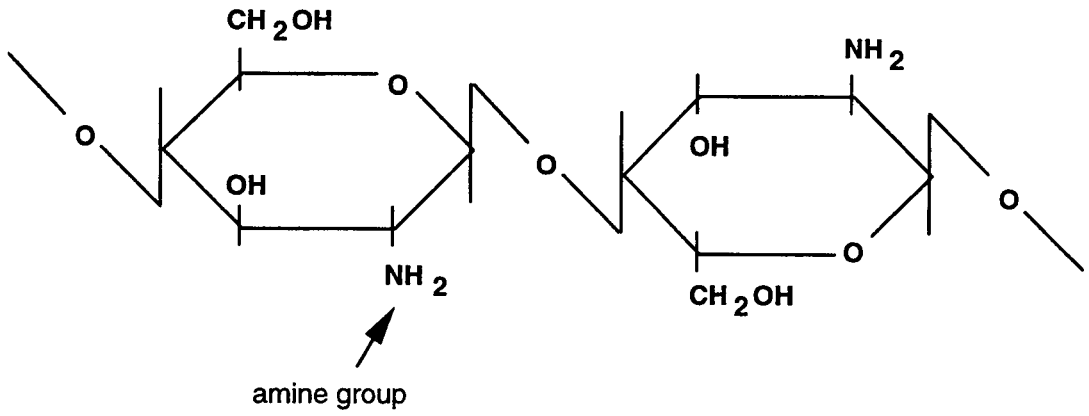

Figure 2.1 Chemical structures. (a) chitosan

Chitosan, like most biopolymers, has two major material limitations which have hindered its development for heavy metal ion separation processes. First, chitosan is nonporous, and so must be ground to a powder to provide a sufficient surface area to mass ratio for high-capacity adsorption of heavy metal ions. Furthermore, the chitosan powder is not suitable for use in packed-bed adsorption columns because of high pressure drop and the potential for bed fouling at low void fractions. Second, chitosan is readily soluble in acid solution. Therefore, the chitosan biopolymer must be engineered to a form suitable for pump-and-treat applications in aggressive chemical environments. Recently, porous beads of chitosan were synthesized for adsorption of ppm-level transition metal ions from aqueous solution (Rorrer et al., 1993 and Kawamura et al., 1993). Rorrer et al. (1993) described the synthesis of large, porous-magnetic chitosan beads for cadmium ion separations from dilute aqueous solutions. Specifically, highly porous 3 mm beads were synthesized using an aqueous, phase-inversion casting

technique followed by freeze drying to remove water without collapsing the porous structure of the hydrophilic chitosan biopolymer. Kawamura et al. (1993) synthesized 0.6 mm chitosan gel beads with a reticular matrix, but did not use freeze drying. Kawamura et al. showed that poly-amination of the amine group significantly improved adsorption capacity for mercury ions. The porous chitosan bead is really a biopolymer-supported reagent which can be chemically modified to alter material properties and heavy metal ion adsorption capacity. Unlike other polysaccharide biosorbents, chitosan possesses an amine group on each glucosamine residue which can serve a reactive site for two attractive chemical modifications. First, N-acylation of chitosan can randomly add hydrocarbon side chains to a fraction of the amine groups (Figure 2.1b). These hydrocarbon site chains can impart a hydrophobic substructure to the biopolymer and also disrupt the hydrogen bonding network between chitosan chains to expose more amine sites for binding with heavy metal ions. Second, inter-chain crosslinking of chitosan with bi-functional reagents such as glutaric dialdehyde can impart a three-dimensional network to the biopolymer (Figure 2.1c). Crosslinking can reduce the solubility of chitosan in aqueous solvents over a broad pH range, and increase resistance to chemical degradation or long-term biological degradation. Like N-acylation, crosslinking also can increase the spacing between chitosan chains to improve the accessibility of metal ions to amine sites.

A few previous studies have described the synthesis of N-acylated chitosan derivatives (Hirano et al., 1976, and Kurita et al., 1988) and glutaric dialdehyde crosslinked chitosan (Masri et al., 1978, Koyama and Tanigiuchi, 1986, and Roberts and Taylor, 1989). However, previous work has not considered how these chemical modifications affect

(b)

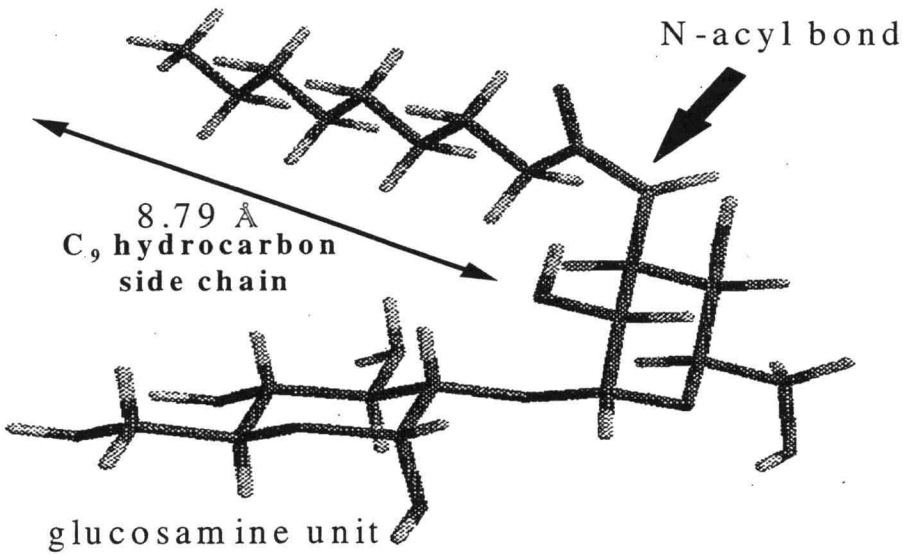

(c)

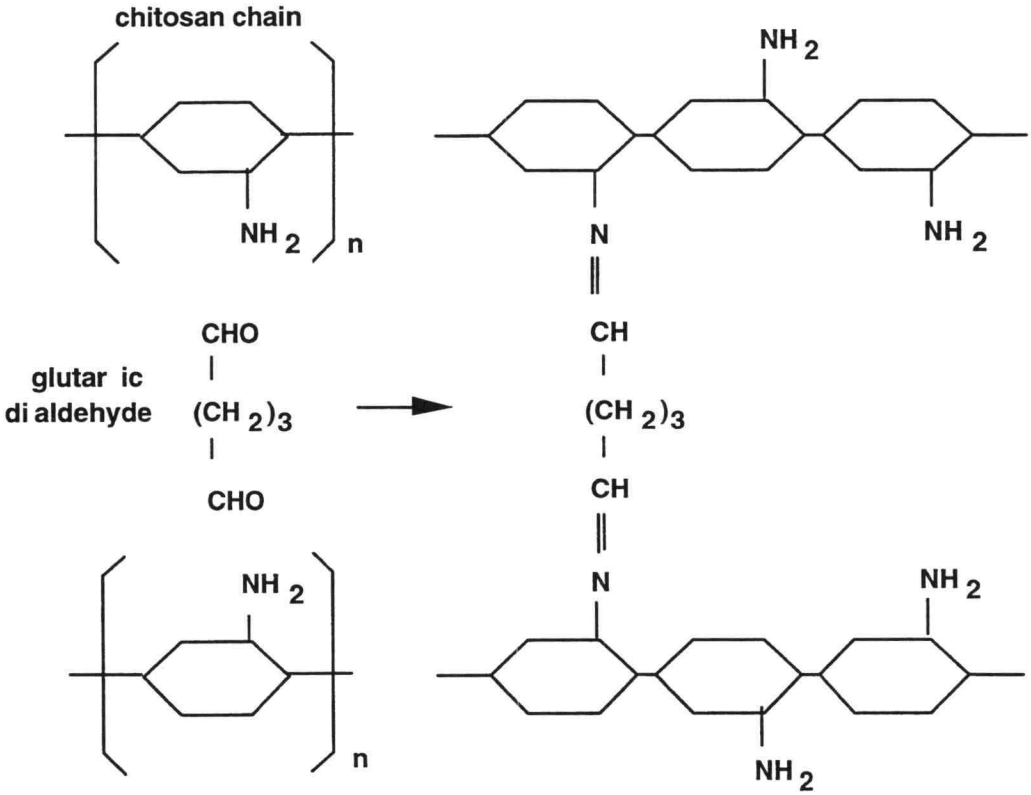

Figure 2.1 (b) N-acylation of chitosan (c) crosslinking of chitosan

material properties for porous chitosan beads.

The first objective of this study is to explore the combined effects of N-acylation and crosslinking on the material properties of porous chitosan beads, and their subsequent effects on the adsorption capacity for the toxic heavy metal cadmium. Specifically, chitosan will be homogeneously N-acylated with nonanoyl chloride at a low degree of substitution (7%) to randomly add C_9 alkyl side chains to chitosan. The N-acylated chitosan will then be cast into gel beads. The chitosan gel beads will then be heterogeneously crosslinked with glutaric dialdehyde and freeze dried (Figure 2.2). The internal surface area, solubility in acid solution, and crushing strength will be measured to characterize the material properties of each adsorbent preparation. Adsorption isotherms for cadmium ions on each adsorbent preparation will be obtained over a broad range of Cd^{+2} concentration (5 to 1500 mg/L) in order to gain insights on how material properties affect the heavy metal ion adsorption.

Another unresolved issue in the development of chitosan biopolymer adsorbents for heavy metal ion separations is selectivity of group III transition metal ions over groups I and II alkali and alkaline earth metal ions. Previous studies have claimed that groups I and II metal ions do not affect adsorption capacity transition metal ions (Kawamura et al., 1993, Muzzarelli and Tubertini, 1969, Muzzarelli and Sipos, 1971, and Randal et al., 1979). Only Kawamura et al. (1993) considered the effect of sodium ion concentration on adsorption capacity for mercury ions (Hg^{+2}), but the data focused on very high Hg^{+2} concentrations of 10 to 70 mM. Therefore, a second objective of this

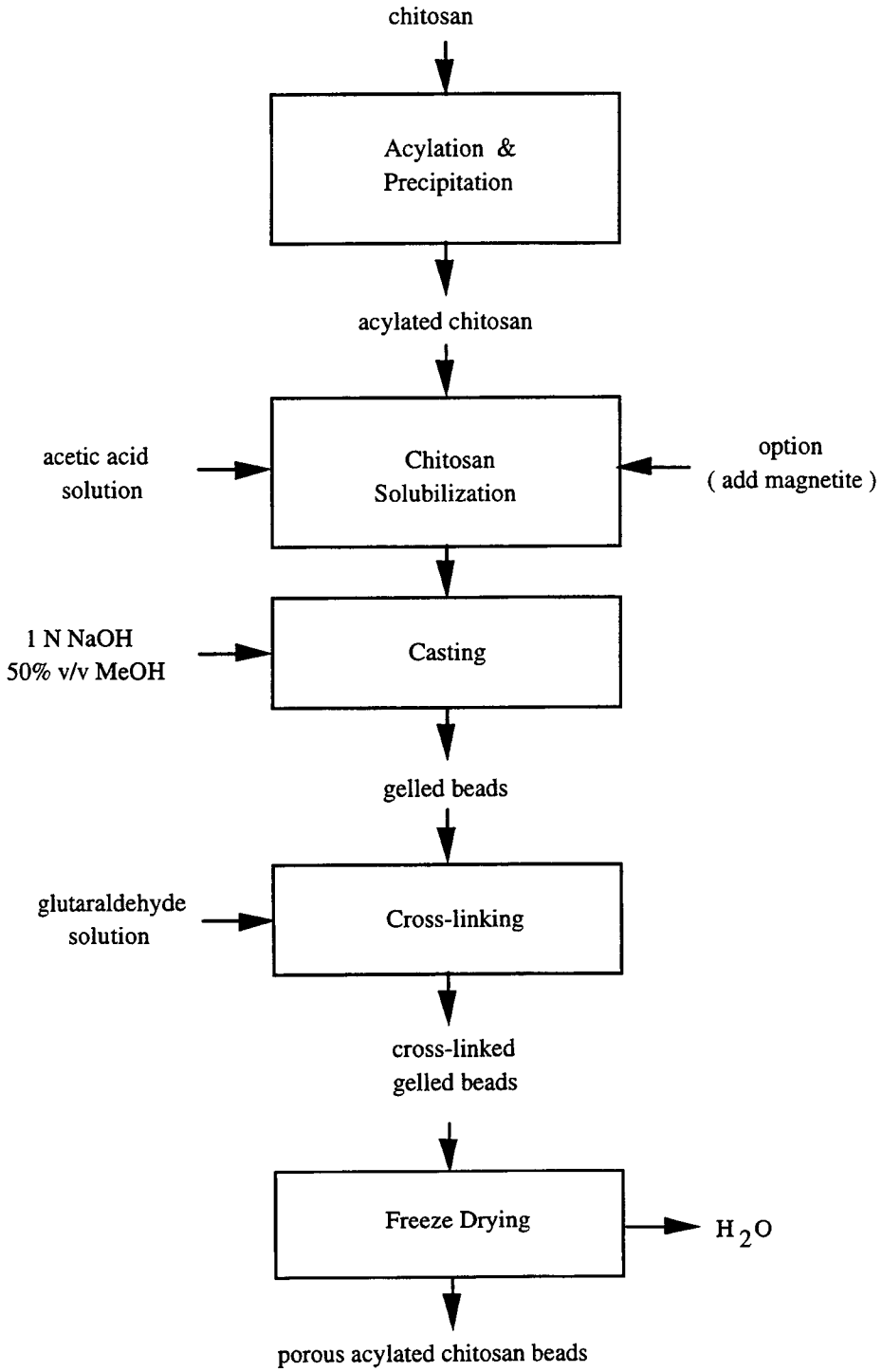

Figure 2.2 Flowchart for synthesis of N-acylated, crosslinked chitosan beads

study is to measure the effect of background sodium ion concentration (0 to 150 mM) on the adsorption isotherm for cadmium ions over a broad range of Cd^{+2} concentration, specifically 5 to 1500 mg Cd^{+2}/L (0.05 to 13.4 mM).

2.2 Materials and Methods

2.2.1 Chemicals

Chitosan flake (94 % deacetylation) was provided by Vansen Chemical Company (Woodinville, WA). The chitosan flake was chopped to a powder and sieved to less than 48 mesh (< 300 μm). All reagents for adsorbent synthesis including acetic acid (Mallinckrodt, 2504-03), methanol (Mallinckrodt, 3041-09), pyridine (Mallinckrodt, 7180-03), glutaric dialdehyde (Aldrich, G400-4), and nonanoyl chloride (Aldrich, 15683-3) were ACS reagent grade. Cadmium nitrate of 98 % purity was obtained from Aldrich (15683-3). The chemicals used for the preparation of eluent and post-column reagents for ion chromatography included oxalic acid (Aldrich, 24117-2), lithium hydroxide monohydrate (Aldrich, 25427-4) and 4-(2-pyridylazo) resorcinol monosodium salt monohydrate (Dionex, PAR P/N 39672), aqueous acetic acid, and ammonium hydroxide.

2.2.2 Bead Synthesis

A complete flow chart for synthesis of N-acylated, crosslinked chitosan beads is shown in Figure 2.2.

Acylation. Chitosan solution was prepared to 5 wt % concentration by dissolving chitosan powder into 0.68 M (4.2 wt %) acetic acid solution. The chitosan solution was mixed on a orbital shaker at 120 rpm for 24 hours at 25 °C. After complete mixing, 70 mL of the chitosan solution was poured into 70 mL of pure pyridine, and then acylated with 0.28 g of nonanoyl chloride ($CH_3(CH_2)_7COCl$) which was added to the final mixture. The mole ratio of nonanoyl chloride to amine groups on chitosan was 0.07. The acylation process was carried at 0 °C for 10 minutes to avoid over reaction. The solution was then stirred at room temperature for one hour and finally mixed on an orbital shaker at 120 rpm for 48 hours at 27 °C. After this time, the reaction was presumed complete, so that 7% of the amine groups on the chitosan chain were randomly N-acylated. The N-acylated chitosan solution was poured into pure ethyl acetate to form a gelatinous suspension of N-acylated chitosan. The ethyl acetate also precipitated pyridinium chloride salts formed by the acylation process. The gelatinous suspension of N-acylated chitosan and the pyridinium chloride salts were filtered from the ethyl acetate. N-acylated chitosan was precipitated from the colloidal suspension with acetone/water (7/1 v/v). The spongy, white precipitate was washed with acetone/water (7/1 v/v) to remove the remaining salts. The N-acylated chitosan precipitate was stored in pure acetone to prevent oxidation.

Bead Casting. The apparatus and procedures for casting chitosan beads were described previously by Rorrer et al. (1993). Chitosan solution was prepared to 5 wt % by dissolving either chitosan or N-acylated chitosan in 0.68 M acetic acid. The chitosan solution was delivered by a peristaltic pump at a flowrate rate of 0.95 mL/min to the spinnerette (0.76 mm ID) and dropped into a precipitation bath containing 500 mL of 2.0

M aqueous sodium hydroxide solution (NaOH). The precipitation bath was mixed at 200 rpm with a 5.5 cm marine blade impeller. Gelled beads were formed by coagulation when the acetic acid was neutralized by NaOH. Gel beads of N-acylated chitosan were prepared similarly using 1.0 M aqueous methanolic sodium hydroxide solution (50 % v/v) as the precipitation bath. Each bead casting run was carried out for a maximum of four hours. The gelled beads were filtered immediately after the casting run was complete. To impart a magnetic component to the bead, magnetite powder (60 to 100 μm) was added to the bead during the casting process as described by Rorrer et al. (1993).

Crosslinking. The chitosan gel beads were heterogeneously crosslinked in aqueous glutaric dialdehyde solution (10 g wet beads in 15 mL aqueous glutaric dialdehyde solution) on an orbital shaker at 120 rpm and 25 °C. The nonacylated chitosan gel beads and dry chitosan powder were crosslinked with 2.5 wt % aqueous glutaric dialdehyde solution. The N-acylated chitosan gel beads were crosslinked at seven glutaric dialdehyde concentrations ranging from 0.125 wt % to 5.0 wt %, which correspond to initial -CHO/-NH_2 ratios ranging from 0.11 to 4.19 (Table 2.1). The crosslinking reaction was carried out for 48 hrs. After crosslinking, the adsorbent was rinsed with cold water then hot water to remove the unreacted glutaric dialdehyde solution.

Drying. Both acylated and nonacylated chitosan gel beads were freeze dried to slowly remove water and impart a porous structure to the beads, as described by Rorrer et al. (7). Crosslinked chitosan powder was dried in air.

Table 2.1 Crosslinking bath parameters for synthesis of N-acylated, crosslinked chitosan beads

Glutaric dialdehyde (GA) concentration in crosslinking bath (g / 100 mL or wt %)	Molar ratio of bulk -CHO to $-NH_2$ in chitosan gel beads
0.125	0.11
0.25	0.21
0.75	0.63
1.25	1.05
2.50	2.11
3.75	3.14
5.00	4.19

2.2.3 Physical Properties of Beads

BET Internal Surface Area. The internal surface area of the freeze-dried chitosan beads and dry chitosan powder was determined by the BET method using N_2 as the adsorbate. The measurements were performed with a Micromeritics ASAP 2000 BET Surface Area and Porosimetry System. Prior to BET analysis the beads were evacuated at 70 °C for 12 hours to remove gases and residual water adsorbed on the sample. The pore size distribution and mean pore size were estimated from the desorption isotherm data by the BJH method of analysis (Barret et al., 1951).

Acid Solubility. The solubility of each chitosan bead preparation in acidic solution was determined by contacting 40 mg of chitosan beads with 40 mL of 1.0 N

acetic acid solution (pH 2.36) under continuous mixing on an orbital shaker at 120 rpm for 24 hours at 25 °C. The % solubility was determined from the initial and final weight of the oven-dried adsorbent after 24 hour contact time (85 °C, 24 hrs).

Crushing Strength. The mechanical stability of the freeze-dried chitosan beads was estimated by a crushing strength test adapted from the ASTM Standard Test Method D-4179-82 (1985). A schematic of the crushing strength apparatus is presented in Figure 3. A single layer of 12 beads rested within the column on the base plate below the

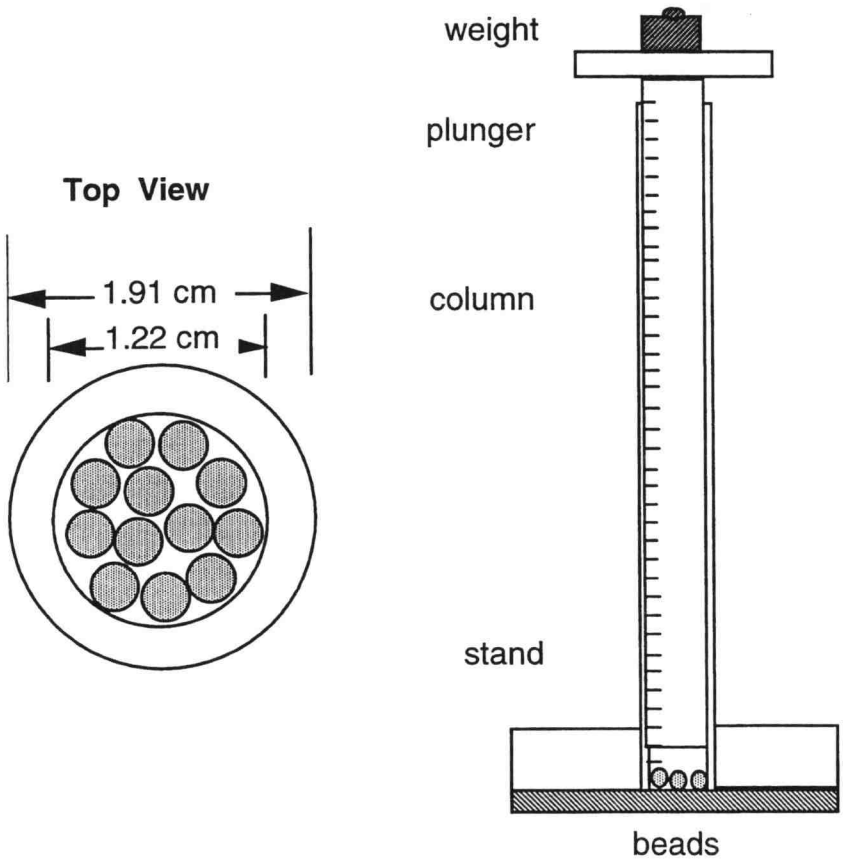

Figure 2.3 Crushing strength test apparatus

plunger. The inner diameter of the column containing the plunger was 1.23 cm. A weight resting on the top plate of the plunger applied a constant force to the sample. The end point force was determined when the irreversible displacement of the plunger was greater than 0.5 mm. The average crushing strength of beads was calculated as pressure based on the end point force applied and the inner diameter of the column.

Diameter. The diameter of the chitosan beads was measured by a Vernier digital caliper. The mean diameter was estimated from a random sample of 20 to 50 beads.

2.2.4 Adsorption Isotherms

Adsorption Capacity. The cadmium solution was prepared by dissolving cadmium nitrate ($Cd(NO_3)_2$) in deionized distilled water. The initial cadmium ion (Cd^{+2}) concentration ranged from 5 to 200 mg Cd^{+2}/L.

Measurements of cadmium adsorption isotherms were conducted in a well mixed batch process which was allowed to proceed to equilibrium. The conditions for the adsorption isotherm measurement are summarized in Table 2.2. Specifically, 40 mg of chitosan beads were contacted with 40 mL of cadmium nitrate solution (1 g beads/L solution) within a 125 mL erlenmeyer flask, and agitated at 120 rpm on an orbital shaker for 60 hours at 25 °C. After 60 hours of adsorption, the cadmium solution was filtered from the beads. The residual cadmium solution was stored in a sealed vial for later analysis. The Cd^{+2} concentration was measured at the beginning and end of the batch

Table 2.2 Summary of conditions for adsorption isotherm measurements

Process Condition	Variable & Units
Contact time	60 hrs
Temperature	25 °C
pH	6.5-7.0
Bead loading	1 g/L
Solution volume	40 mL in 125 mL flask
Agitation	120 rpm (orbital shaker)
Initial cadmium concentration	5 to 1500 mg Cd^{+2}/L

adsorption experiment by ion chromatography. The final loading of cadmium adsorbed on the beads was determined by

$$Q_f = \frac{(C_o - C_f)V}{m_b} \qquad (2\text{-}1)$$

where C_o is the initial concentration of Cd^{+2} (mg Cd^{+2}/L), C_f is the final concentration of Cd^{+2} at equilibration (mg Cd^{+2}/L), m_b is the mass of beads, Q_f is the adsorption capacity of Cd^{+2} on the bead (mg Cd^{+2}/g-adsorbent), and V is the volume of solution (L).

Ion Chromatography. The Cd^{+2} concentration in each sample was determined by ion chromatography (IC) using a Dionex model DX-300 Ion Chromatograph. The IC hardware system consisted of an automatic sample injector with 100 μL sample loop, dual-piston gradient high pressure pump, PAR post-column reaction coil, and a UV/VIS variable wavelength detector. All wetted parts were constructed of non-metallic materials, including polyetherether ketone (PEEK). A Dionex CG-5 guard column and

CS-5 transition metal analysis column (4 mm ID, 25.4 cm packing length) were used to profile the transition metal ions in the sample. The UV/VIS detector was connected to an AST-286 PC equipped with Peaksimple II 19-bit interface board and software (SRI Instruments).

Prior to analysis, 0.5 mL of sample was added to 0.5 mL of 20.5 mg/L cobalt (Co^{+2}) in 1 wt % HNO_3. The Co^{+2} served as an internal standard. A 100 µL aliquot of the solution (Cd^{+2} plus Co^{+2} as the internal standard) was injected into the IC system and separated by the CS-5 column at 25 °C using 0.07 M oxalic acid as the eluent at a constant flowrate of 1.00 mL/min. The eluent was adjusted to pH 4.8 with lithium hydroxide monohydrate (0.095 M). The separated metal ions were chelated with 4-(2-pyridylazo) resorcinol monosodium salt monohydrate (PAR) to form a chromophore in the PAR post column reaction coil, and then profiled by the UV/VIS detector at an absorbance of 520 nm. The retention times for Cd^{+2} and Co^{+2} (the internal standard) were 5.8 min and 7.3 min respectively. The metal ion peaks were integrated, and the concentration of Cd^{+2} was determined by the internal standard method.

2.3 Results and Discussion

2.3.1 Physical Properties of Porous Chitosan Beads

The physical properties of the chitosan adsorbents, including diameter, BET surface area, solubility, and crushing strength are summarized in Table 2.3.

As shown in Table 2.3, the combination of N-acylation and crosslinking resulted in the highest internal surface area for the chitosan beads. The average internal surface area of the N-acylated chitosan gel beads crosslinked with 2.5 wt % glutaric dialdehyde was 223.6 m^2/g after freeze drying, versus 192.4 m^2/g for nonacylated chitosan beads crosslinked and freeze dried under the same conditions. The average internal surface area of uncrosslinked N-acylated chitosan beads was only 42.6 m^2/g, showing clearly that crosslinking was required to impart a high internal surface area to the bead. However, heterogeneous crosslinking of the chitosan powder reduced the internal surface area from 15.9 m^2/g to only 1.9 m^2/g, indicating that only heterogeneous crosslinking of the chitosan gel bead followed by freeze drying improved the final internal surface area. Therefore, N-acylation, bead casting, crosslinking, and freeze drying steps must be combined to maximize the internal surface area of the chitosan adsorbent.

The material properties of the N-acylated chitosan beads were significantly affected by crosslinking with glutaric dialdehyde. The concentration of glutaric dialdehyde in the crosslinking bath was the most critical variable for the crosslinking process. Figure 2.4 shows the effect of the glutaric dialdehyde concentration in the crosslinking bath on the internal surface area and acid solubility of the 3 mm N-acylated chitosan beads. The internal surface area of the crosslinked N-acylated chitosan beads increased as the concentration of glutaric dialdehyde in the crosslinking bath increased from 0.125 to 2.5 wt %. However, the internal surface area decreased slightly when the glutaric dialdehyde concentration was increased to 5.0 wt %.

Table 2.3 Summary of physical properties for selected chitosan adsorbent preparations

Chitosan Adsorbent	Mean Particle Diameter (mm)	Magnetite Content (wt %)	N_2-BET Surface Area[(a)] (m^2/g)	Acid Solubility (wt %)	Differential Crushing Strength (psi)
Uncrosslinked Chitosan Powder	< 0.3	0.0	15.9	99.3	N/A
Crosslinked Chitosan Powder	< 0.3	0.0	1.9	12.4	N/A
Uncrosslinked Chitosan Beads	3.3 ± 0.3	13.2	60.1 ± 7.7 (n = 2)	99.0	16.4
Crosslinked Chitosan Beads	3.2 ± 0.1	12.2	192.4 ± 20.7 (n = 3)	4.6	4.8
N-acylated Chitosan Beads	3.3 ± 0.2	13.8	42.6 ± 12.9 (n = 4)	96.5	16.4
N-acylated Crosslinked Beads	3.2 ± 0.1	13.8	223.6 ± 10.6 (n = 3)	0.3	2.3

Notes (a) average values and standard deviations reported for "n" repeat batch preparations

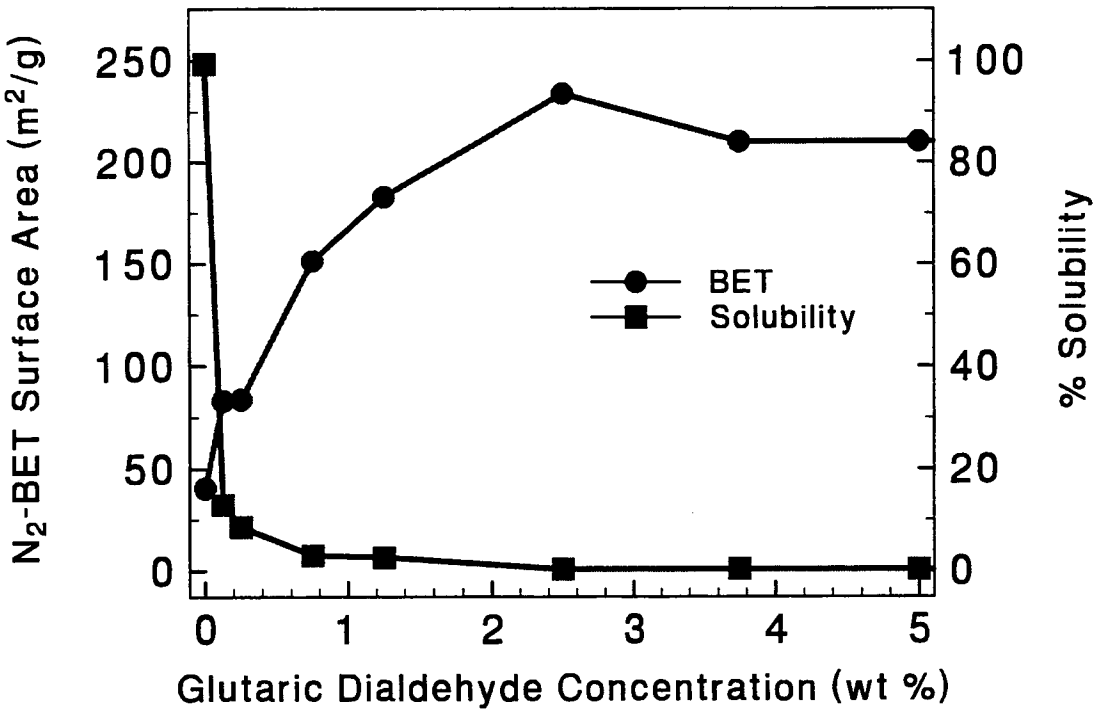

Figure 2.4 Effect of glutaric dialdehyde concentration in the crosslinking bath on internal surface area and acid solubility for N-acylated chitosan beads

Crosslinking also significantly reduced the solubility of chitosan in dilute acid. Chitosan adsorbents that were not crosslinked were readily soluble. The solubility of chitosan adsorbents was determined by measuring the percentage of chitosan that did not dissolve in 1 M acetic acid solution (pH 2.36) after 24 hours at room temperature. On average, 96.5 % of the chitosan in the uncrosslinked N-acylated chitosan beads dissolved in the acetic acid solution after 24 hours. The solubility of the crosslinked N-acylated

chitosan beads decreased drastically from 96.5 % to 0.3 % as the glutaric dialdehyde concentration in the crosslinking bath increased to 2.5 wt % (Figure 2.5).

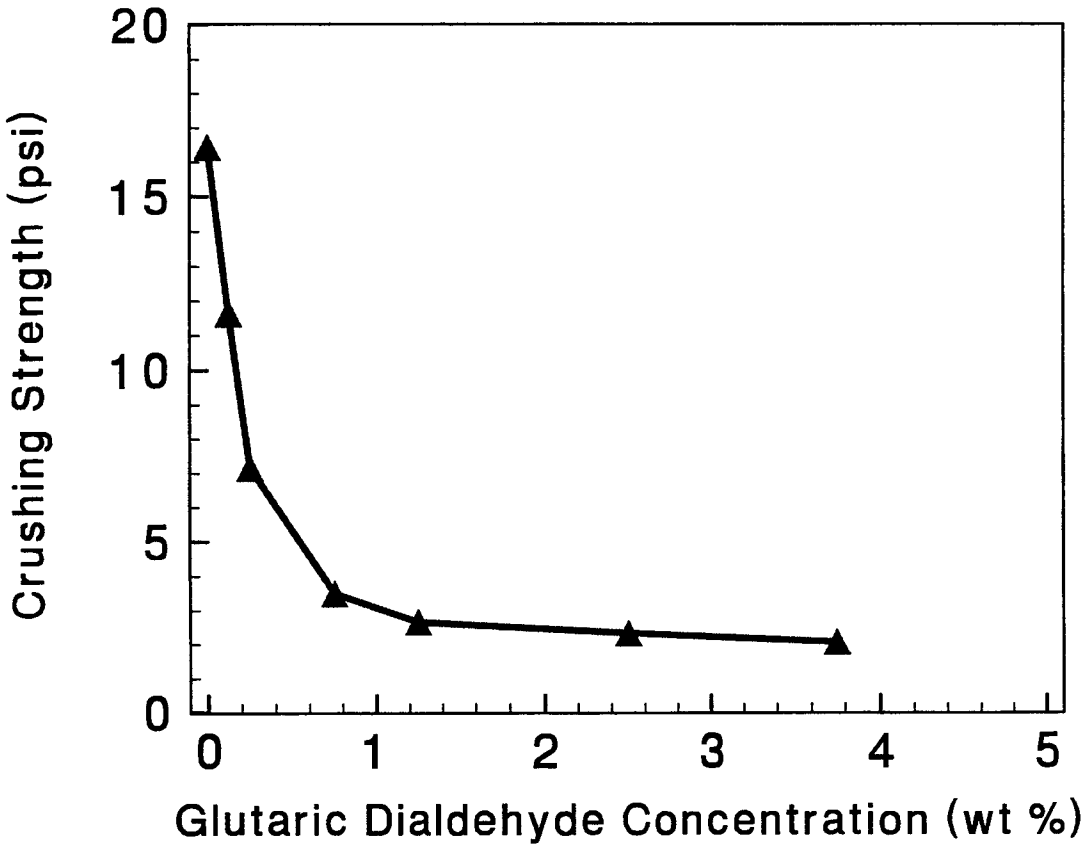

Figure 2.5 Effect of glutaric dialdehyde concentration in the crosslinking bath on the crushing strength of the N-acylated chitosan beads

The type of the chitosan adsorbent used for crosslinking also affected the acid solubility. N-acylated, crosslinked chitosan beads had the lowest solubility of 0.3 wt %, compared to

4.6 wt % for the nonacylated crosslinked chitosan beads, and 12.4 wt % for the crosslinked chitosan powder (Table 2.3). Apparently, the hydrocarbon chains on N-acylated, crosslinked chitosan beads increased the hydrophobicity of the biopolymer and hence helped to reduce the acid solubility. However, N-acylation alone was not successful in reducing acid solubility (Table 2.3).

The effect of glutaric dialdehyde concentration in the crosslinking bath on the crushing strength of N-acylated chitosan beads is presented in Figure 2.5. Crushing strength measurements were performed only on the final freeze-dried chitosan beads, not the chitosan gel beads before freeze drying. The uncrosslinked N-acylated chitosan bead had the highest crushing strength, 16.4 psi. The differential crushing strength of N-acylated chitosan beads decreased as the glutaric dialdehyde concentration in the crosslinking bath increased from 0.125 wt % to 2.5 wt %, and then leveled off at 3.75 wt %. The differential crushing strength of the N-acylated chitosan bead crosslinked in 3.75 wt % glutaric dialdehyde solution was 2.0 psi, 8 times smaller than the uncrosslinked N-acylated chitosan beads. N-acylation of the chitosan bead without crosslinking did not have a significant effect on crushing strength (Table 2.3).

Crosslinking may have reduced the crushing strength of bead by the shifting the void fraction from macropores to mesopores as the internal surface area increased. Crosslinking may have also rendered the biopolymer itself less elastic to compression forces. In particular, the rigid double bond between the dialdehyde groups and amine groups for the crosslinked chitosan may have reduced the elasticity of the linear chitosan chain and disrupted the hydrogen bonding network between the chitosan chains, making the material more brittle.

In summary, crosslinking of chitosan beads between the dialdehyde group (-CHO) on glutaric dialdehyde and amine group ($-NH_2$) on chitosan increased the internal surface area, reduced the acid solubility, and reduced the crushing strength. However, the internal surface area, acid solubility, and crushing strength of beads leveled off at high concentrations (2.5 wt %) of glutaric dialdehyde in the crosslinking bath. Apparently, at high glutaric dialdehyde concentrations, a significant fraction of the amine groups near the outer surface of the bead were crosslinked. This highly crosslinked outer shell most likely determined the final material properties of the chitosan bead. The consumption of glutaric dialdehyde in the crosslinking bath was not measured, and so the true extent of crosslinking in this outer shell is not known. Conditions of bead casting, N-acylation, and crosslinking must ultimately be optimized to synthesize chitosan beads of desired internal surface area, stability in acid solution, and crushing strength.

2.3.2 Cadmium Ion Adsorption Isotherms

Adsorption isotherms for cadmium ions on chitosan beads and chitosan powder were obtained at pH 6.5 and 25 °C. The effects of background sodium ion concentration, crosslinking, and N-acylation on the adsorption isotherms were considered.

The cadmium adsorption isotherms for nonacylated, crosslinked chitosan beads in background concentrations of $NaNO_3$ ranging from 0 to 150 mM are shown in Figure 2.6. The cadmium uptake of nonacylated, crosslinked chitosan beads was not affected the presence of sodium ions at 50 and 150 mM over the cadmium ion concentrations

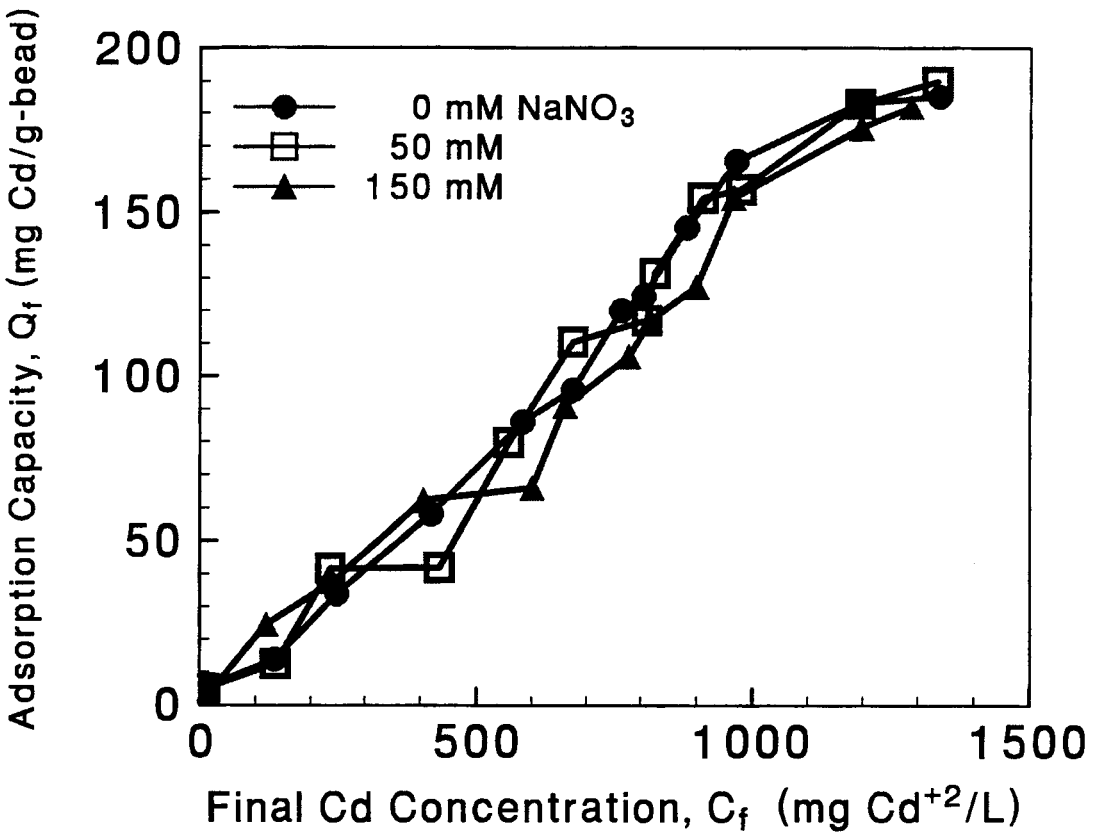

Figure 2.6 Effect of background $NaNO_3$concentration on the cadmium adsorption isotherm for nonacylated, crosslinked chitosan beads

ranging from 5 to 1500 mg/L. The effect of alkali and alkaline earth metal ions on transition metal adsorption capacity has not been investigated thoroughly, especially for Cd^{+2} binding on chitosan. Jha et al. (1988) showed that the presence of 5 mM Ca^{+2} decreased the Cd^{+2} adsorption rate on chitosan powder during the first 24 hours of adsorption. After 24 hours, the adsorption capacity decreased only 7% at cadmium ion concentrations ranging from 1 to 10 mg/L. Muzzarellii and Tubertini (1969) showed that the presence of sodium ions in seawater did not affect the adsorption capacity of

transition metal ions on chitosan, but data were obtained at only one transition metal ion concentration of 0.044 mM.

The results show that sodium cations do not hinder the chelation of Cd^{+2} ions with the amine groups on chitosan. The electron orbital configuration of Na^{+}, a group IA alkali metal, has only s and p electrons in its outer shell. In contrast, Cd^{+2} possesses s, p, and unsaturated d electron orbitals in its outer shell. Thus, Cd^{+2} selectively binds to chitosan by the chelation of unfilled d electron orbitals on the Cd^{+2} ion with the p orbital on the amine group, similar to the Co^{+2} binding on ammonia ligands (Huheey, 1983). Hayes and Leckie (1987) presented that Cd^{+2} ion adsorption onto goethite is relatively unaffected by changing the ionic strength of $NaNO_3$ solution. They also suggested that Cd^{+2} adsorption as a function of ionic strength is best modeled as an inner-sphere surface reaction.

The effect of crosslinking on the cadmium adsorption isotherms for the nonacylated chitosan beads is shown in Figure 2.7. Both of the isotherms have a similar stepped shape. The behavior of the stepped shape of the adsorption isotherm was discussed earlier by Rorrer et al. (1993). The uncrosslinked chitosan beads have a slightly higher adsorption capacity than the crosslinked chitosan beads at final cadmium ion concentrations ranging from 100 to 500 mg/L. The adsorption capacity did not change significantly between the uncrosslinked and crosslinked nonacylated chitosan beads at final cadmium concentrations ranging from 600 to 1500 mg/L. These results are surprising since the internal surface area of the uncrosslinked chitosan beads (60.1 m^2/g) was significantly lower than the crosslinked chitosan beads (192.4 m^2/g). Apparently, the cadmium was not loaded uniformly in the bead. Therefore, other material properties,

such as the pore size distribution or the structure of crosslinked outer shell, may have also affected the adsorption capacity. In particular, the highly-crosslinked outer shell could have hindered diffusion of Cd^{+2} ions into the center of the bead. A diffusion mechanism which further suggests that the metal would be preferentially loaded near the outer surface of the porous bead is described by Rorrer et al. (1993).

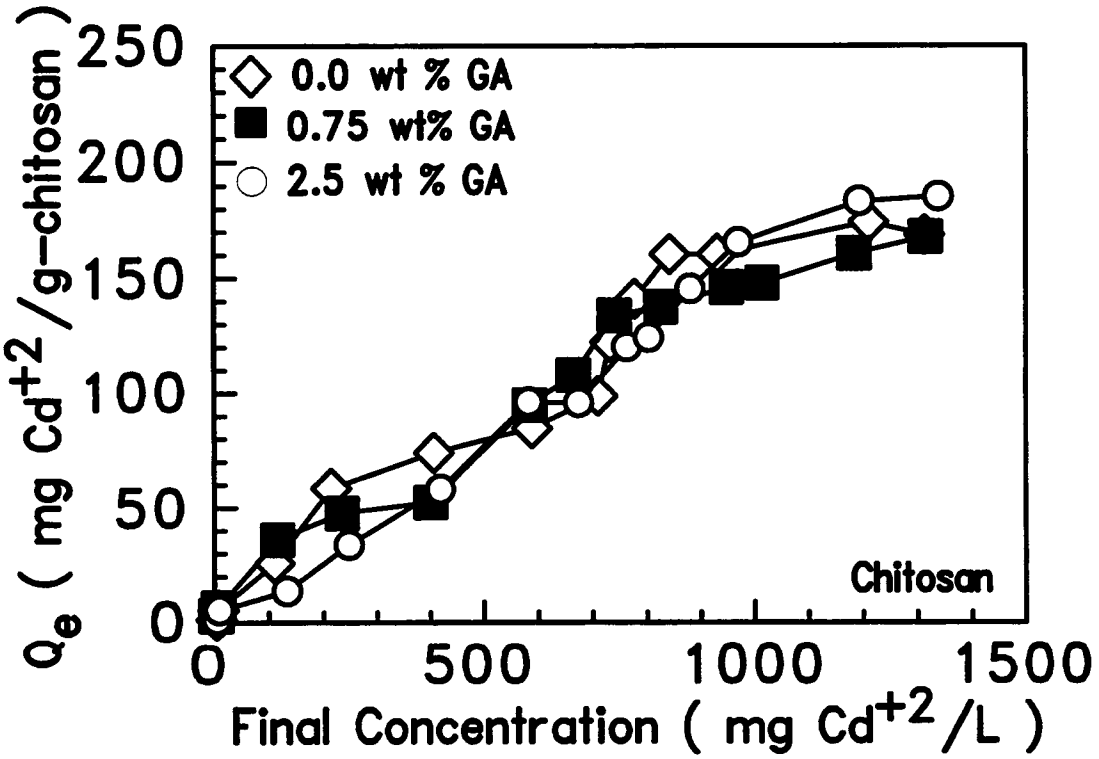

Figure 2.7 Effect of crosslinking on the cadmium ion adsorption isotherm for nonacylated chitosan beads

The effect of crosslinking on the cadmium adsorption isotherms for the finely-ground nonacylated chitosan powder is presented in Figure 2.8. Although the chitosan powder was sieved below 300 μm, a significant fraction of the particles were around 100 μm. At saturation, the uncrosslinked chitosan powder had twice the cadmium adsorption capacity of the crosslinked chitosan powder. Yang and Zall (1984) proposed that the overall adsorption rate of metal ions was controlled by the diffusion rate into the chitosan powder. Apparently, the majority of the adsorbed cadmium was concentrated near the surface of the chitosan powder. The reduction in adsorption capacity for the nonacylated crosslinked chitosan powder probably resulted from the reduction of exposed amine sites near the surface as the result of the heterogeneous crosslinking process. To support this conclusion, the BET surface area of the uncrosslinked chitosan powder was 15.9 m^2/g versus only 1.91 m^2/g for the crosslinked chitosan powder.

Masri et al. (1978) suggested that the adsorption capacity of transition metal ions on chitosan powder was reduced by a heterogeneous crosslinking process with glutaric dialdehyde. In contrast, Koyama and Taniguchi (1986) homogeneously crosslinked chitosan with glutaric dialdehyde in acetic acid solution and claimed that the adsorption capacity for Cu^{+2} increased as result of the crosslinking process. Specifically, they proposed that the homogeneous crosslinking chitosan at an initial -CHO/-NH_2 ratio of 0.7 increased the hydrophilicity of chitosan and improved the accessibility of metal ions to amine groups by disruption of the crystalline structure. In this study, when the chitosan beads were synthesized, both the porosity of the bead and the crosslinking reaction affected the number of readily accessible amine sites. The amine groups consumed by

crosslinking were presumably compensated for by an increase in the number amine sites exposed by the increased internal surface area. However, the true number of exposed amine sites within the porous matrix could not be measured directly. Direct titration of the exposed basic amine sites with acid was not possible as the hydrogen ions would penetrate into the nonporous regions of the chitosan bead and swell the biopolymer.

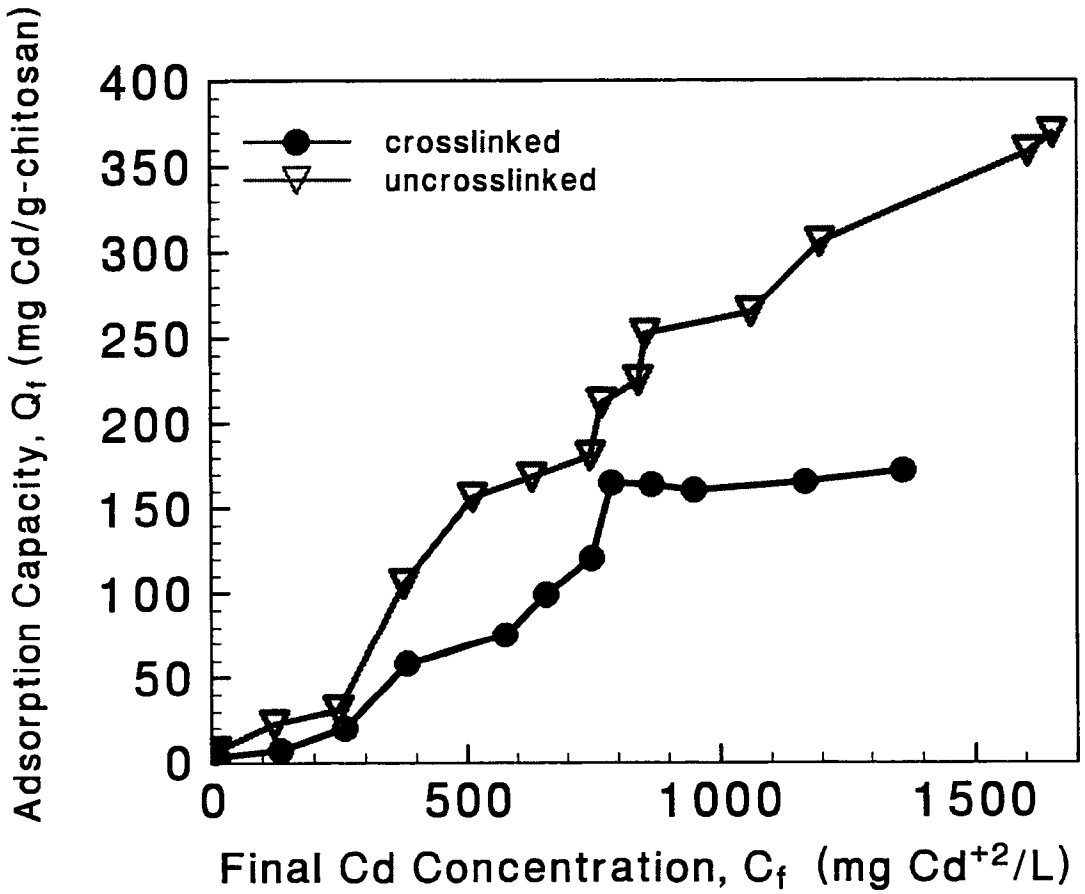

Figure 2.8 Effect of crosslinking on the cadmium ion adsorption isotherm for nonacylated chitosan powder

The effect crosslinking on the cadmium adsorption isotherms for the N-acylated chitosan beads is shown in Figure 2.9. There was no significant difference in adsorption capacity between the N-acylated chitosan beads at final cadmium ion concentrations

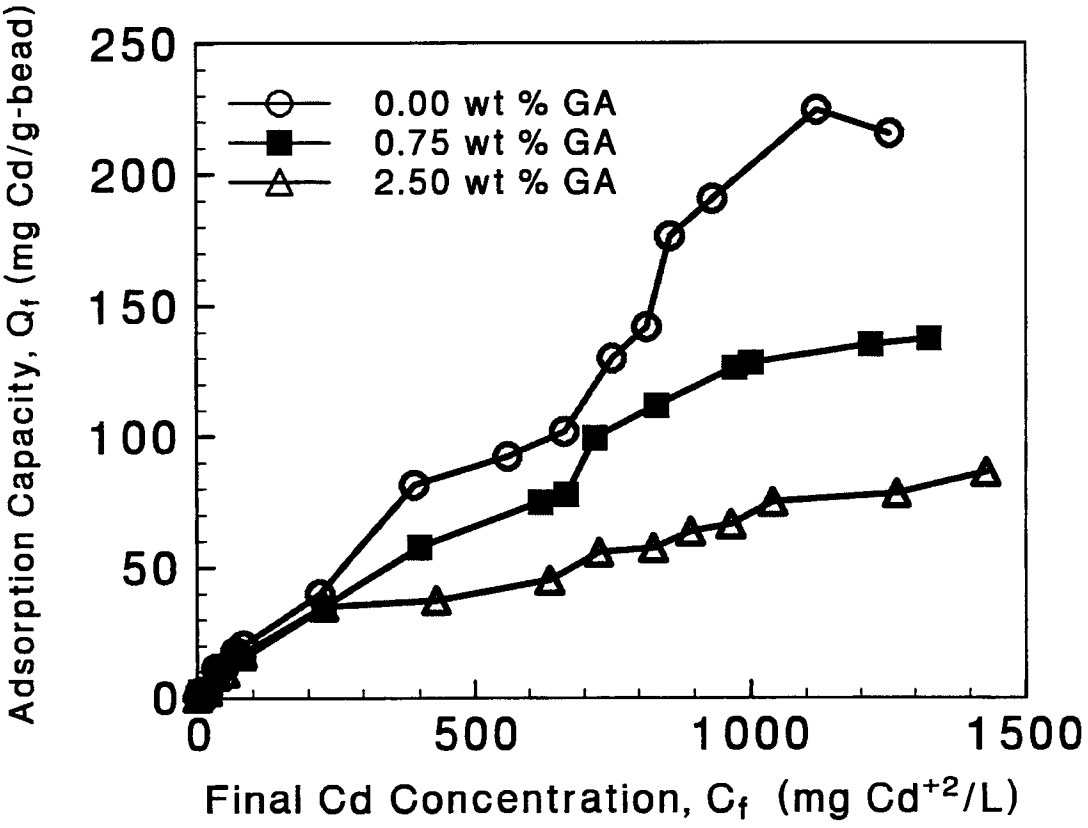

Figure 2.9 Effect of glutaric dialdehyde concentration in the crosslinking bath on the cadmium ion adsorption isotherm for N-acylated chitosan beads

ranging from 4 to 200 mg/L. However, the difference in adsorption capacity became significant when the final Cd^{+2} ion concentration was above 700 mg/L. In particular, the slope of the adsorption isotherm decreased drastically when the N-acylated chitosan bead

was crosslinked at higher glutaric dialdehyde concentrations. This reduction in adsorption capacity may have resulted from the combined stearic hindrance of amine, alkyl, and aldehyde functional groups to the binding of cadmium ions to exposed amine sites within the chitosan bead.

N-acylation without crosslinking improved adsorption capacity for Cd^{+2} on the chitosan beads at concentrations exceeding 1000 mg Cd^{+2}/L. The saturation adsorption capacity was 216 mg Cd^{+2}/L for the N-acylated, uncrosslinked chitosan beads, versus 169 mg Cd^{+2}/L for nonacylated, uncrosslinked chitosan beads, an increase of about 28%.

Low Cd^{+2} concentration adsorption isotherms over the range of 4 to 80 mg Cd^{+2}/L are presented in Figure 2.10. The nonacylated, uncrosslinked chitosan beads had the highest adsorption capacity. The adsorption capacity of the N-acylated, crosslinked chitosan beads were comparable with one another. The binding of Cd^{+2} on the N-acylated, crosslinked chitosan beads exhibited type V isotherm behavior, suggesting weaker adsorbate/adsorbent interactions in mesoporous solids (Gregg and King, 1982). At low Cd^{+2} concentrations, the driving force for diffusion of Cd^{+2} ions into the porous bead was low. Thus, the binding of Cd^{+2} to the chitosan may have been localized near the outer surface of bead. The nonacylated, uncrosslinked chitosan beads had the highest number of potential external adsorption sites near the surface. In contrast, the number exposed amine sites on the N-acylated, crosslinked chitosan bead were decreased by N-acylation and crosslinking reactions.

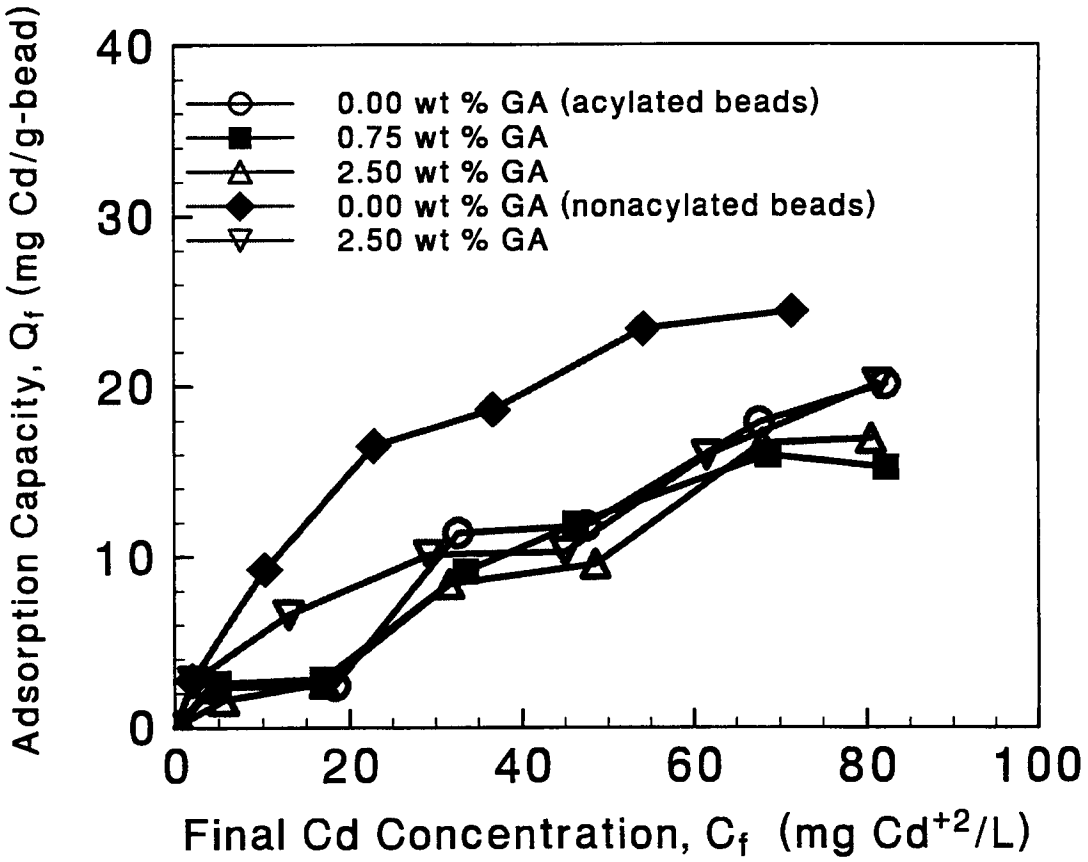

Figure 2.10 Low concentration adsorption isotherms (4-80 mg Cd^{+2}/L)

Isotherm data over the low concentration range of 4 to 80 mg Cd^{+2}/L were fitted to the Freundlich isotherm, given by

$$Q_e = K C_e^{1/n} \qquad (2\text{-}2)$$

where K and n are adjustable parameters. The parameter K is a measure of the binding strength, whereas 1/n is a measure of distribution of adsorption energies (Sposito, 1984). The value for n is also an indicator of the distribution of bond strengths. When $n > 1$, then the bonding energy decreases with increasing surface concentration. Log-log plots

of Q_e vs. C_e data have slope 1/n and intercept log K. Values for K and n are given in Table 2.4. The data fitted the Freundlich isotherm model reasonably well with 3 of the 5 isotherms having an r^2 value of 0.95 or above. N-acylation of chitosan reduced the values for both K and n. This analysis suggests that N-acylation decreases the adsorption capacity and binding strength while promoting monolayer coverage of the adsorbed metal on the exposed surfaces of the adsorbent at low Cd^{+2} concentrations. It is interesting to note that the n values for N-acylated chitosan beads are near 1.0 while the n values for nonacylated chitosan beads are close to 2.0. The difference in the n value may suggest that the N-acylated chitosan beads exhibit a more uniform energy distribution of active sites for cadmium chelation reaction than the nonacylated chitosan beads.

Table 2.4 Freundlich parameters for low-concentration Cd^{+2} isotherm data

Adsorbent Preparation	K	n	r^2
Uncrosslinked Chitosan Beads	2.01	1.61	0.98
Crosslinked Chitosan Beads (2.5 wt% GA in crosslinking bath)	1.76	1.97	0.97
N-acylated, Uncrosslinked Chitosan Beads	0.59	1.30	0.81
N-acylated, Crosslinked Chitosan Beads (0.75 wt% GA in crosslinking bath)	0.61	1.35	0.87
N-acylated, Crosslinked Chitosan Beads (2.5 wt% GA in crosslinking bath)	0.26	1.06	0.95

2.4 Summary and Conclusions

Glucosamine biopolymers such as chitosan are a promising new class of adsorbents for heavy metal ion separations. However, the chitosan biopolymer must be engineered into a form which exhibits high adsorption capacity and stability in low-pH chemical environments. To address these needs, 3 mm porous chitosan beads were fabricated using an aqueous phase inversion technique to cast gel beads followed by freeze drying of the gel beads to remove water without collapsing the pore structure. In the attempt to simultaneously improve material properties and cadmium ion adsorption capacity, two chemical modifications to the chitosan beads were considered. First, before bead casting, C_9 alkyl side chains were added to chitosan at a 7% degree of substitution by homogeneous N-acylation with nonanoyl chloride. Second, the chitosan gel bead was heterogeneously reacted with the bifunctional reagent glutaric dialdehyde to form a highly crosslinked outer shell. Both acylation and crosslinking attempted to impart hydrophobicity to the biopolymer and increase the spacing between biopolymer chains, in order to reduce solubility and improve access of transition metal ions to amine adsorption sites.

The combination of acylation, bead casting, crosslinking, and freeze-drying steps produced a highly porous chitosan bead which was insoluble in 1 M acetic acid solution (pH 2.4) and possessed an internal surface area of 224 m^2/g. The concentration of glutaric dialdehyde in the crosslinking bath was the most important process variable for determining the material properties. N-acylation and crosslinking also effected the adsorption capacity for cadmium ions. N-acylation of uncrosslinked chitosan beads

improved the saturation adsorption capacity from 169 to 216 mg Cd^{+2}/g-bead. However, crosslinking of the N-acylated chitosan beads reduced the saturation adsorption capacity down to 136 and 86 mg Cd^{+2}/L when the glutaric dialdehyde concentration in the crosslinking bath was increased to 0.75 wt % and 2.5 wt % respectively. In contrast, at low concentrations of 4 to 80 mg Cd^{+2}/L, the adsorption capacities were comparable. Analysis of the Freundlich isotherm parameters for nonacylated and N-acylated chitosan beads inferred that N-acylation decreased the adsorption capacity and binding strength for Cd^{+2} while promoting monolayer coverage of the adsorbed metal on exposed surfaces of the adsorbent. All trends suggested that the cadmium metal was preferentially loaded near the outer surface of bead, as there was no clear relationship between internal surface area and the adsorption capacity.

This paper has shown that chitosan is a facile biopolymer-supported reagent for chemical modifications leading to improved material properties. However, the relationship between the material properties and the cadmium ion adsorption capacity is complex. Future studies will attempt to more clearly define this relationship by relating chemical microstructure of the bead to the distribution of adsorbed metal within the bead.

CHAPTER 3

GLUTARIC DIALDEHYDE CROSSLINKING MECHANISM AND ITS EFFECT ON CADMIUM ADSORPTION CAPACITY FOR CHITOSAN BEADS

Tzu-Yang Hsien and Gregory L. Rorrer*

Department of Chemical Engineering
Oregon State University
Corvallis, Oregon 97331

(tel) 503-737-3370, (fax) 503-737-4600

* corresponding author

3.1 Introduction

The extent of glutaric dialdehyde crosslinking on chitosan gel beads and its effect on the cadmium adsorption capacity have not been thoroughly investigated. In this work, the crosslinking kinetics were characterized, and the overall extent of crosslinking (X_T) was correlated to the saturation cadmium ion adsorption capacity. The possible roles of crosslinking time, initial glutaric dialdehyde concentration, pH, and glutaric dialdehyde polymer (PGA) formation on the crosslinking process are examined. These insights are used to help validate the modified shrinking core model for crosslinking process.

3.2 Materials and Methods

3.2.1 Gel Bead Synthesis

The synthesis of chitosan gel beads, including acylation and gel bead casting, was described in previous studies (Rorrer et al., 1993, Hsien and Rorrer, 1995). First, 5 wt % chitosan solution (x_B) was prepared by dissolving chitosan powder (Vansen Chemical Company, Redmond, WA) into a 0.68 M acetic acid solution and mixing for 72 hours. The chitosan solution was then delivered by a peristaltic pump to a spinnerette. The spinnerette formed spherical particles, which dropped into a 2.0 M aqueous sodium hydroxide precipitation bath and coagulated to form gel beads. To prepare 7 % N-acylated chitosan, 70 mL of 5 wt % chitosan solution was acylated with 0.28 g of nonannoyl chloride ($(CH_2)_7CH_3COCl$, Aldrich Chemical Company, Milwaukee, WI) described by Hsien and Rorrer (1995). The same gel bead casting procedures were than

followed, using 1.0 M aqueous methanolic sodium hydroxide solution (50 % v/v) as the precipitation bath. After partial N-acylation, the free amine group content was estimated as 5.769 mmole NH_2/g chitosan (Y_B). The density for the 7 % N-acylated gel beads was measured by volumetric displacement. The density (ρ_b) of the 7 % N-acylated gel beads was 1.06 ± 0.03 g/cm^3 (n=2).

3.2.2 Crosslinking

Crosslinking of Gel Beads. The chitosan gel beads were crosslinked with aqueous glutaric dialdehyde (GA, $COH(CH_2)_3COH$, Aldrich Chemical Company, Milwaukee, WI). In the crosslinking bath, the gel beads were added to an aqueous glutaric dialdehyde solution at a ratio of 6.4 g of gel beads (m_b) to 9.6 mL of crosslinking bath solution (V_c) and mixed on an incubated orbital shaker at 120 rpm and 27 °C. The initial glutaric dialdehyde concentration in the crosslinking bath (C_{A0}) ranged from 0.125 to 5.0 wt %. The initial molar ratio of glutaric dialdehyde to free -NH_2 groups is given in Table 3.1. The glutaric dialdehyde solution was filtered from the gel beads after crosslinking times ranging from 1 to 48 hours. The concentration of glutaric dialdehyde solution was measured by gas chromatography, and the retention of the crosslinked reagent in the gel beads was measured gravimetrically. Alternately, if only the glutaric dialdehyde concentration in the crosslinking bath was desired, than a small sample aliquot (0.6 μL) was withdrawn directly from the crosslinking bath at desired time intervals over the crosslinking process.

GC Analysis of Glutaric Dialdehyde in Crosslinking Bath. The glutaric dialdehyde concentration in the crosslinking bath (C_A) was determined by a gas chromatography (GC) using Hewlett Packard 5890 Series II GC system. Specifically, 0.6 μL of sample solution was injected into the GC system at an injector temperature of 150 °C, and separated on a HP-FFAP column (10 m x 0.53 mm x 1.0 μm) at 100 °C. The existing sample vapors were detected by a Flame Ionization Detector (FID) at 155 °C. The carrier gas was helium at 10 mL/min. The retention time of glutaric dialdehyde was 2.7 min under these analysis conditions. The value for X_T, defined as the total moles of glutaric dialdehyde consumed per total mole of amine groups in the gel beads, was determined at a given measured value for C_A by equation (3-3).

Stability of Glutaric Dialdehyde. The pH of different aqueous glutaric dialdehyde concentrations was measured by a pH electrode (Table 3.1). The stability of the aqueous glutaric dialdehyde solution during the crosslinking process was tested by mixing 9.6 mL of 2.5 wt % glutaric dialdehyde (GA) solution on an orbital shaker at 120 rpm and 27°C for 48 hours. The glutaric dialdehyde concentration was constant over the 48 hours of incubation time, demonstrating that the aqueous glutaric dialdehyde solution was stable during the crosslinking process.

Gravimetric Measurement of Crosslinking. After 48 hours of crosslinking, the chitosan gel beads were filtered from the glutaric dialdehyde solution, air-dried at room temperature for 24 hours, weighed and then oven-dried at 85 °C for 4 hours and weighed again to ensure that the final weight of the crosslinked product (w_A) was obtained. As a

control, the weight of the uncrosslinked gel beads was also determined by soaking 6.4 g of gel beads in 9.6 mL distilled water for 48 hours, followed by filtration and drying as

Table 3.1 Initial pH value and GA/-NH_2 ratio in the crosslinking bath

C_{A0} (g GA/100 mL)	Initial pH	Initial GA/-NH_2 mole ratio	
		N-acylated Beads	Nonacylated Beads
0.125	4.163	0.065	0.047
0.25	4.069	0.130	0.093
0.75	3.676	0.390	0.279
2.50	3.402	1.300	0.930
5.00	3.246	2.600	1.861

described above (w_{A0}). The retention of glutaric dialdehyde in the bead after drying, expressed as mole of glutaric dialdehyde crosslinked per total mole of NH_2 groups in the gel bead, was estimated by

$$X_R = \frac{(w_{A0} - w_A)}{m_b x_B Y_B M_A} \qquad (3\text{-}1)$$

where M_A is the mass of crosslink formed per mole of reacted glutaric dialdehyde.

3.2.3 Adsorption Capacity

Batch Adsorption Measurements. The cadmium solution was prepared by dissolving 98 % pure cadmium nitrate ($Cd(NO_3)_2$, Aldrich Chemical Company, Milwaukee, WI) in deionized distilled water. The initial cadmium ion concentration was 2000 mg Cd^{+2}/L. The cadmium adsorption process was conducted in a well mixed batch

system until equilibrium was reached. Specifically, 0.79 g of the gel beads (0.040 g chitosan basis) were contacted with 40 mL of cadmium nitrate solution within a 125 mL Erlenmeyer flask and agitated at 120 rpm on an orbital shaker at 25 °C for 60 hours. The solution was filtered from the gel beads and analyzed for cadmium ion concentration by ion chromatography (IC). The cadmium adsorption capacity measurements for the freeze-dried chitosan beads crosslinked at different initial glutaric dialdehyde concentrations were also obtained. Specifically, 40 mg of crosslinked, freeze-dried chitosan beads were contacted with a 2000 mg Cd^{+2}/L solution at 25 °C for 60 hours.

The cadmium ion concentration was measured by ion chromatography as previously described (Hsien & Rorrer, 1995) using a Dionex CS-5 column. The final cadmium loading in the gel beads was determined by

$$Q_f = \frac{(C_o - C_f)\,V}{m_b\ x_B} \tag{3-2}$$

where C_o is the initial cadmium concentration (mg Cd^{+2}/L), C_f is the final cadmium concentration (mg Cd^{+2}/L), Q_f is the final cadmium loading on the gel beads (mg Cd^{+2}/g chitosan), and V is the volume of cadmium solution (L).

3.2.4 EDAX Sample Preparation

The cadmium adsorption process was also followed by Energy Dispersive X-Ray/Scanning Electron Microscopy analysis (EDAX/SEM). To prepare the cadmium-absorbed sample, a 40 mg of freeze-dried nonacylated chitosan beads was contacted with 40 mL of cadmium nitrate solution at an initial concentration of 1026 mg Cd^{+2}/L in a 125

mL Erlenmeyer flask and agitated for 60 hours at 25 °C. After 60 hours of adsorption, the beads were filtered under vacuum until no water remained at the outer surface, and then immediately immersed in liquid nitrogen. The frozen beads were fractured open by a razor blade. The exposed cross sectional surface was not smooth. The freeze-fractured chitosan beads were then air dried at 25°C for 48 hours to remove the water remaining in the pores of the bead.

To prepare the fractured sample for EDAX/SEM analysis, the exposed surface was sputter coated with carbon to drain the electrostatic charges from the sample. The carbon coated cross sectional surface was scanned by a electron beam at a beam current of 100 +/- 5 microamperes at 20 kilovolts, using a pulse sharping time constant of 8 microseconds and a total acquisition time of 120 seconds. The analysis was performed on a Kevex 7077 XES, SN 2973 EDAX/SEM system with a spectrometer resolution of 10 eV per channel.

3.2.5 Modified Shrinking Core Model for Diffusivity Estimation

The heterogeneous crosslinking of the spherical chitosan gel beads with the bifunctional crosslinking agent glutaraldehyde is carried out in a well mixed batch reactor under isothermal conditions at constant volume. The depletion of glutaraldehyde in the crosslinking bath is balanced by the formation of crosslinked chitosan within the gel bead as the glutaraldehyde monomer diffuses into the chitosan gel and reacts between available amine groups on adjacent chitosan chains to form the crosslink assembly.

Therefore, the first goal of the model development is to develop a system of material balance equations which will predict the extent of chitosan crosslinking within the gel bead and the depletion of glutaraldehyde in the crosslinking bath as a function of time. The second goal of the model development is develop a model equation, called the modified shrinking core model, which can be used to estimate the effective diffusivity of glutaraldehyde into the crosslinked layer within the gel bead given glutaraldehyde

$$(C_{AO} - C_A)\, V_C = X_T\, m_b\, x_B\, Y_B \qquad (3\text{-}3)$$

concentration (C_A) vs. time data in the crosslinking bath.

The overall material balance for glutaraldehyde in the batch crosslinking bath is The term X_T, which is defined as moles of glutaraldehyde consumed by the gel bead to the

$$X_T = \overline{X}\,\beta \qquad (3\text{-}4)$$

total moles of amine ($-NH_2$) groups within the chitosan gel bead, is related to the extent of crosslinking, (moles of $-NH_2$ crosslinked/total moles of $-NH_2$) by

In accordance with the shrinking core model, the crosslinked chitosan is found in an outer shell of the gel bead bounded by $r = R$ to $r = r_c$, where r_c represents the moving boundary between the crosslinked zone and the uncrosslinked zone. In this context, is also defined as

$$\overline{X} = 1 - \left[\frac{r_c}{R}\right]^3 \qquad (3\text{-}5)$$

Since the heterogeneous crosslinking process is unsteady state, both C_A and will change with time. Differentiation of equations (3-3) and (3-5) with respect to time yields

$$\frac{dC_A}{dt} = - \frac{d\overline{X}}{dt} \frac{m_b \; x_B \; Y_B \; \beta}{V_C} \tag{3-6}$$

$$\frac{d\overline{X}}{dt} = - \frac{3}{R^3} r_C^2 \frac{dr_C}{dt} \tag{3-7}$$

At any time t, the total glutaraldehyde uptake rate into "n" gel beads is balanced by the rate of depletion of glutaraldehyde in the crosslinking bath. Therefore

$$-4 \pi R^2 \; N_{AS} \; n = \frac{d(V_C \; C_A)}{dt} \tag{3-8}$$

If the flux of glutaraldehyde into the gel bead is limited by molecular diffusion of the glutaraldehyde monomer, then for a dilute system Fick's First Law defines N_{AS} as

$$N_{AS} = - D_{Ae} \frac{d\overline{C}_A}{dr}\Big|_{r=R} \tag{3-9}$$

In equation (3-8), the number of beads in the crosslinking bath (n) is estimated from macroscopic properties by

$$n = \frac{3 \; m_b}{4 \pi R^3 \; \rho_b} \tag{3-10}$$

Finally, by continuity through Fick's Second Law, N_{AS} is related to N_A by

$$R^2 \; N_{AS} = r^2 \; N_A \tag{3-11}$$

Combining equations (3-8) to (3-11) gives

$$\frac{dC_A}{dt} = \frac{3\ m_b\ D_{Ae}}{V_C\ R^3\ \rho_b}\ r^2\ \frac{d\overline{C}_A(r)}{dr} \tag{3-12}$$

Equation (3-12) relates the depletion of glutaraldehyde in the crosslinking bath to the diffusion limited concentration profile of glutaraldehyde within the crosslinked zone of the gel bead. The concentration profile $C_A(r)$ needs to be eliminated from equation (3-12). Under the pseudo steady state assumption, there is no accumulation of free glutaraldehyde within the crosslinked zone of the gel bead. Consequently, at a given instant in time, dC_A/dt is constant, and variables $_A$ and r in equation (3-12) can be separated. Furthermore, for a rapid crosslinking reaction at unreacted core boundary $r_{C,A}$ is zero. Therefore, the integral setup for equation (3-12) becomes

$$\int_{\overline{C}_{AS}}^{0} d\overline{C}_A = \frac{dC_A}{dt}\ \frac{V_C\ R^3\ \rho_b}{3\ m_b\ D_{Ae}}\ \int_R^{rc}\ \frac{dr}{r^2} \tag{3-13}$$

If external mass transfer resistances are negligible, then $C_{AS} = C_A$. Under this assumption, the evaluated integral for equation (3-13) is

$$\frac{dC_A}{dt} = \frac{-3\ m_b\ D_{Ae}\ C_A}{V_C\ R^3\ \rho_b \left[\frac{1}{r_C} - \frac{1}{R}\right]} \tag{3-14}$$

The depletion of glutaraldehyde in the crosslinking bath is related to crosslink formation through r_C. Equations (3-6), (3-7), and (3-14) are combined to give

$$r_C^2\ \frac{dr_C}{dt} = -\frac{D_{Ae}\ C_A}{x_B\ \rho_b\ Y_B\ \beta \left[\frac{1}{r_C} - \frac{1}{R}\right]} \tag{3-15}$$

$$1 - 3\left[\frac{r_C}{R}\right]^2 + 2\left[\frac{r_C}{R}\right]^3 = \frac{6\ D_{Ae}}{x_B\ \rho_b\ Y_B\ \beta\ R^2}\int_0^t C_A\ dt \qquad (3\text{-}16)$$

Separation of variables r_C and t and integration from $t = 0$, $r = R$, to $t = t$, $r = r_C$ gives

$$F(\overline{X}) = 1 - 3(1 - \overline{X})^{\frac{2}{3}} + 2(1 - \overline{X}) = \frac{6\ D_{Ae}}{x_B\ \rho_b\ Y_B\ \beta\ R^2}\int_0^t C_A\ dt \qquad (3\text{-}17)$$

In terms of defined in equation (3-5), equation (3-16) is re-written as

Using equation (3-17), the effective diffusion coefficient of glutaraldehyde through the crosslinked zone to reaction boundary r_C can be estimated from C_A vs. t data. First, at time t is calculated by equations (3-3) and (3-4) given the current value for C_A at time t. Second, the integral on the right hand side of equation (3-17) is numerically evaluated from C_A vs. t data from $t = 0$ to the current time t at which is determined. Finally, $F(\overline{X})$ in equation (3-17) is plotted vs $\int C_A\ dt$ to yield a straight line with slope $6\ D_{Ae} / x_B\ \rho_b\ Y_B\ \beta R^2$, from which D_{Ae} is determined.

Once D_{Ae} is estimated, C_A and can be predicted as a function of crosslinking time t at a given initial concentration C_{AO} by numerical integration of equations (3-6), (3-7) and (3-15) over t.

The prediction of r_C, C_A and as a function of crosslinking time t is accomplished by numerical integration. Specifically, rearrangement of equation (3-15) gives

$$\frac{dr_C}{dt} = - \frac{D_{Ae}\ C_A}{x_B\ \rho_b\ Y_B\ \beta \left[\frac{1}{r_C} - \frac{1}{R} \right] r_C^2} \tag{3-18}$$

Equation (3-18) contains C_A, the current concentration of glutaraldehyde in the crosslinking bath. Rearrangement of equation(3-3) relates C_A to $\overline{X}$ via

$$C_A = C_{AO} - \frac{\overline{X}\ \beta\ m_b\ x_B\ Y_B}{V_C} \tag{3-19}$$

Combination of equations (3-5), (3-18), and (3-19) yields a first-order ordinary differential equation explicitly in terms of r_C

$$\frac{dr_C}{dt} = - \frac{D_{Ae} \left[C_{AO} - \frac{\beta\ m_b\ x_B\ Y_B}{V_C} \left[1 - \left(\frac{r_C}{R} \right)^3 \right] \right]}{x_B\ \rho_b\ Y_B\ \beta \left[\frac{1}{r_C} - \frac{1}{R} \right] r_C^2} \tag{3-20}$$

Equation (3-19) is numerically integrated by the 4th order Runge-Kutta Method. Values for and C_A at r_C for a given time t are obtained by equations (3-5) and (3-19) respectively. In equation (3-20), a discontinuity exists at the initial condition $t = 0$, $r_C = R$. However, at very short times C_A approximates C_{AO}, and so the analytical solution for equation (3-18) is

$$1 - 3 \left[\frac{r_C}{R} \right]^2 + 2 \left[\frac{r_C}{R} \right]^3 = \frac{6\ D_{Ae}\ C_{AO}\ t}{x_B\ \rho_b\ Y_B\ \beta\ R^2} \tag{3-21}$$

Equation (3-21) is used to obtain a value for r_c a very small value for t, which is subsequently used as the initial condition for equation (3-20). The constant parameters C_{AO}, D_{Ae}, m_b, R, V_C, Y_B, β, ρ_b are all input parameters to the model.

3.3 Results

The crosslinking process affects the material properties and the cadmium adsorption capacity of the chitosan gel beads. In this present work, the crosslinking kinetics for both chitosan gel beads and N-acylated chitosan gel beads are determined as a function of initial glutaric dialdehyde concentration in the crosslinking bath. The effect of the extent of crosslinking on cadmium adsorption for the gel and freeze-dried beads is also considered. Finally, EDAX/SEM images for adsorbed cadmium within the crosslinked chitosan bead are presented in order to provide further insights on how crosslinking affects the cadmium ion adsorption process.

3.3.1 Crosslinking Kinetics

The overall extent of absorbed and reacted glutaric dialdehyde (X_T) for the 3 mm N-acylated chitosan gel beads is presented in Figure 3.1 (a) as a function of crosslinking time for an initial glutaric dialdehyde concentration of 0.75 wt % in the crosslinking bath. The pH profile in the crosslinking bath is also presented in Figure 3.1(a). The X_T and pH versus time profiles show a similar trend. Values for both X_T and pH leveled off after 12 hours. The pH value only increased slightly in the last 36 hours of crosslinking.

(a)

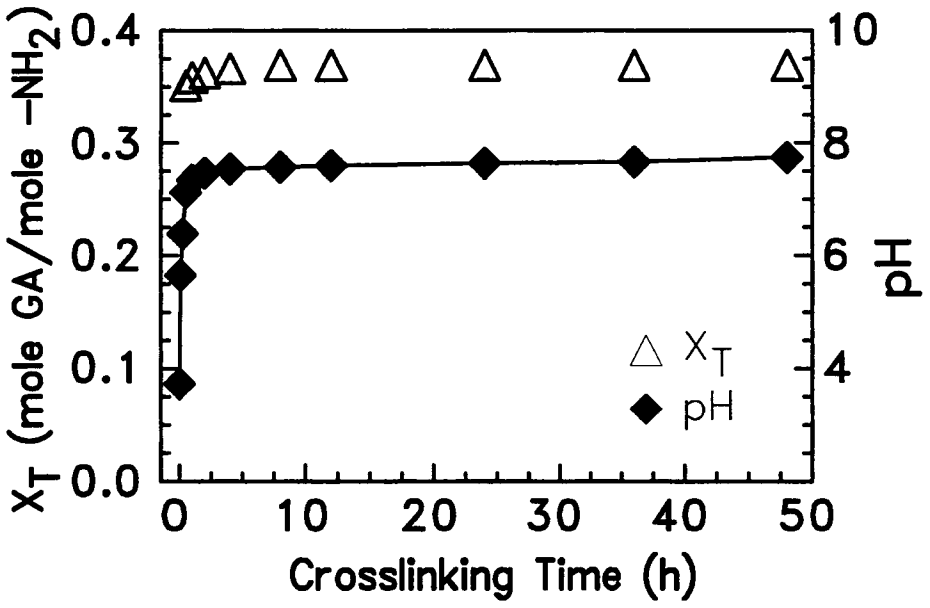

(b)

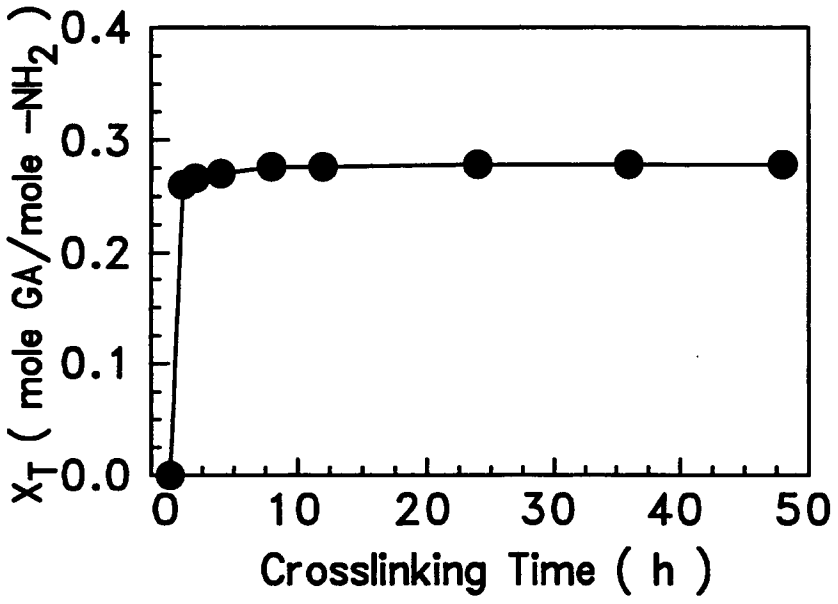

Figure 3.1 (a) X_T and pH profiles for 3 mm 7 % N-acylated gel beads at C_{A0} = 0.75 g/100 mL (b) X_T vs. T for 3 mm chitosan gel beads at C_{A0} = 0.75 g/100 mL

Similarly, the X_T versus time profile at the same initial glutaric dialdehyde concentration for the 3 mm chitosan gel beads is provided in Figure 3.1 (b). Values for X_T leveled off after 24 hours of crosslinking but the final value for X_T was 25 % lower than the final value of X_T for the 7 % N-acylated gel beads.

The crosslinking kinetics for gel beads depend on the initial glutaric dialdehyde concentration in the crosslinking bath. Therefore, the effect of initial glutaric dialdehyde concentration on the extent of crosslinking was also considered. The X_T and pH versus time profiles at a higher initial glutaric dialdehyde concentration of 2.5 wt % in the crosslinking bath are provided in Figure 3.2. The value of X_T for 7 % N-acylated gel beads increased significantly during the first 8 hours of crosslinking and then modestly increased over the following 40 hours of crosslinking. The X_T versus time profile for the 3 mm chitosan gel beads behaved similarly, but again had lower values for X_T.

The effect of mixing speed on the crosslinking kinetics for 7 % N-acylated gel beads at 120 rpm and 240 rpm is shown in Figure 3.3. The mixing speed did not affect the extent of crosslinking (X_T) versus time profile for 7 % N-acylated gel beads. Therefore, the crosslinking kinetics were not affected by the external mass transfer resistances.

3.3.2 Effect of Initial Glutaric Dialdehyde Concentration on the Extent of Crosslinking

The effect of initial glutaric dialdehyde concentration in the crosslinking bath on X_R defined in equation (3-1) and X_T defined in equation (3-2) after 48 hours of

(a)

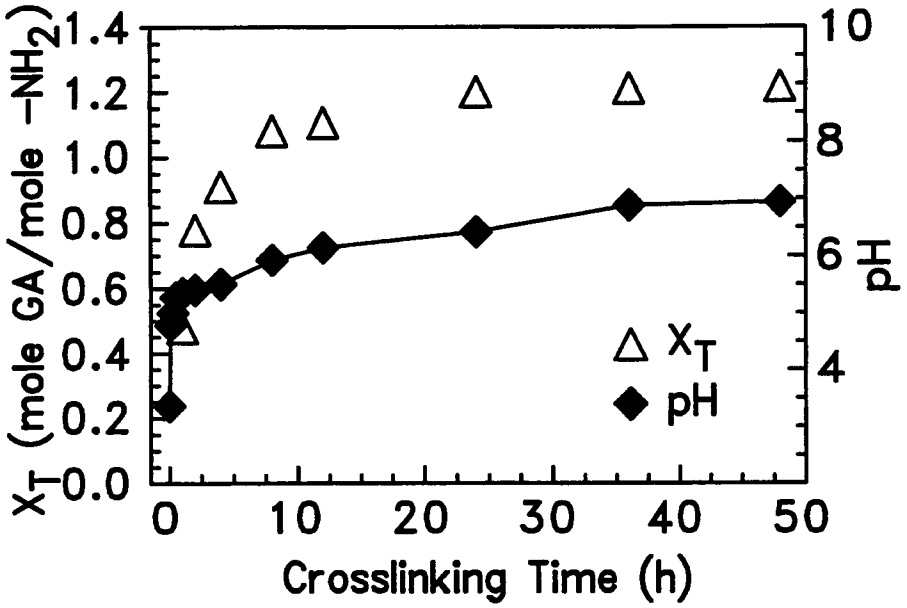

(b)

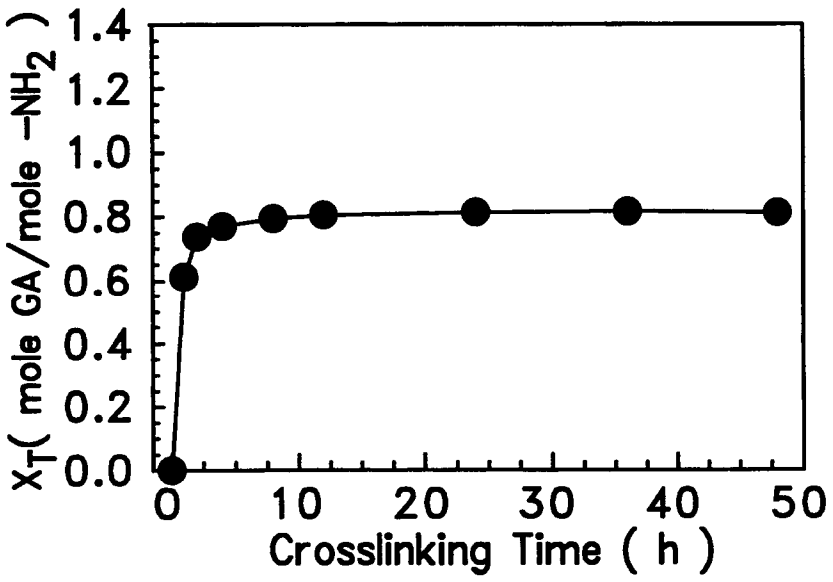

Figure 3.2 (a) X_T and pH profiles for 3 mm 7 % N-acylated gel beads at C_{A0} = 2.5 g/100 mL (b) X_T vs. T for 3 mm chitosan gel beads at C_{A0} = 2.5 g/100 mL

crosslinking are presented in Figure 3.4. The change in X_T for 7 % N-acylated gel beads varied linearly with increasing initial glutaric dialdehyde concentration. Values of the X_T for 3 mm nonacylated chitosan gel beads also increased linearly as the initial glutaric dialdehyde concentration in the crosslinking bath increased. Values for X_R and X_T were similar when initial glutaric dialdehyde concentration in the crosslinking bath was below 0.75 wt %, which corresponded to an initial ratio of 0.39 mole GA per mole of

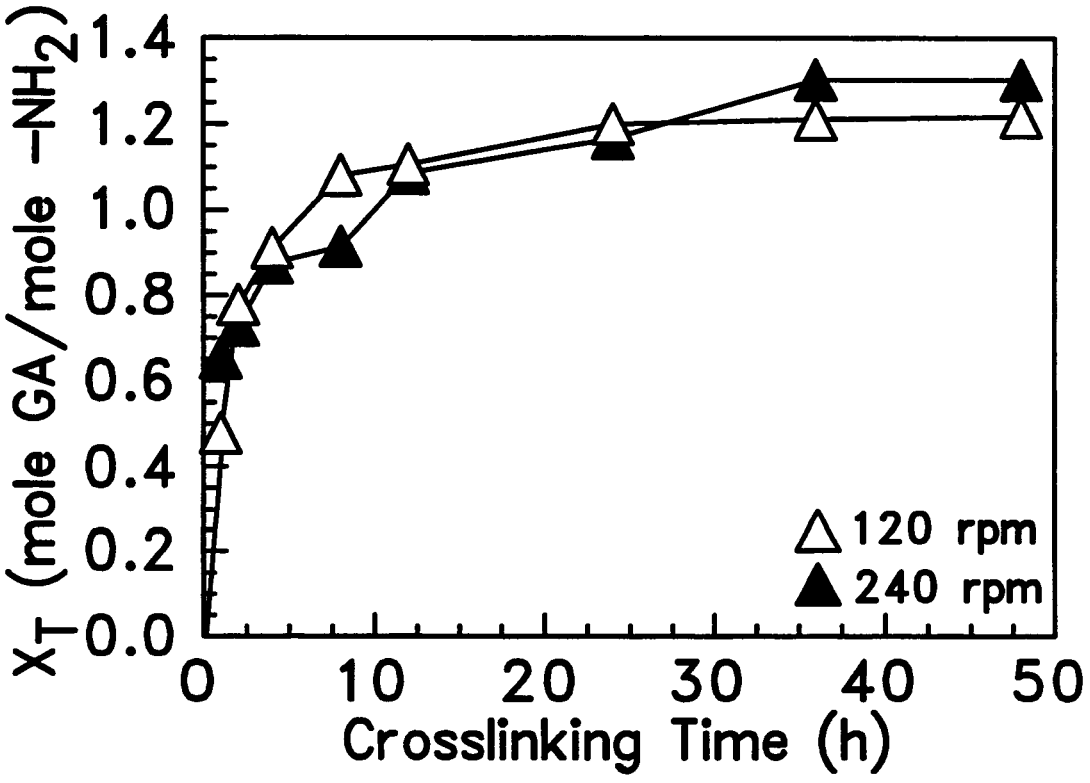

Figure 3.3 Effect of mixing speed on the overall extent of crosslinking for 3 mm 7 % N-acylated gel beads at C_{A0} = 2.5 g/100 mL

(a)

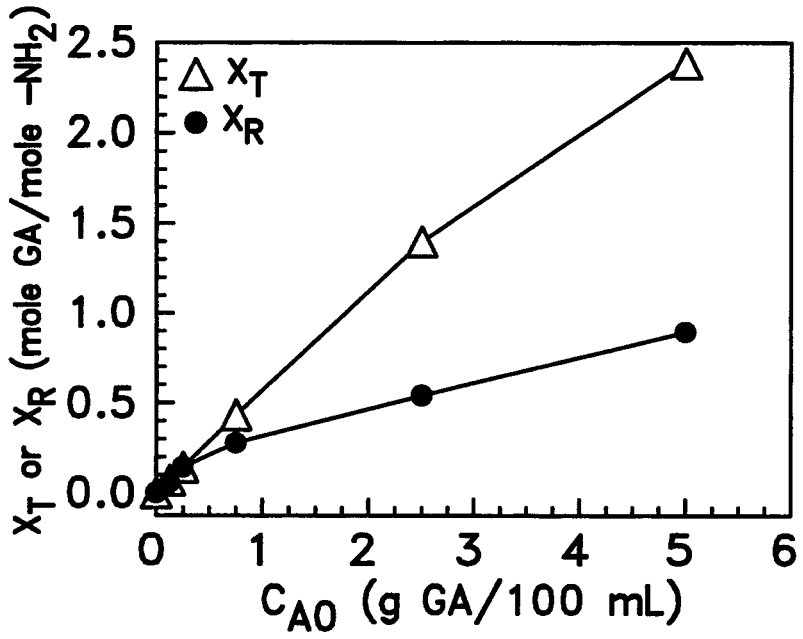

(b)

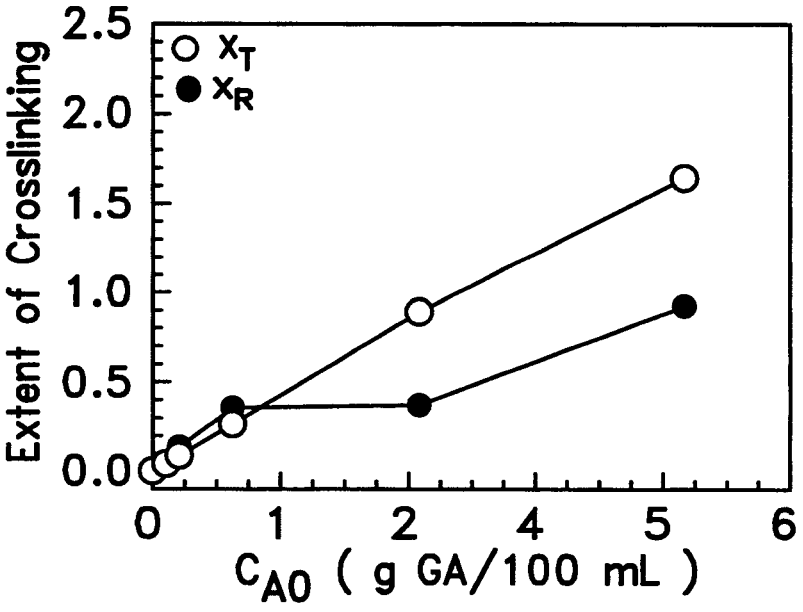

Figure 3.4 X_R and X_T vs. C_{A0} at t = 48 hours (a) 3 mm 7 % acylated gel beads
(b) 3 mm chitosan gel beads

NH_2. At higher initial glutaric dialdehyde concentrations, X_T was higher than X_R, and X_R began to level off. At an initial glutaric dialdehyde concentration of 5.0 wt % in the crosslinking bath, values for X_R were less than 50 % of the values of X_T. Also, the final X_T value for 7 % N-acylated gel beads was 1.45 times higher than X_T for the chitosan gel beads.

To determine if any glutaric dialdehyde was reversibly absorbed within the crosslinked gel beads, 6.4 g of crosslinked gel beads were filtered from the crosslinking bath, immersed into 9.6 mL of deionized water, and then agitated in an orbital shaker at 120 rpm and 27 °C for 48 hours. The glutaric dialdehyde concentration in the water was measured. As shown in Table 3.2, only a small amount of glutaric dialdehyde was released back to the water. Therefore, the uptake of glutaric dialdehyde into the gel bead was irreversible.

Table 3.2 Residual glutaric dialdehyde concentration after soaking crosslinked chitosan gel beads in water (C_{A0} = 2.5 g GA/100 mL)

Crosslinking time (hour)	GA concentration in water (wt %)	$\frac{\textit{mole}\ \text{GA released}}{\text{mole GA consumed}}$
0	0.000	0.0000
1	0.002	0.0014
2	0.008	0.0053
4	0.019	0.0100
8	0.010	0.0046
12	0.014	0.0061
24	0.011	0.0045
36	0.010	0.0040
48	0.021	0.0084

A homogeneous crosslinking experiment was also performed at conditions consistent with the heterogeneous crosslinking of the chitosan gel beads. Specifically, 9.6 mL of 2.5 wt % aqueous glutaric dialdehyde solution was added into 6.4 g of 5.0 wt % chitosan solution at 25 °C and manual briskly stirred. The light yellow color and firm texture of the crosslinked chitosan gel quickly formed within 60 seconds. Apparently, the homogeneous crosslinking reaction was very fast relative to the heterogeneous crosslinking of the 3 mm chitosan gel beads .

The average initial pH value within 7 % N-acylated gel beads was estimated from a hydrogen ion balance. Specifically, the hydrogen ion consumption was determined by the difference in the pH value for glutaric dialdehyde solution before and after crosslinking plus the amount of hydrogen ions needed to protonate $-NH_2$ to $-NH_3^+$ (the $_pk_a$ of chitosan is 6.3). The average initial pH value within the gel bead was calculated to be 12.1.

3.3.3 Cadmium Adsorption Isotherms

The cadmium ion adsorption capacity of the gel beads and freeze-dried beads were compared. Representative adsorption isotherms for 7% N-acylated beads crosslinked at an initial concentration of 0.75 wt % in the crosslinking bath are given in Figure 3.5. On a chitosan basis, the gel beads had a slightly higher cadmium adsorption capacity than the freeze-dried beads. Isotherms for both the gel and freeze-dried beads possessed a step-shaped profile. However, for 7 % N-acylated chitosan gel beads, a rapid increase in adsorption capacity at final cadmium ion concentrations between 420

and 500 mg/L was observed. The saturation cadmium adsorption capacities were 161 and 138 (mg Cd^{+2}/g-bead) respectively for 7 % N-acylated chitosan gel and freeze-dried beads.

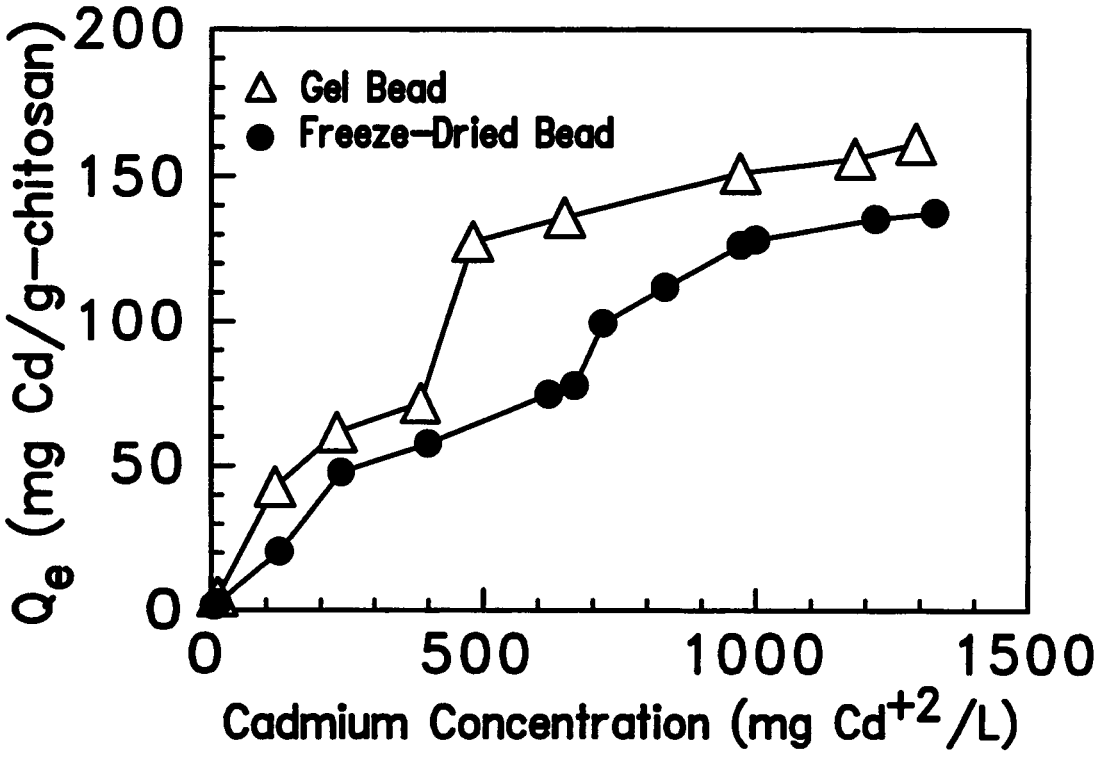

Figure 3.5 Cadmium adsorption isotherms for 7 % N-acylated chitosan gel beads and freeze-dried beads crosslinked with C_{A_0} = 0.75 g GA/100 mL

The cadmium adsorption isotherms for the freeze-dried 7 % N-acylated and nonacylated chitosan beads crosslinked with three different initial glutaric dialdehyde concentrations are compared in Figure 2.9. As shown in Figure 2.9, there was no

significant difference in the adsorption capacity between the freeze-dried N-acylated chitosan beads at final cadmium ion concentrations ranging from 4 to 200 mg/L. However, at final cadmium ion concentrations higher than 600 mg/L, the adsorption capacity decreased as the initial glutaric dialdehyde concentration in the crosslinking bath increased. In Figure 2.7, the uncrosslinked freeze-dried chitosan beads exhibited a slightly higher adsorption capacity than the crosslinked chitosan beads at final cadmium ion concentrations between 100 and 500 mg/L. There was no significant effect of the initial glutaric dialdehyde concentration on the saturation cadmium adsorption capacity.

The behavior of these isotherms suggest that the extent of crosslinking affects the cadmium ion adsorption capacity. This effect would be more readily observed by measuring the saturation adsorption capacity as a function of the extent of crosslinking for the gel bead preparation.

3.3.4 Saturation Cadmium Adsorption Capacity vs. Extent of Crosslinking

The saturation cadmium adsorption capacity in the chitosan beads as a function of the extent of crosslinking is presented in Figure 3.6. The cadmium adsorption capacity decreased as the extent of crosslinking increased. The relationship between cadmium adsorption capacity and X_R for 7 % N-acylated gel beads and nonacylated chitosan gel beads was similar.

It is interesting to note in Figure 3.4 (b) that the values of X_R at initial glutaric dialdehyde concentration of 0.75 wt % and 2.5 wt % are nearly equal. Consequently, the saturation adsorption capacities at these extents of crosslinking are almost equal (Figure

(a)

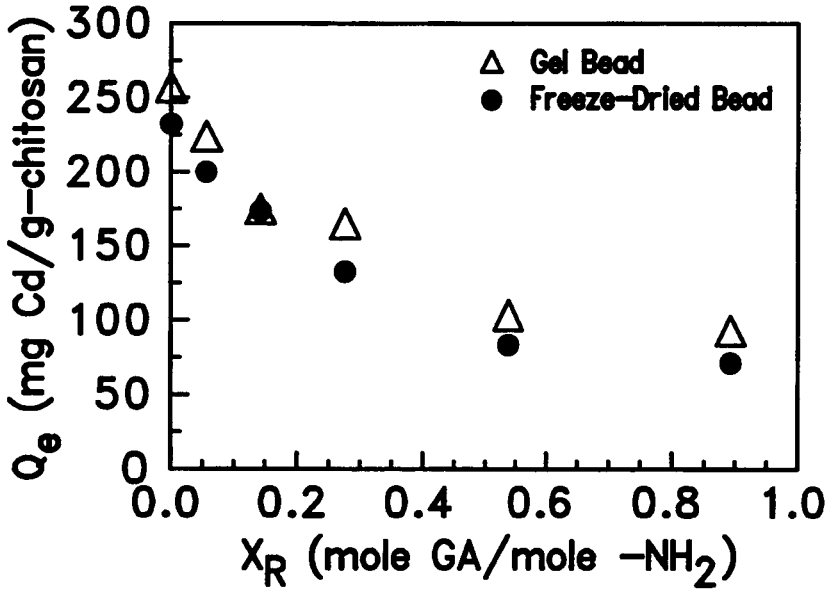

(b)

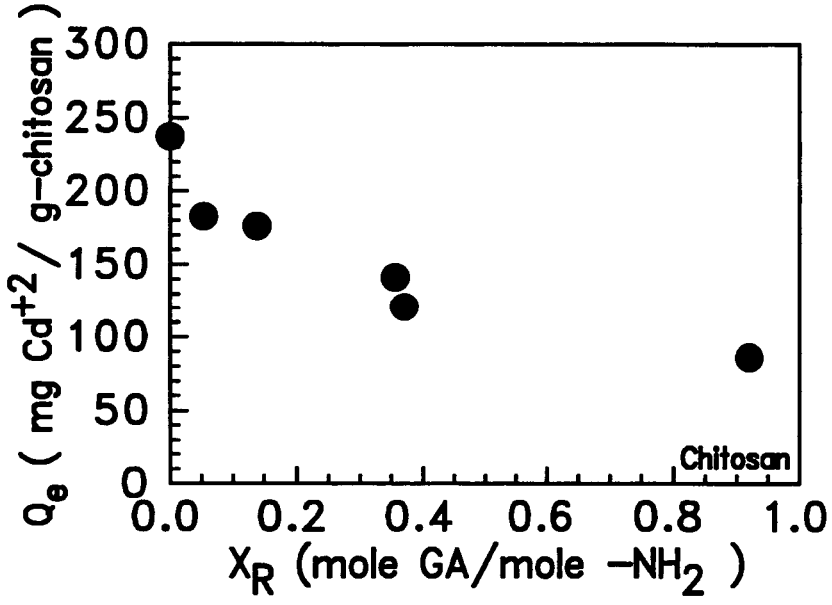

Figure 3.6 Qe vs. X_R at saturation for (a) 7 % 3 mm N-acylated and (b) nonacylated chitosan gel beads

3.6 b) and the isotherms are nearly the same as well (Figure 2.7). It is also interesting to note that the 3 mm 7 % N-acylated gel beads and nonacylated chitosan gel beads crosslinked with 5.0 g GA/100 mL solution still showed appreciable cadmium adsorption capacity. The cadmium adsorption capacity for freeze-dried N-acylated chitosan beads at different estimated values of X_R are also given in Figure 3.6 (a). The crosslinked gel beads had a higher adsorption capacity than the freeze-dried chitosan beads at the same extent of crosslinking.

3.3.5 EDAX Profiles for Adsorbed Cadmium

EDAX line and mapping images for 3 mm crosslinked, freeze-dried chitosan beads adsorbed with 139 mg cadmium per gram of chitosan beads are presented in Figure 8. The extent of crosslinking (X_R) was estimated at 0.36 (mole GA consumed/total mole of (-NH_2) from Figure 3.4 (b). The sample cross section was prepared by freeze fracturing as opposed to the microtome sectioning and so does not exhibit a smooth surface.

The SEM image in Figure 3.7 (a) shows two distinct morphologies: a reticular tightly woven shell, and an amorphous core. The outer shell is presumably crosslinked chitosan formed during the heterogeneous crosslinking process. The EDAX line profile in Figure 3.7 (a) shows that the cadmium signal intensity bisecting the chitosan bead is significantly higher at the outer shell than the interior core. The majority of adsorbed

(a)

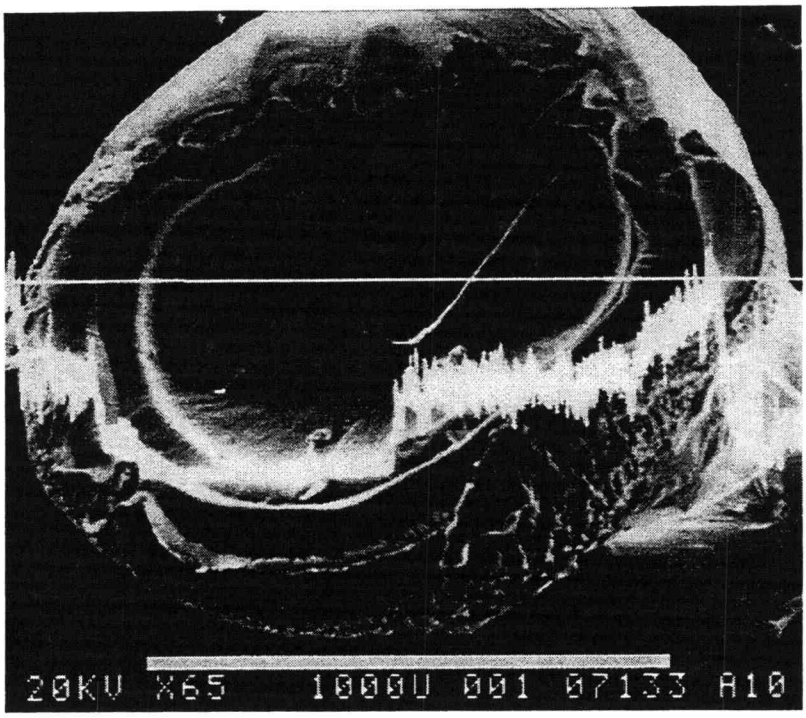

(b)

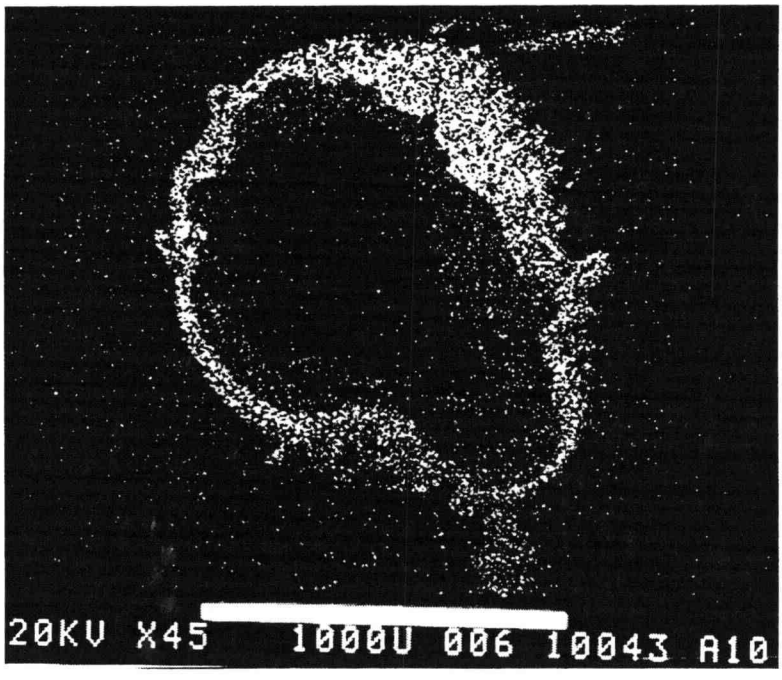

Figure 3. 7 Representative EDAX images for 3 mm crosslinked chitosan beads with cadmium (C_o = 1026 mg Cd/L). (a) line (b) mapping

cadmium was detected within this outer shell of the chitosan bead. There was no appreciable Cd signal within the interior of the bead. In Figure 3.7 (b), the EDAX mapping profile obtained from the same sample cross section also confirms that the majority of the adsorbed cadmium is localized in the outer shell near the surface of the bead. In contrast, the EDAX mapping image for 3 mm freeze-dried uncrosslinked chitosan beads shows that the chelated cadmium is uniformly distributed through the particle (Figure 3.7 c).

(c)

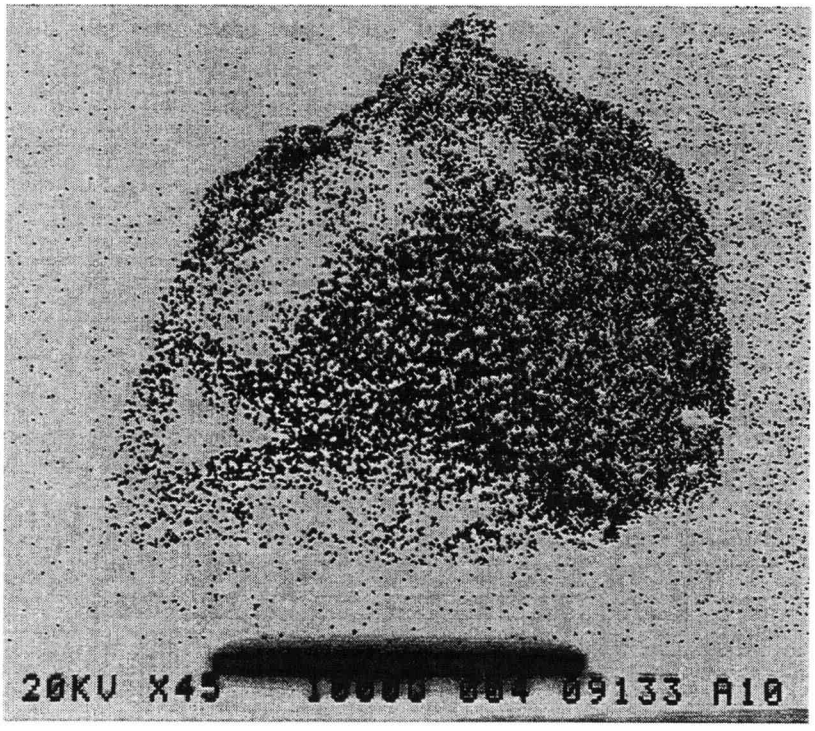

Figure 3.7 (c) Mapping image for 3 mm uncrosslinked chitosan beads

3.4 Discussion

3.4.1 Crosslinking Mechanism

Chemistry of Glutaric Dialdehyde. Kawahara et al. (1992) showed that glutaric dialdehyde in dilute aqueous solution at pH 3-8 existed in monomeric form. The molecular weight of GA as determined by light scattering was 100, the molecular weight of GA monomer. However, Hardy et al.(1969) showed that in weakly alkaline solution (pH 8), glutaric dialdehyde readily polymerized. Margel and Pembunm (1980) further showed that the polymerization of glutaric dialdehyde was promoted in an alkaline environment. In this present work, the initial pH of glutaric dialdehyde in the crosslinking bath at GA concentrations ranging from 0.75 wt % to 5.0 wt % was between 3.7 and 4.2. Also, the final pH in the crosslinking bath was below 8. Therefore, the glutaric dialdehyde should exhibit a monomeric structure in the aqueous crosslinking bath.

The GA structure resulting from crosslinking with amine groups has not been investigated in detail. According to Richards and Knowles (1968), when aqueous glutaric dialdehyde was used as a protein crosslinking reagent, the glutaric dialdehyde polymerized through aldol condensation to form α,β-unsaturated aldehydes and then reacted with amine groups on the protein. Although Hardy et al. (1969) proposed that this crosslinking reaction involved monomeric glutaric dialdehyde or its hydrates in neutral aqueous solution, Kawahara et al. (1992) suggested that the glutaric dialdehyde may slowly polymerize to yield a cyclic hemiacetal structure during the crosslinking

reaction to form a Schiff 's base between glutaric dialdehyde and the amine groups on protein even at near neutral pH. According to the crosslinking mechanism proposed by Monsan et al. (1975), the structure of the glutaric dialdehyde polymers within the crosslinked protein was verified by NMR analysis to consist of 8 monomeric units of glutaric dialdehyde over a wide pH range of 1.9 to 10.5. This result verified Korn's (1972) earlier crosslinking study, which indicated that 4 moles of glutaric dialdehyde reacted with one mole of free amine on lysine and hydroxylsine.

The glutaric dialdehyde polymer structure proposed by Monsan et al. (1975) is reasonable. Therefore, it is accepted and applied to this present study for the crosslinking reaction between NH_2 on chitosan gel beads and aldehyde groups on glutaric dialdehyde. Since the initial pH value within the 7 % N-acylated gel beads is 12.1, we propose that glutaric dialdehyde monomers polymerize within the alkaline gel environment and then react with NH_2 in the gel beads. The molecular structures of the glutaric dialdehyde polymer and the glutaric dialdehyde polymer crosslinked with the glucosamine unit on chitosan are presented in Figures 3.8 (a) and (b). The β value, defined as mole of glutaric dialdehyde consumed to form a crosslink per mole of $-NH_2$ crosslinked is 4. If the glutaric dialdehyde is only in monomeric form, then the β value could be 1 if the GA monomer reacted with a free amine groups, or 0.5 if both aldehyde groups on the GA monomer reacted with two $-NH_2$ groups on adjacent chitosan chains to form a crosslink.

Roberts and Taylor (1989) claimed objections to the previous postulated crosslinking mechanism. By the analysis of UV/visble and NMR spectra of glutaric dialdehyde, they found that only a very small fraction of the aldehyde groups had

(a)

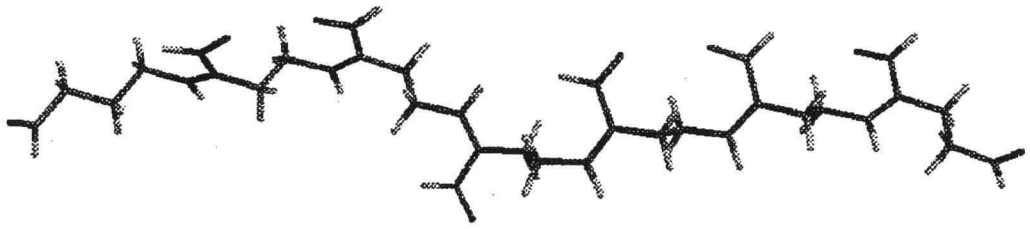

$$CHO(CH_2)_3CH=[C(CHO)CH_2)_2CH]_6=C(CHO)(CH_2)_2CHO$$

(b)

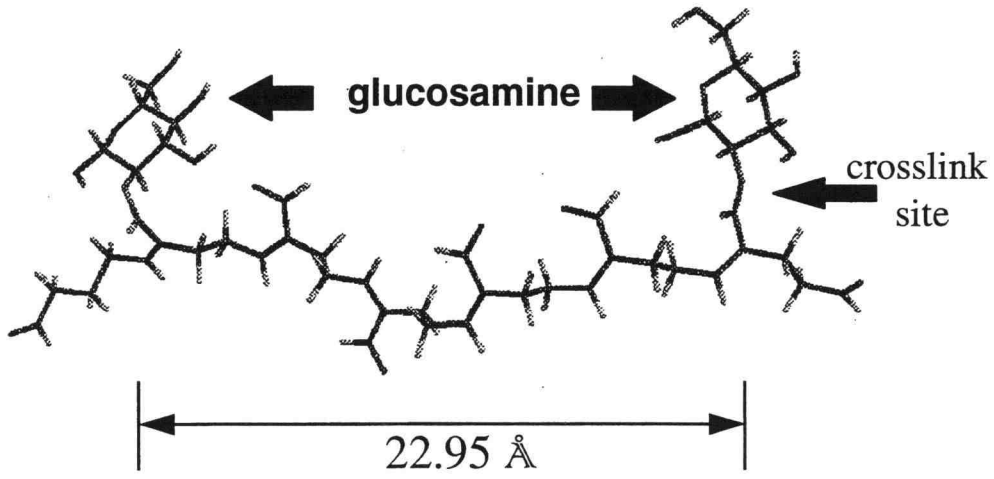

Figure 3.8 Molecular structures (a) glutaric dialdehyde polymer (b) crosslinked glutaric dialdehyde polymer

undergone an aldol condensation reaction to α,β-unsaturated aldehyde groups. Therefore, they suggested that the crosslinking mechanism involved the formation of Schiff 's base (-C=N-) structures instead of Michael-type (-C-N-) adducts, a result consistent with the crosslinked structure in this study.

Modified Shrinking Core Model for Diffusivity Estimation. Based on the above discussion, the following crosslinking mechanism is proposed. The crosslinking process is believed to include three main steps: 1) mass transfer of glutaric dialdehyde monomers to the surface of the gel beads; 2) diffusion of glutaric dialdehyde monomers and polymers to the active sites within the gel beads; 3) crosslinking reaction between NH_2 in the gel beads and aldehyde groups (-CHO) of the glutaric dialdehyde polymer. The modified shrinking core model proposes that the heterogeneous crosslinking of the chitosan gel bead is diffusion controlled. Our own experimental work and previous studies on crosslinking in polymer gels confirm this assumption. The external mass transfer resistances on the crosslinking process were negligible (Figure 3.3). Also, the homogeneous crosslinking reaction between NH_2 and aldehyde groups was very fast relative to heterogeneous crosslinking of gel beads.

Gudmund et al. (1989) suggested that the gelation of polymers was characterized by the strong site binding of the crosslinking agent to the polymer. The rate of diffusion of the crosslinking agent into the gel was the limiting process. Dusek and MacKnight (1987) further suggested that diffusion control limited the overall rate of polymerization leading to a crosslinked polymer network. In this present study, it is believed that the glutaric dialdehyde monomers polymerized in the alkaline environment of the chitosan

gel beads. The glutaric dialdehyde subsequently crosslinked with free NH_2 groups within the chitosan gel. Therefore, the modified shrinking core model was developed assuming that diffusion rate of GA through the crosslinked shell of gel bead was the rate limiting step.

The relationship between $F(\bar{X})$ and the $\int C_A dt$ for 7 % N-acylated gel beads at initial glutaric dialdehyde concentration of 2.5 wt % is shown in Figure 3.9. The data is

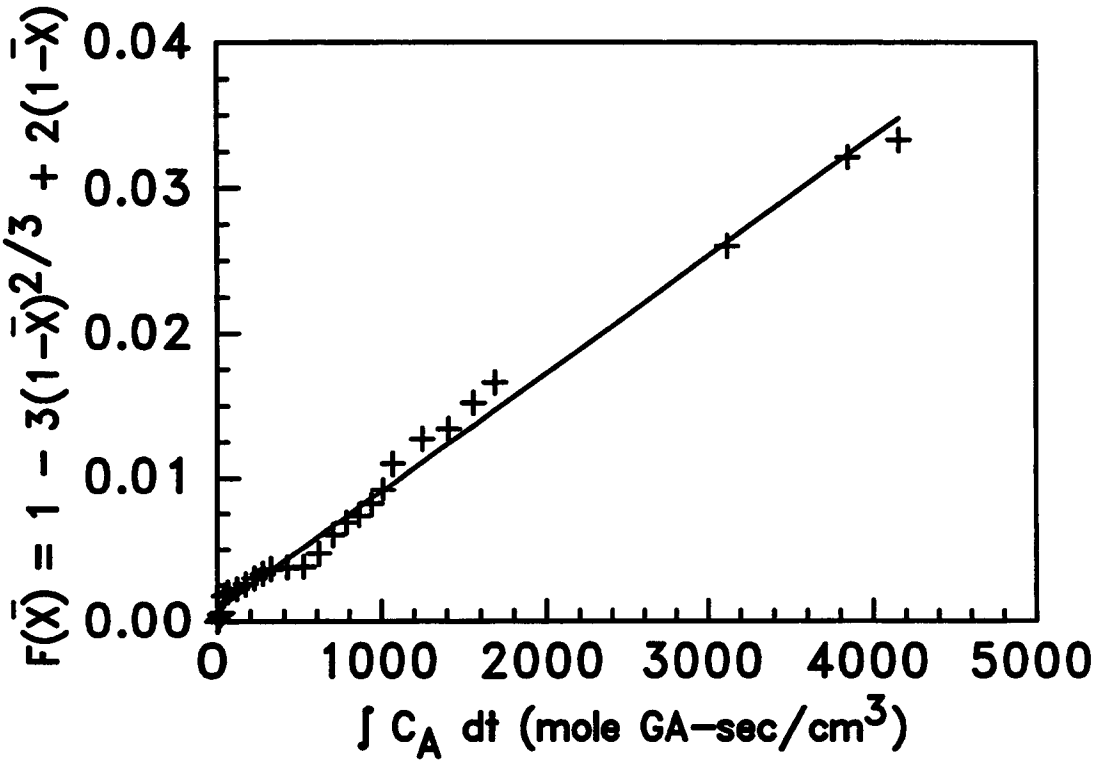

Figure 3.9 Modified shrinking core model plot for 7 % N-acylated chitosan gel beads crosslinked at C_{Ao} = 2.5 g GA/100 mL

linear, which demonstrates the validity of the modified shrinking core model for describing the diffusion limits heterogeneous crosslinking of the chitosan gel bead. The experimental data closely matched the correlated line. Specifically, the effective diffusivity for glutaric dialdehyde in the gel beads, estimated from the slope of the straight line, is $4.11 \cdot 10^{-8} \pm 8.17 \cdot 10^{-10}$ (1s) cm^2 / s with a regression coefficient of 0.99.

The molecular diffusivity evaluated by Wilke and Chang correlation (Wilke and Chang, 1955) for glutaric dialdehyde in aqueous medium at infinite dilution is $8.97 \cdot 10^{-6}$ cm^2 / s. The effective diffusivity for glutaric dialdehyde in the gel bead is considerably smaller than this value. This effective diffusivity might represent the average diffusivity of glutaric dialdehyde monomers, dimers, trimers, and higher polymers in the gel beads during the crosslinking process.

The effective diffusivity of glutaric dialdehyde in the gel beads was used to predict the overall extent of crosslinking within the gel beads as a function of crosslinking time at different initial glutaric dialdehyde concentrations (Figure 3.10). The diffusion limited model prediction shows that the change in X_T with crosslinking time at 0.75 wt % initial GA concentration is faster than an initial GA concentration of 2.5 wt %, which is observed experimentally. Values of X_T by model prediction are consistent with the X_T data at initial glutaric dialdehyde concentrations of 0.75 wt % and 2.5 wt %, except at very short crosslinking times. At very short crosslinking times, the crosslinking reaction may be the rate limiting step for the heterogeneous crosslinking process when the crosslinked shell is very thin (Appendix B-4).

(a)

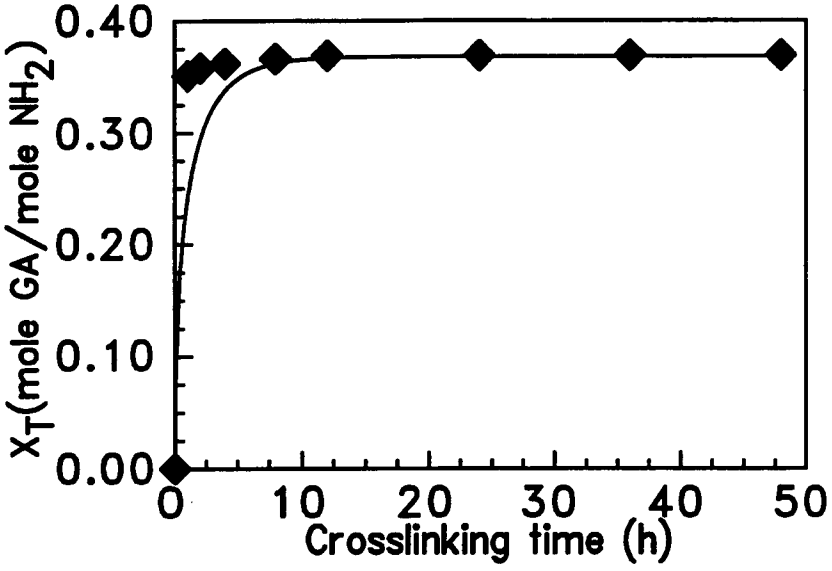

(b)

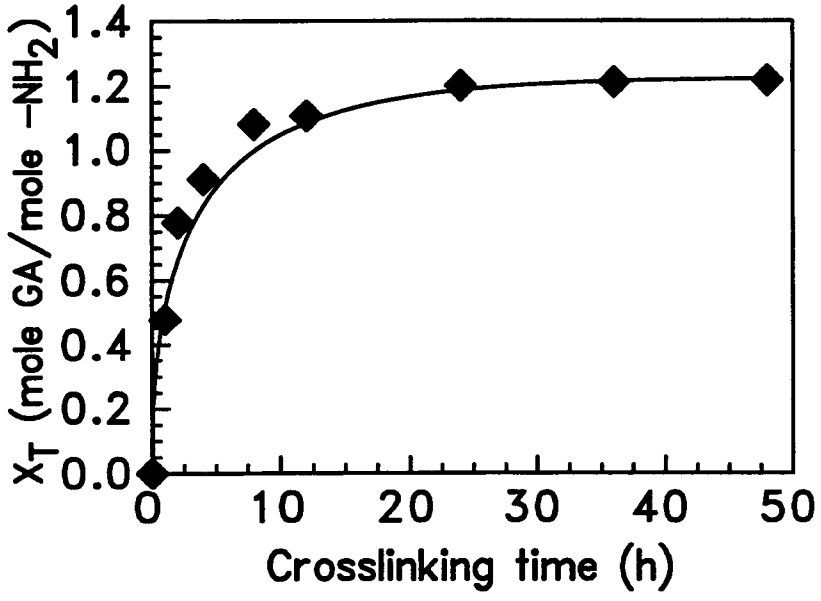

Figure 3.10 Predicted $X_{T,model}$ vs. Time for (a) C_{Ao} = 0.75 g GA/100mL and (b) C_{Ao} = 2.5 g GA/100mL

The pH profiles (Figures 3.1 and 3.2) at an initial glutaric dialdehyde concentration of 0.75 wt % leveled off faster than those at an initial glutaric dialdehyde concentration at 2.5 wt % . The faster pH rise might result in a higher rate of polymerization for glutaric dialdehyde monomers at 0.75 wt % initial glutaric dialdehyde concentration. Furthermore, more GA polymers could react with amine groups in gel beads within certain period of crosslinking time. Thus, there was a higher concentration gradient existing between glutaric dialdehyde monomers in the crosslinking bath and the glutaric dialdehyde polymers in the gel beads during the initial crosslinking. This concentration gradient could force glutaric dialdehyde to be more rapidly absorbed and react with NH_2 in gel beads.

Figure 3.5 suggested that higher initial glutaric dialdehyde concentrations resulted in higher extents of crosslinking (X_T and X_R) after 48 hours of crosslinking. The difference between the value of X_T and X_R became significant as the initial glutaric dialdehyde concentration increased. Perhaps a fraction of the glutaric dialdehyde monomers became trapped within the crosslinked gel network and did not react. Therefore, when the gel beads were dried to obtain the X_R measurement, the trapped, unreacted GA volatilized with water during the oven drying.

3.4.2 Effect of Crosslinking on Cadmium adsorption Capacity

The extent of crosslinking (X_T and X_R) could play a major role in determining cadmium adsorption capacity for the chitosan gel beads and freeze-dried chitosan beads. Crosslinking of gel beads at an optimum -CHO/-NH_2 mole ratio could decrease the

affinity of the biopolymer chain to water and at the same time improve accessibility of cadmium ions to the chelating sites (free NH_2) by optimizing the matrix structure in the gel beads. However, crosslinking also reduced the free amine group content (Koyama and Taniguchi, 1986).

Kurita (1987) and Koyama et al. (1986) indicated that the maximum Cu^{+2} adsorption for crosslinked chitosan was reached at a low extent of homogeneous crosslinking, corresponding to an initial GA to $-NH_2$ mole ratio of 0.139. In contrast, Masri et al. (1978) found that the adsorption capacity for transition metal ions decreased when chitosan powder was heterogeneously crosslinked at an initial GA to $-NH_2$ mole ratio of 0.215.

Homogeneous crosslinking of the chitosan solution was performed at conditions consistent with the heterogeneous crosslinking of chitosan gel beads. Specifically, 9.6 mL of 2.5 wt % GA solution was added into 6.4 g of 5.0 wt % chitosan solution to form a firm textured crosslinked chitosan gel. Then 0.79 g of the homogeneous crosslinked gel (0.040 g chitosan basis) was mixed with 40 mL of cadmium nitrate solution (C_0: 2000 mg Cd/L) in a 125 mL Erlenmeyer flask and agitated at 120 rpm by an orbital shaker at 25 °C for 60 hours. The filtered cadmium solution was analyzed by ion chromatography (IC) to determine the saturation cadmium capacity for the homogeneous crosslinked gel. The saturation cadmium adsorption capacity was 49.6 (mg Cd^{+2}/g-bead). Apparently, the effect of the homogeneous crosslinking on the saturation cadmium capacity was much more significant than for heterogeneous crosslinking.

In this present study, the gel beads exhibited slightly higher cadmium adsorption

capacities than the freeze-dried beads (Figure 3.5). When the water in the porous gel matrix was removed during the freeze drying process, the hydrated chitosan chains collapsed. Therefore, the cadmium ions could diffuse deeper into the gel and chelate with more of the amine groups in gel bead than in the freeze-dried chitosan bead.

The proposed cadmium chelation scheme is presented in Figure 3.11. Chelation involves the attachment of cadmium ion onto at least two nitrogen atoms by electrostatic interaction. If the distance between the nitrogen atoms is less than the radius of the cadmium ions, then chelation occurs. Two kinds of chelation reactions, inter-molecular and intra-molecular, may occur. The inter-molecular chelation assumes that cadmium ion is chelated by at least two nitrogen atoms of imino groups on crosslinked chitosan. In contrast, intra-molecular chelation assumes that the cadmium ion is bound by nitrogen atoms of a crosslinked imino group and an uncrosslinked amine group within the gel. Stability constant data for metal complexes on organic ligands (IUPAC, 1979) showed that both imino and amine exhibit similar binding strength for transition metal ions.

Saturation cadmium adsorption capacity data (Figures 3.5 & 2.9) was used to develop a relationship between the extent of heterogeneous crosslinking and cadmium adsorption capacity. The data showed that the increasing of the extent of crosslinking lowered the cadmium adsorption capacity. Although both crosslinked imino groups (-C=N-) and uncrosslinked amine groups ($-NH_2$) may exhibit a similar chelating ability with cadmium ions, the hindrance effect by the corsslinked molecular could hinder the binding of cadmium ions to crosslinked imino groups, or impede diffusion of Cd^{+2} ion deeper into the bead to reach the uncrosslinked amine groups within the bead.

The 7 % acylated chitosan gel beads had a higher cadmium adsorption capacity than the nonacylated chitosan gel beads at similar extents of crosslinking. The 7 % N-

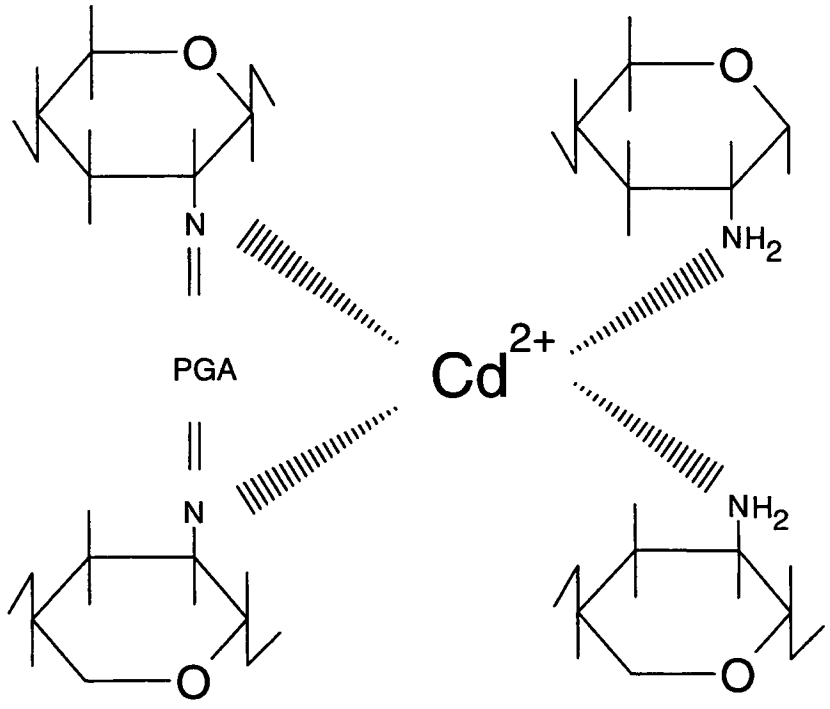

Figure 3.11 Chelation scheme of Cd^{+2} in crosslinked chitosan

acylated gel beads have a more open gel matrix relative to the nonacylated chitosan gel beads. Specifically, the long chain annoyl residues attached to the selected amine group of chitosan to create an open gel matrix which facilitated cadmium penetration.

Adsorption Model. The effect of the extent of crosslinking ($\overline{X}$) on the saturation cadmium capacity (Q_c) for partially N-acylated gel beads indicated that the saturation cadmium capacity obviously decreased as the extent of crosslinking increased. However, after a certain level of crosslinking the saturation cadmium capacity was not affected by further crosslinking. The adsorption model presented below attempts to estimate the cadmium unsaturation zone (r_M) in the N-acylated gel beads at different extents of crosslinking. This estimation is based on the changes of the thickness of the cadmium saturated zone ($R-r_M$) and the thickness of the crosslinked layer ($R-r_C$) at different extents of crosslinking.

The EDAX mapping images for 3 mm uncrosslinked and crosslinked freeze-dried chitosan beads (Figure 3.7) shows that the thickness of the cadmium loading zone for the uncrosslinked bead is larger than that for the crosslinked bead. This might suggest that the penetration distance of cadmium ions within the chitosan bead gradually decreased as the extent of crosslinking increased. The penetration cadmium ions were retarded by the crosslinked layer. Therefore, cadmium penetration and adsorption into the gel bead could be represented as a shrinking core process. At low $\overline{X}$, the cadmium ions penetrate deeper into the gel beads without a serious resistance from the thin crosslinked layer. In this case, the value of r_C is much greater than r_M. As $\overline{X}$ increases, r_M increases and r_C slowly decreases. After a certain level of $\overline{X}$ is approached, r_M approaches r_C. The adsorbed cadmium is now completely localized into the cadmium saturation zone ($R-r_M$).

As pervious described, the binding strength of the imino (-N=C-) site with cadmium ions might be close to the binding strength of the $-NH_2$ site. The crosslinked

shell could hinder cadmium ion penetration into the uncrosslinked zone of the gel beads. Cadmium ions could easily chelate with nitrogen atoms of imino sites within the crosslinked zone and additional cadmium ions penetrate into the uncrosslinked zone to chelate with $-NH_2$ sites at low extents of crosslinking. However, only a partial of the cadmium could penetrate deeper into the interior of the gel to chelate with the nitrogen atoms of $-NH_2$ sites in the uncrosslinked zone as the crosslinked layer gradually increased. Therefore, the saturation cadmium capacity at different extents of crosslinking should include the adsorption capacities for -N=C- sites in the crosslinking layer and fraction of $-NH_2$ sites in the interior uncrosslinked zone.

The theoretical loading of the cadmium ion in the active sites (=N or $-NH_2$ groups) in chitosan gel bead ($\overline{Q}_e$) can be determined by

$$\overline{Q}_e = \frac{Y_B M_{w,Cd^{+2}}}{\nu} \tag{3-22}$$

where $M_{w,Cd^{+2}}$ is the molecular weight of the cadmium ions (g/mole), and ν is the chelation coordination number for cadmium (2 moles active sites/mole Cd^{+2}). The saturation cadmium capacity for crosslinked N-acylated gel beads is the sum of the cadmium loading in the crosslinked zone (imino groups) and the fraction of amine groups in the uncrosslinked zone. Therefore, the saturation cadmium capacity can be expressed as

$$\begin{aligned} Q_e &= \overline{X}\,\overline{Q}_1 + \overline{Q}_2 (1 - \overline{X}) \frac{\frac{4}{3}\pi r_C^{\,3} - \frac{4}{3}\pi r_M^{\,3}}{\frac{4}{3}\pi r_C^{\,3}} && \text{as } X_M \geq \overline{X} \\ &= X_M\,\overline{Q}_1 && \text{as } X_M \leq \overline{X} \end{aligned} \tag{3-23}$$

The volume fraction of N-acylated gel beads containing adsorbed cadmium (X_M) can be defined as

$$X_M = 1 - \left(\frac{r_M}{R} \right)^3 \tag{3-24}$$

Recall that: $$\overline{X} = 1 - \left(\frac{r_C}{R}\right)^3$$

After rearrangement, equation (3-23) is simplified as

$$\begin{aligned} Q_e &= \overline{X}\,\overline{Q}_1 + \overline{Q}_2 (X_M - \overline{X}) \qquad \text{as } X_M \geq \overline{X} \\ &= X_M \overline{Q}_1 \qquad\qquad\qquad\qquad\quad \text{as } X_M \leq \overline{X} \end{aligned} \tag{3-25}$$

where $\overline{Q}_1$ and $\overline{Q}_2$ are the theoretical maximum loading of the cadmium ion in the crosslinked and uncrosslinked zones, respectively. Based on the similar binding strength of the imino and amine groups to the cadmium ion, $\overline{Q}_1$ and $\overline{Q}_2$ are equal to $\overline{Q}_e$.

Subsitution of $\overline{X}$ and X_M into equation (3-25), yields

$$Q_e = \frac{Y_B M_{w,Cd^{+2}}}{v} \left\{ \left[1 - \left(\frac{r_C}{R} \right)^3 \right] + \left\{ 1 - \left[1 - \left(\frac{r_C}{R} \right)^3 \right] \right\} \left[1 - \frac{r_M^3}{r_C^3} \right] \right\} \tag{3-26}$$

The change of the thickness of the cadmium unsaturation zone (r_M) and the uncrosslinked zone (r_C) versus X_T for N-acylated gel beads is presented in Figure 3.12. It is noteable that the values of r_C decrease and r_M increase as the extent of crosslinking increases, a result consistent with the assumption of the adsorption model.

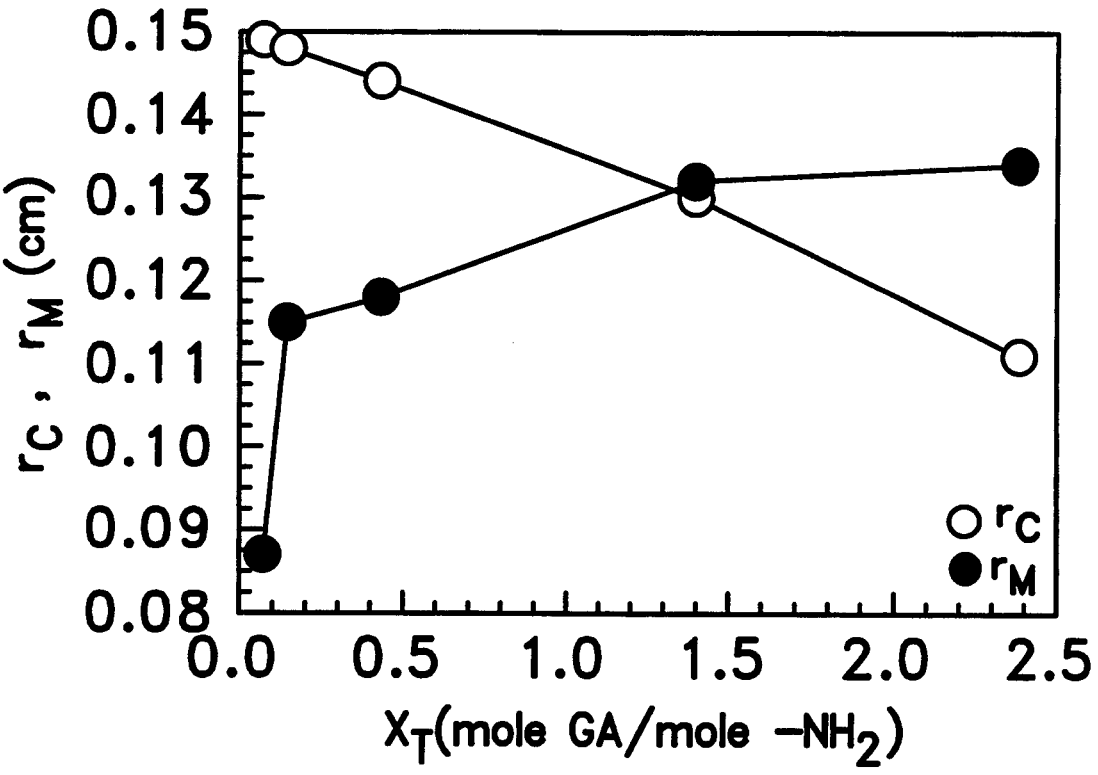

3. 12 The change of the thickness of the cadmium unsaturation zone (r_M) and the uncrosslinked zone versus X_T for N-actlated gel beads

CHAPTER 4

DESORPTION OF CADMIUM FROM CHITOSAN BEADS

Tzu-Yang Hsien and Gregory L. Rorrer*

Department of Chemical Engineering
Oregon State University
Corvallis, Oregon 97331

(tel) 503-737-3370, (fax) 503-737-4600

* corresponding author

Submit to Journal of *Environmental Science & Technology*

4.1 Introduction

The pH affects cadmium adsorption and desorption on the chitosan beads. In this present study, the adsorption and desorption kinetics for single stage adsorption desorption experiments are determined in a spinning basket reactor. The hydrogen ion capacity of the chitosan beads and the pH of the cadmium solution in the vessel are also measured as a function of time. Finally, an equilibrium model for the desorption process is presented in order to describe the competitive relationships associated with displacing adsorbed cadmium ions with hydrogen ions.

4.2 Materials and Methods

4.2.1 Chitosan Beads Synthesis

The synthesis of chitosan beads, including chitosan solution preparation, gel beads casting, crosslinking and freeze drying was described in previous studies (Rorrer et al., 1993, Hsien and Rorrer, 1995). Specifically, a 5 wt % chitosan solution was casted in the precipitation bath to form chitosan gel beads and then crosslinked with a 2.5 wt % aqueous glutaric dialdehyde. The wet crosslinked chitosan beads were freeze-dried to remove the remaining humidity. The chitosan beads crosslinked with a 2.5 wt % initial glutaric dialdehyde solution were used in this study.

4.2.2 Single Stage Desorption

Two types of desorption experiments, single stage and multiple stage, were performed. In the single stage experiment, the adsorbed cadmium ions on chitosan beads were released back to the bulk solution by the single addition of a large amount of H^+. Batch adsorption/desorption experiments were conducted at 25 °C in a spinning-basket reactor (Figure 4.1), inspired by a basket reactor from Carberry (1976). Prior to desorption, the adsorption process was carried out. Specifically, 0.5 g of chitosan beads were packed into the hollow impeller basket assembly and contacted with 200 mL of 200 mg /L cadmium ion solution at 150 rpm and 25 °C for at least 48 hours to ensure that adsorption equilibrium was achieved. After adsorption, 65 mL of 0.1 N HNO_3 solution was added to the vessel to load the bulk solution with the H^+ ions needed to affect the complete desorption and to reach a final pH value of 2.0. The adsorption/desorption parameters for spinning basket reactor experiments are summarized in Table 4.1.

Table 4.1 The adsorption/desorption parameters for spinning basket reactor experiments

Process Condition	Variable and Units
Temperature	25 °C
Bead loading (m_b)	0.5 g
Initial solution volume (V)	200 mL
Initial Cd^{+2} concentration (C_o)	200 mg Cd/L
Acid (HNO_3) concentration (C_a)	0.0001 - 0.1 N
Agitation	150 rpm

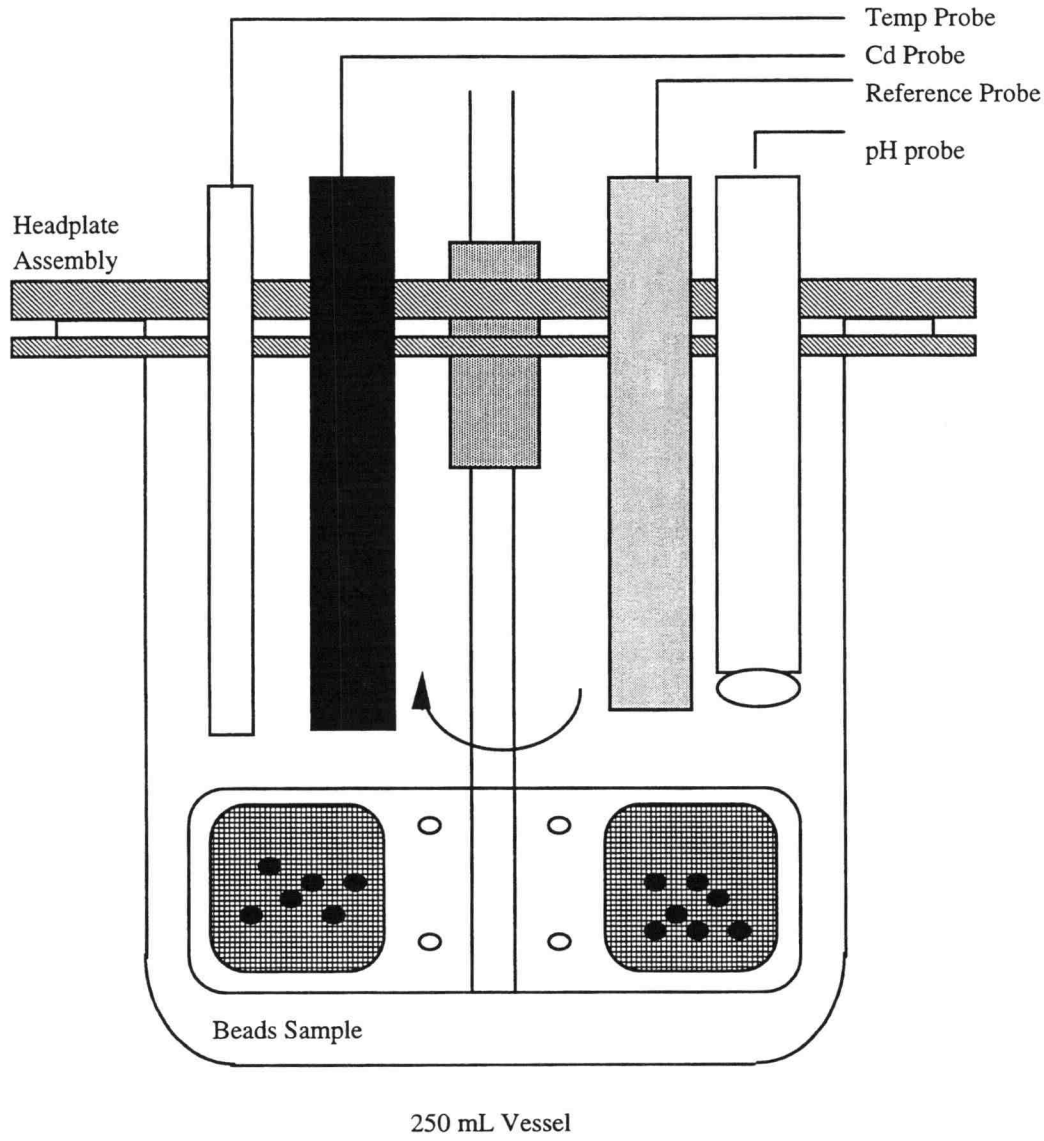

Figure 4.1 Spinning basket reactor

The high concentration of hydrogen ions loaded to the vessel displaced the adsorbed cadmium ions. The kinetics of cadmium release and H^+ adsorption were

followed by measuring the cadmium ion concentration and pH of the bulk solution phase with time. The pH was monitored continuously, whereas 0.5 mL samples were periodically removed from the reactor and analyzed for Cd^{+2} concentration by ion chromatography (IC).

Two control experiments were performed. In the first control experiment, the pH curve for the chitosan beads was measured to determine the extent of H^+ consumed by adsorption for the case where no cadmium ions were present in the system. Specifically, 0.5 g of chitosan beads were packed in the hollow propeller cells of the spinning-basket reactor and immersed in 200 mL of deionized distilled water for 48 hours. The pH at the start of the experiment was about 7.0. The mixing speed was 150 rpm. Then, 65 mL of 0.1 N HNO_3 solution was added to the vessel and the pH was measured continuously until an equilibrium pH value was reached. During this time, the pH of the bulk solution increased as hydrogen ions adsorbed onto weakly basic $-NH_2$ sites on chitosan.

In the second control experiment, the stability of chelated cadmium ions adsorbed on chitosan beads was tested. Specifically, the cadmium adsorbed chitosan beads were immersed in 200 mL distilled water within the reactor at 25 ° C and mixed at 150 rpm. Samples were removed from bulk solution at 123 and 171 hours and analyzed for cadmium ion concentration by ion chromatography (IC).

Shake flask experiments were carried out to determine the equilibrium hydrogen and cadmium loading on the chitosan beads at different pH levels. Specifically, 0.1 g of chitosan beads were mixed with 40 mL of 200 mg /L cadmium ion solution in a 125 mL

Erlenmeyer flask and agitated at 120 rpm and 25 °C for 51 hours to ensure that adsorption equilibrium was reached. After adsorption, different doses (1 to 4 mL) of HNO_3 solution (10^{-4} to 1 N) was added to the flask to process the desorption for another 140 hours. The adsorption/desorption parameters for shake flask experiments are summarized in Table 4.2.

Table 4.2 The adsorption/desorption parameters for shake flask experiments

Process Condition	Variable and Units
Temperature	25 °C
Bead loading (m_b)	0.1 g
Initial solution volume (V)	40 mL
Initial Cd^{+2} concentration (C_o)	200 mg Cd/L
Acid (HNO_3) concentration (C_a)	0.0001 - 0.1 N
Agitation	120 rpm

4.2.3 Multiple Stage Desorption

In the multiple stage experiment, adsorbed cadmium was gradually displaced by the series addition of small doses of H^+. A discrete volume of 0.1 N HNO_3 was added to the vessel. If the equilibrium pH was above 2.0, then additional 0.1 N HNO_3 was added. The experiment was completed when an equilibrium pH of 2.0 was achieved.

A modified titration procedure suggested by previous works (Kunin, 1958; Helfferich, 1962) for studying ion exchange or adsorption characteristics was modified in the present study to determine hydrogen ion adsorption on chitosan beads. Specifically, a 0.5 g of chitosan beads were packed into the hollow propeller cells of the spinning-basket reactor and immersed in 200 mL of deionized distilled water at 150 rpm for 48 hours. After the chitosan beads were saturated with water, a discrete volume of 0.1 N HNO_3 was added to the vessel to initiate hydrogen ion adsorption on chitosan beads. Until an equilibrium pH value was reached, a different amount of 0.1 N HNO_3 solution was sequentially added to the vessel.

4.2.4 pH and Cadmium Ion Concentration Measurements

The pH measurements were performed with an Orion model 91-02 combination pH electrode and Orion model 720A ion selective electrode (ISE) meter. The pH readings were recorded by a computer every ten minutes during the experiment. The pH saturation curve was expressed as the amount of hydrogen ion sorbed per gram of chitosan beads versus the equilibrium pH of the bulk solution.

The cadmium ion concentration was measured by IC analysis as described earlier. The cadmium adsorption capacity is calculated by

$$Q = \frac{(C_0 - C(t))V}{m_b} \qquad (4.1)$$

where C(t) is the cadmium ion concentration in the vessel at different adsorption or desorption times (mg Cd/L), C_0 is the initial cadmium concentration in the vessel before adsorption (mg Cd/L), m_b is the mass (g) of chitosan beads in the spinning basket reactor impeller assembly, Q is the cadmium adsorption capacity on the chitosan beads (mg Cd/g-chitosan), and V is the current cadmium solution volume loaded in the spinning basket reactor vessel (L).

The percentage of cadmium desorbed from the beads is calculated by

$$D(\%) = \left(1 - \frac{C(t) - C_{min}}{C_0 - C_{min}}\right) \cdot 100 = \left(1 - \frac{Q(t)}{Q_f}\right) \cdot 100\ \% \quad (4.2)$$

or

$$D(\%) = \left(1 - \frac{C(t) - C_{min,i}}{C_{0,i} - C_{min,i}}\right) \cdot 100 = \left(1 - \frac{Q_i(t)}{Q_{i,f}}\right) \cdot 100\ \% \quad (4.3)$$

where D (%) is the percentage of cadmium desorbed at a given desorption time, C_{min} is the lowest cadmium concentration along the adsorption or desorption process (mg Cd/L), $C_{0,i}$ is the initial cadmium concentration in the spinning basket reactor at specific desorption stage " *i* " (mg Cd/L), and $C_{min,i}$ is the lowest cadmium concentration along the adsorption or desorption process at a specific desorption stage (mg Cd/L), Q_f is the final cadmium adsorption capacity on the chitosan beads (mg Cd^{+2}/g chitosan) .

The hydrogen ion adsorption capacity ($\Delta Q_i (H^+)$) on the chitosan beads was based on pH measurements of the bulk solution in the vessel. The hydrogen ion adsorption capacity at ith desorption stage $\Delta Qi(H^+)$ is given by

$$\Delta Q_i (H^+) = \frac{C_a V_a - (10^{-pH_t} \cdot V_t)}{m_b} \quad (4.4)$$

where C_a is the concentration of HNO_3 (mole H^+/L) added into the spinning basket reactor before desorption, pH_t is the pH value at different adsorption or desorption times, $\Delta Q_i (H^+)$ is the hydrogen ion adsorption capacity for chitosan beads at the *i*th desorption stage (mg H/g-chitosan), V_a is the acid volume (L) added into the spinning basket reactor, V_t is the volume (L) of solution in the spinning basket reactor at a given time.

The accumulated hydrogen ion adsorption capacity $Q(H^+)$ is given by

$$Q (H^+) = \sum_{i=1}^{n} \Delta Q_i \quad (4.5)$$

where n is the number of the desorption stage, $Q(H^+)$ is the accumulated hydrogen ion adsorption capacity in the present stage (mg Cd/g-chitosan).

4.3 Results and Discussion

4.3.1 Kinetics of Adsorption and Desorption

The cadmium ion concentration versus time profile in the spinning basket reactor is presented in Figure 4.2 (a) for a single stage adsorption/desorption experiment. The cadmium ion concentration decreased significantly from 200 to 183 mg Cd^{+2}/L during the first four hours of adsorption and then slightly decreased to reach a final cadmium concentration of 179 mg Cd^{+2}/L at 51 hours. The total solution volume was 196 mL.

After adsorption, 65 mL of 0.1 N nitric acid was added to the vessel to initiate the desorption process. The cadmium concentration increased sharply during the first 12 hours of desorption following the addition of nitric acid, and then leveled off after 75 hours of desorption. The hydrogen ion capacity for the chitosan beads and the pH change in the cadmium solution are provided in Figure 4.2 (b) for both the adsorption and desorption processes. Similarly, the hydrogen ion capacity gradually increased and reached a final value between 8.6 and 9.5 mmole H^+/g chitosan. The pH of the cadmium solution also decreased with the addition of nitric acid and then rose to a final value of 2.17.

The stability of the adsorbed cadmium ions in the chitosan beads was determined. Specifically, the cadmium-adsorbed chitosan beads were immersed in 200 mL of distilled water within the spinning basket reactor at 25 °C and mixed at 150 rpm for 93 hours. Only a trace amount of cadmium ions were released back into the water during the desorption (Table 4.3). Form this control experiment, we conclude that the exchange

Table 4.3 Stability of the adsorbed cadmium ion in distilled water at pH 6.0

Time (h)	Q (mg Cd/g)	pH	Cd^{+2} concentration (mg Cd^{+2}/L)
51	9.86	6.73	0.00
87	9.55	6.31	0.78
144	9.18	6.20	1.71

(a)

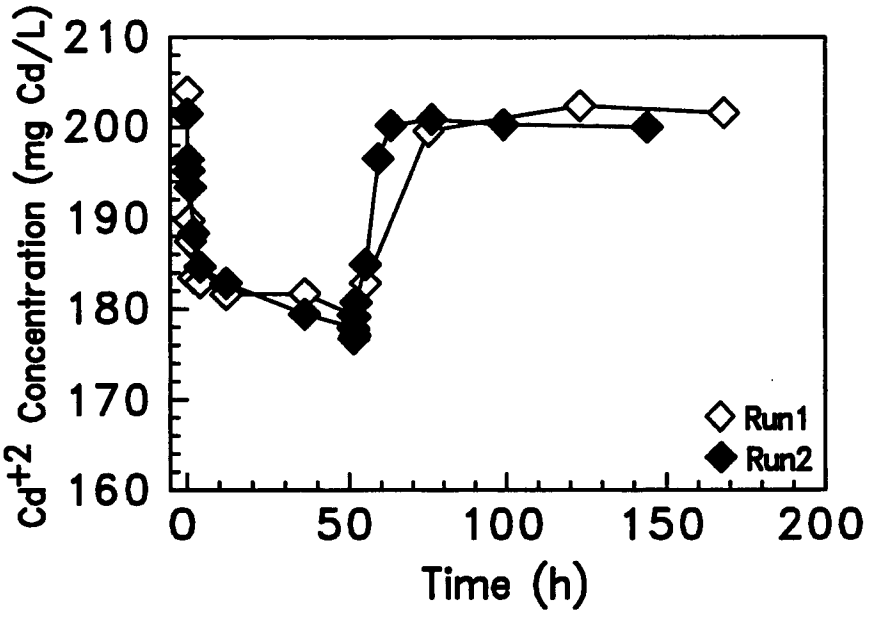

(b)

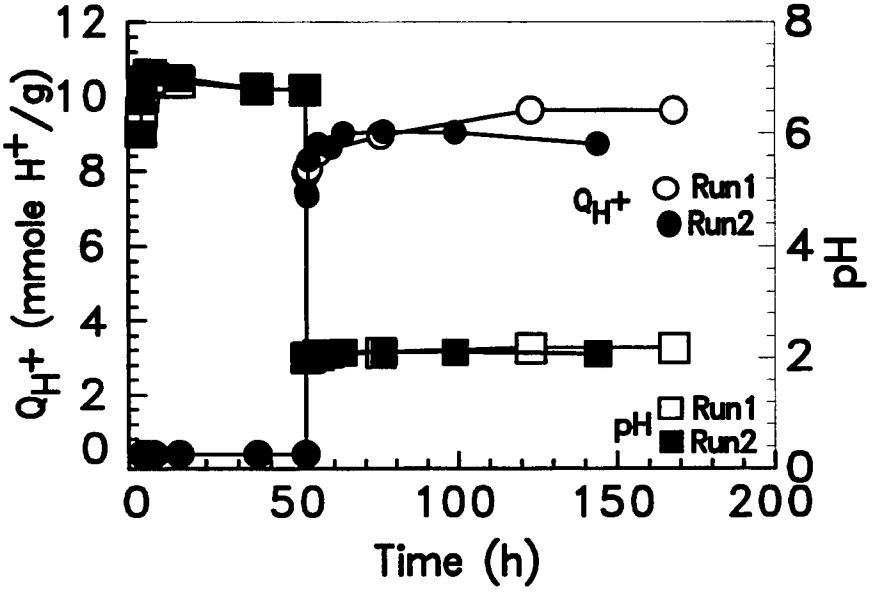

Figure 4.2 (a) cadmium ion concentration versus time (b) hydrogen ion capacity and the pH change in the cadmium solution in the spinning basket reactor for a single stage adsorption/desorption experiment

between the adsorbed cadmium ions with the hydrogen ions on active sites (-NH_2 groups) of the chitosan beads during the desorption process requires hydrogen ions from the addition of the nitric acid.

In another control experiment using the spinning basket reactor, 65 mL of 0.1 N nitric acid were added to 0.5 g chitosan beads to determine the hydrogen ion capacity in cadmium-free water. Profiles for the hydrogen ion consumption and pH are presented in Figure 4.3. From Figure 3, 8.9 mmole H^+ per gram of chitosan and a final pH value of 2.06 were reached 140 hours after the addition of nitric acid. It is notable that the hydrogen ion consumption of 8.9 mmole H^+/g chitosan is consistent with the hydrogen ion consumption data presented in Figure 4.2 (b).

4.3.2 Optimum pH and Hydrogen Ion Consumption

Hydrogen ions are needed to replace the cadmium ions adsorbed on the amine groups of the chitosan beads. Therefore, different amounts of hydrogen ion were added into the vessel to determine the effect of hydrogen ion consumption on the percentage of cadmium desorbed and the final pH value of the cadmium solution obtained in the single stage desorption process. The percentage of cadmium desorbed is presented in Figure 4.4 as a function of desorption time for different amounts of hydrogen ion initially charged to the vessel. Specifically, after cadmium adsorption, different amounts of 0.1 N nitric acid (22.2 mL , 50 mL and 65 mL respectively) were dosed into the reactor. At a final pH

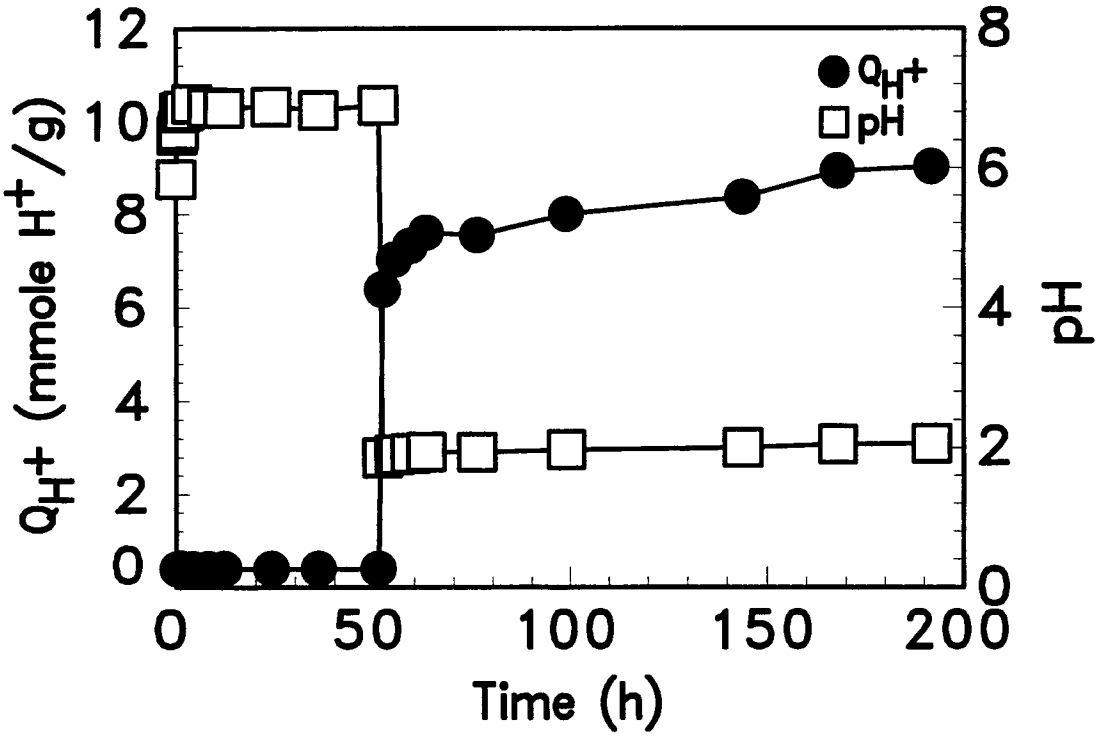

Figure 4.3 The hydrogen ion consumption and pH versus time for cadmium-free water saturation experiment

value of 2.0, 94 % of cadmium desorption was achieved and 8.3 mmole H^+ per gram of beads were consumed. It is interesting to note that even at a final pH of 4.7, 80 % of cadmium desorption was accomplished.

The multiple stage desorption experiment was carried out by a series addition of nitric acid solution into the spinning basket reactor. The effect of pH on the percentage of cadmium desorbed is given in Table 4.4. After 6 stages of desorption in series, 95.7 % of the cadmium desorption was achieved at a final pH of 3.0. Even at an equilibrium pH

Table 4.4 The effect of pH adjustment on the % of cadmium desorbed (D) for the multiple stage desorption experiment

Stage	Time (h)	pH	D (%)
A-1	48	7.00	
D-1	67	6.80	7.01
D-2	78	6.64	27.42
D-3	90	5.80	39.75
D-4	101	5.48	39.33
D-5	119	4.36	84.66
D-6	141	3.00	95.72

of 4.36, 84.6 % of cadmium desorption was reached, consistent with the single stage desorption process (Figure 4.4).

Previous researchers used shake flask experiments to study the effect of pH on heavy metal ion adsorption capacity. Eric and Roux (1992) used the shake flask experiment to study the influence of pH on the heavy metal ion binding onto a fungus-derived biosorbent. Inoue et al. (1995) also used the shake flask experiment to evaluate the effect of the hydrochloric acid concentration on the adsorption of platinum group metal ions onto chemically modified chitosan.

Shake flask desorption experiments were also performed in this present study and compared to the results from the spinning basket reactor experiments and to previous works. Data for the percentage of cadmium desorbed is plotted as a function of the

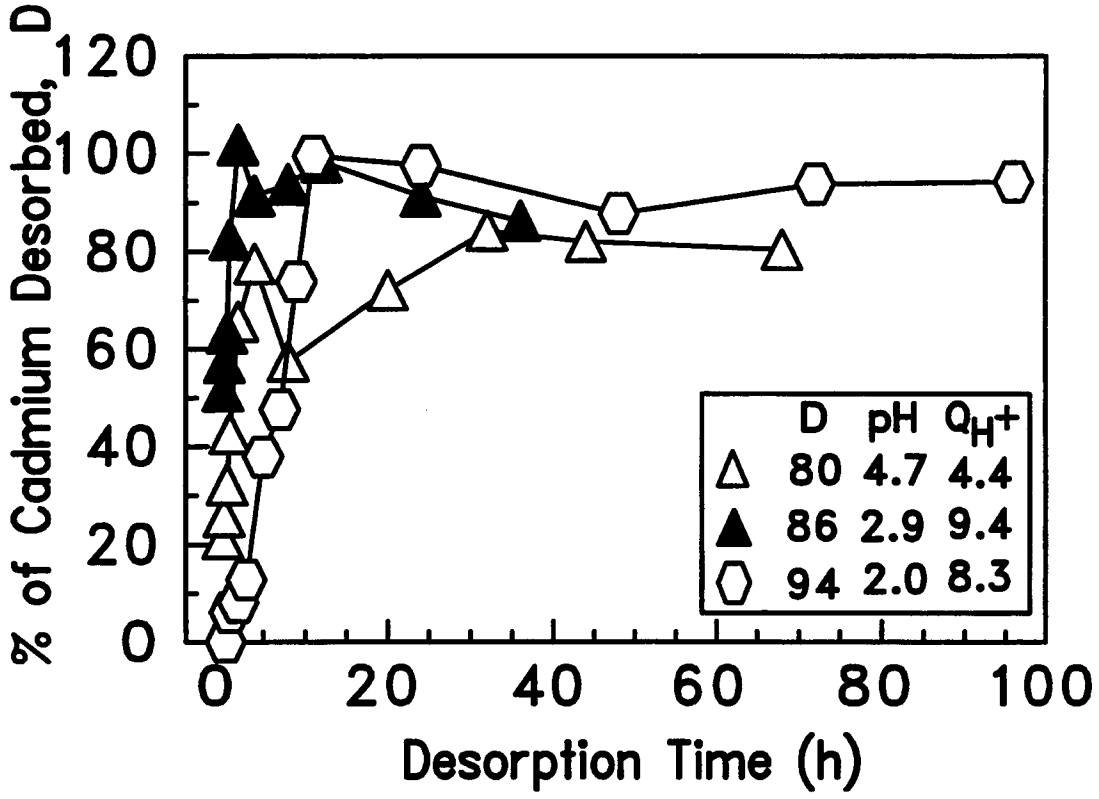

Figure 4.4 The percentage of cadmium desorbed versus desorption time for different amounts of hydrogen ion initially charged to the vessel

equilibrium pH in Figure 4.5. At an equilibrium pH of 2.1, 100 % cadmium desorption was achieved. Increasing the equilibrium pH decreased the percentage of cadmium desorbed according to an S-shaped profile. This S-shaped profile was also observed by Schultz et al. (1987) and Aldor et al. (1995). Jha et al. (1988) also found that 88 % of cadmium desorption was obtained 24 hours after addition of 0.01 N hydrochloric acid to 100 mg of cadmium-loaded chitosan. Also, 80 % cadmium desorption occurred at pH 3.0, a similar result as the present study. Hayes and Leckie (1987) presented an S-

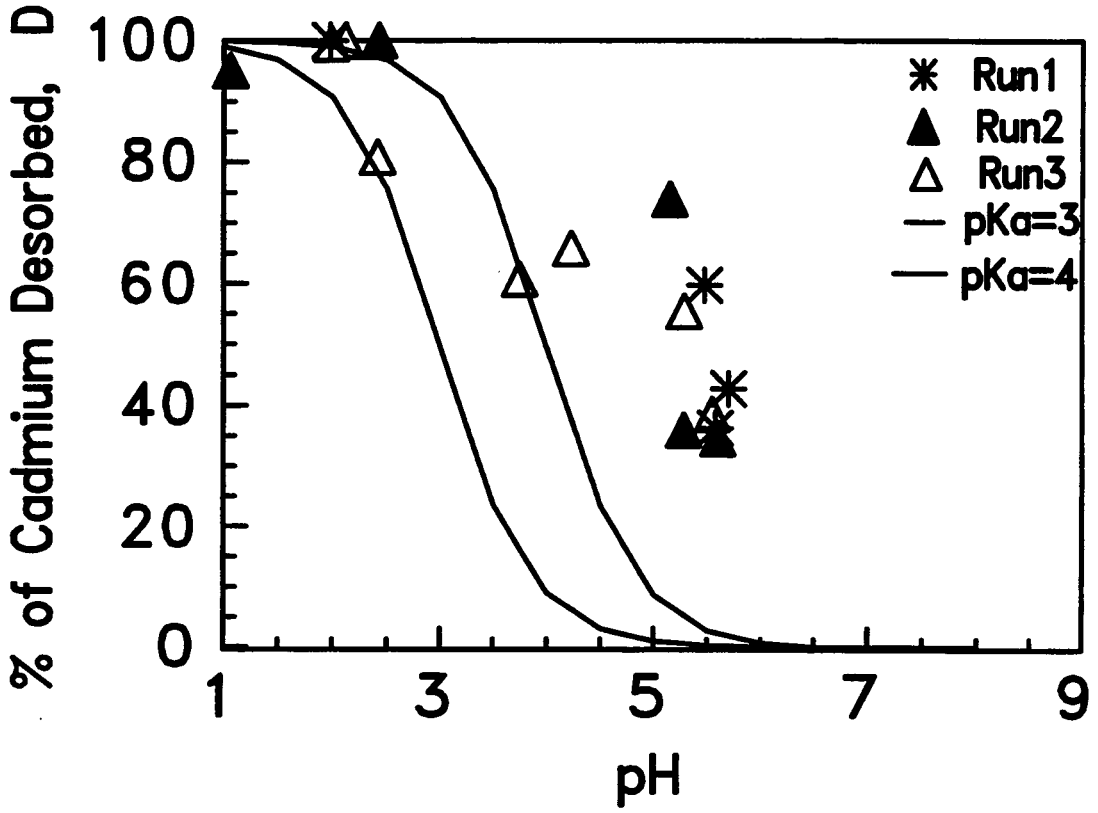

Figure 4.5 The experimental and predicted percentages of cadmium desorbed versus equilibrium pH for shake flask experiments

shaped profile for Cd^{+2} and Pb^{+2} adsorption on goethite, which has a complimentary profile to the present desorption study.

Results of the percentage of cadmium desorbed from the shake flask desorption experiment were consistent with the spinning basket desorption experiment. However, the results for hydrogen ion consumption were quite different. The inconsistent hydrogen ion consumption may be due to the sensitivity of the pH measurement. A small change in

the results for hydrogen ion consumption were quite different. The inconsistent hydrogen ion consumption may be due to the sensitivity of the pH measurement. A small change in pH near 2 resulted in a significant difference in hydrogen ion consumption. Also the modes of mixing between the spinning basket reactor experiment and the shake flask experiment were different. The mixing in the spinning basket reactor was more uniform and resulted in more repeatable and reliable pH measurements. Therefore, the measurements for H^+ adsorption on the chitosan beads for the shake flask experiments at low pH need to be interpreted with caution.

The titration curve describing the equilibrium relationship between the pH and hydrogen ion capacity on the crosslinked chitosan beads is presented in Figure 4.6. A similar titration curve was observed by Yoshida et al. (1994) for adsorption of hydrochloric acid on poly(ethylene imine) chitosan. The titration curve in Figure 4.6 apparently has two equivalent points. For the first equivalent point of 4.0, hydrogen ions exchange with the imino groups (=NH) on the chitosan beads within the crosslinked outer shell. The second equivalent point at pH of 2.5 shows that hydrogen ions penetrate deeper to the uncrosslinked core of bead to exchange with the free amine groups ($-NH_2$).

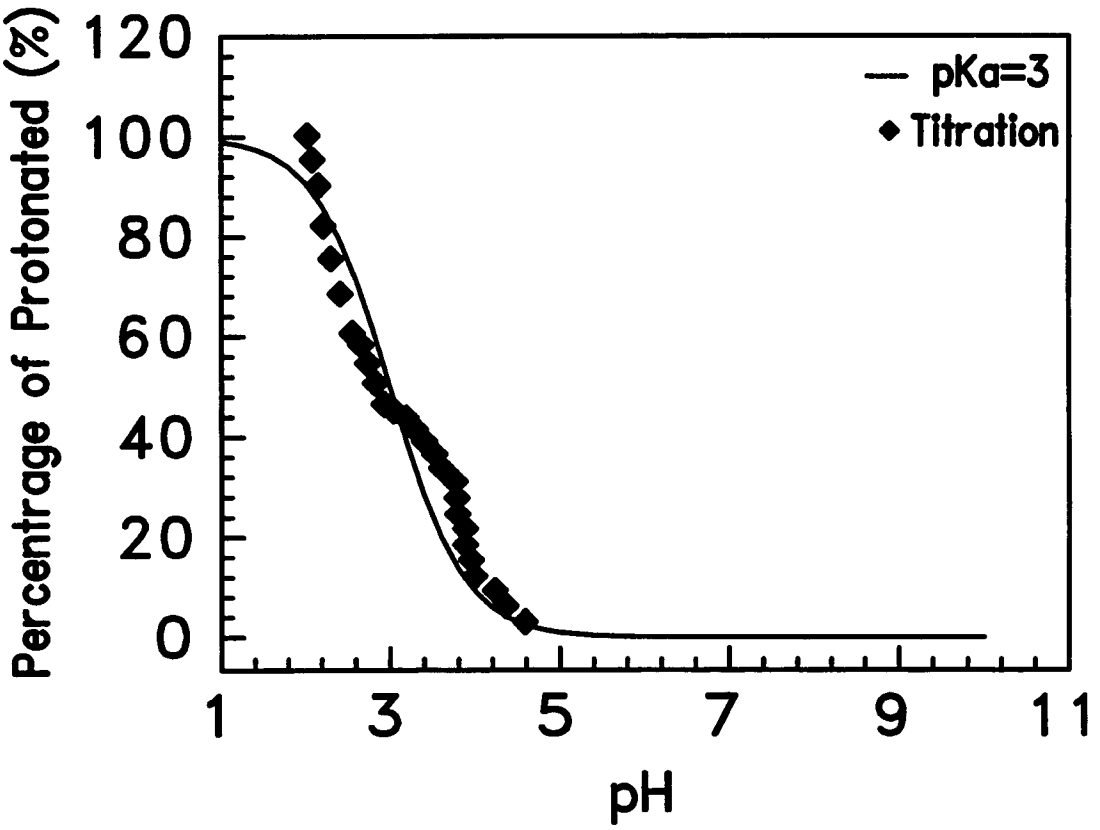

Figure 4.6 The titration curve for crosslinked chitosan beads

4.3.3 Exchange Between Cadmium Ions and Hydrogen Ions

The proposed competitive ion exchange scheme for cadmium ions and hydrogen ions with nitrogen atoms on crosslinked chitosan is presented in Figure 4.7. The addition of hydrogen ions displaces the adsorbed cadmium ions. A Langmuir-Freundlich equation for multiple components is developed below to model the competition between the hydrogen ions and the adsorbed cadmium ions on the crosslinked chitosan beads.

Model Development. Three major assumptions are made for the equilibrium model. First, the adsorption of cadmium ions on the crosslinked chitosan beads may follow the chelation binding mechanism validated by Inoue et al. (1988), which shows that divalent cadmium ions adsorb onto amine groups of chitosan to form metal-chelate complexes with composition of 1 mole of cadmium to 2 mole of glucosamine unit. Second, the Cd^{+2} ions chelate only with imino (-CH=N-) groups in the outer shell of the crosslinked chitosan. In Chapter 3, it was shown that the crosslinked chitosan bead

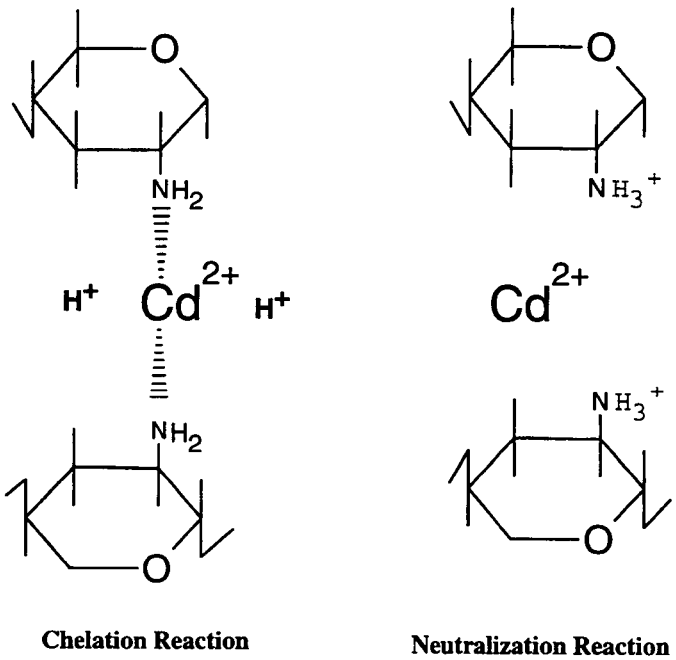

Figure 4.7 The competitive ion exchange scheme

contains a crosslinked outer shell where all amine groups are derivativized to imino (-CH=N-) crosslinks, and an inner core of uncrosslinked chitosan containing free amine (-NH_2) groups. In the present desorption experiments, the maximum adsorption capacity was around 15 mg Cd^{+2}/g chitosan. Thus, the value for r_M from equation (3-24) is 1.32 mm, which is larger than r_c value of 1.29 mm for the crosslinked chitosan beads used in the desorption experiments. Consequently the adsorbed cadmium is only localized in the crosslinked outer shell of the chitosan beads where only imino chelation sites are present. Therefore, the chelation reaction is expressed as

$$2\ -C=NH\ +\ Cd^{+2} \overset{K_{Cd}}{\Leftrightarrow} 2\ \text{-C=NH} \bullet Cd^{+2} \qquad (4\text{-}6)$$

The third assumption is that the equilibrium constants for the adsorption of hydrogen ions on the chitosan beads may follow the acid/base neutralization reactions of the form

$$-C=NH + H^+ \overset{K_a'}{\Leftrightarrow} \text{-C=}NH_2^+ \qquad (4\text{-}7\ a)$$

$$or\quad \text{-C-}NH_2 + H^+ \overset{K_a'}{\Leftrightarrow} \text{-C-}NH_3^+ \qquad (4\text{-}7\ b)$$

In other words, the equilibrium constant K_a' is assumed to be the same for either imino or amine groups. Consequently, Figure 4.6 is assumed to have only one apparent pK_a value at pH 3.0. From equations (4-6) and (4-7), K_{cd} and K_a' are defined as

$$K_{Cd} = \frac{[\ -C=NH \bullet Cd^{+2}\ ]}{[\ -C=NH\ ]\ [\ Cd^{+2}\ ]^{1/2}} \tag{4-8}$$

$$K_a' = \frac{[\ -C=NH_2^{+}\ ]}{[\ -C=NH\ ]\ [\ H^{+}\ ]} \tag{4-9}$$

If the overall active number of adsorption sites on the crosslinked chitosan bead is conserved, then the equilibrium constants K_{cd} and K_a' can be expressed as

$$K_{Cd} = \frac{2\ q_{Cd}}{(\ Q_M - 2\ q_{Cd} - q_H\ )\ C_e^{\ 1/2}} \tag{4-10}$$

$$K_a' = \frac{q_H}{(\ Q_M - 2\ q_{Cd} - q_H\ )\ C_{ae}} \tag{4-11}$$

where C_e is the equilibrium cadmium ion concentration in the vessel (mole /L), C_{ae} is the equilibrium hydrogen ion concentration in the cadmium solution (mole/L), K_a' is the equilibrium constant $(mole/L)^{-1}$ for the neutralization reaction, K_{cd} is the equilibrium constant $(mole/L)^{-1/2}$ for chelation, Q_M is the theoretical maximum capacity of chitosan (6.2 mmole active sites/g chitosan), q_{Cd} is the equilibrium cadmium ion capacity of the crosslinked chitosan beads (mmole Cd^{+2}/g chitosan), and q_H is the equilibrium hydrogen ion capacity of the crosslinked chitosan beads (mmole H^{+}/g chitosan).

By solving for q_{Cd} and q_H from equations (4-10) and (4-11), the following Langmuir-Freundlich equations were derived, based on the binary mixture model presented by Ruthven (1984):

$$q_{Cd} = \frac{K_{Cd}\ C_e^{\ 1/2}\ Q_M\ /\ 2}{1 + K_a'\ C_{ae} + K_{Cd}\ C_e^{\ 1/2}} \tag{4-12}$$

$$q_H = \frac{K_a'\ C_{ae}\ Q_M}{1 + K_a'\ C_{ae} + K_{Cd}\ C_e^{\ 1/2}} \tag{4-13}$$

The sum of q_{Cd} and q_H is expressed as q, given by

$$q = q_{Cd} + q_H = \frac{K_{Cd} C_e^{1/2} Q_M / 2 + K_a' C_{ae} Q_M}{1 + K_a' C_{ae} + K_{Cd} C_e^{1/2}} \qquad (4\text{-}14)$$

In equations (4-12) and (4-14), $Q_M/2$ is equal to 3.1 mmole Cd^{+2}/g chitosan.

Recall from equation (4-3) that the percentage of cadmium desorbed (D) is given by

$$D(\%) = \left(1 - \frac{q_{Cd}}{q_{Cd,f}}\right) \cdot 100\ \%$$

where $q_{Cd,f}$ is the final cadmium adsorption capacity before the desorption process is initiated (mmole Cd^{+2}/g chitosan). Therefore, the percentage of the cadmium desorbed into the cadmium solution during the desorption process is expressed as

$$D(\%) = \left(1 - \frac{K_{Cd} C_e^{1/2} Q_M / 2}{1 + K_{Cd} C_e^{1/2} + K_a' C_{ae}} \frac{1}{q_{Cd,f}}\right) \cdot 100\ \% \qquad (4\text{-}15)$$

Estimation of Equilibrium Constants. The pK_a value of the crosslinked chitosan beads was obtained from the pH value at which 50 % of the active sites were protonated. The pK_a value estimated from Figure 4.6 was 3.0. In other words, the pK_b value of the conjugated base was 11.0 (Snoeyink and Jenkins, 1982). In this study K_a' is defined as the inverse of K_a. Based on the relationship between pK_a and K_a ($pK_a = -\log K_a$), the value of K_a' was equal to 10^{pKa}. Therefore, the K_a' value was 1000 $(mole/L)^{-1}$. Muzzarelli (1977) found that the pK_a value for chitosan was 6.3. Similarly, the pK_b for the base -C-NH_2 was 7.7. The pK_b differences may suggest that the crosslinked imino group (=NH) on chitosan is a weaker base than the uncrosslinked amine group (-NH_2).

Both the titration curve for adsorption of hydrochloric acid onto poly(ethylene imine) chitosan beads and the derived pK_a value of 4.0 by Yoshida et al. (1994) are similar with the results of this present work.

Once K_a' was obtained, K_{cd} was estimated. The $q_{Cd,f}$ values at C_e around 200 mg Cd^{+2}/L (1.79 mmole Cd^{+2}/L) and pH at 6.5 to 7 were between 0.13 and 0.17 mmole Cd^{+2}/g chitosan. After substitution of K_a', C_{ae}, C_e, Q_M, and $q_{Cd,f}$ values into equation (4-15), K_{cd} was determined when the minimum sum of squares between the data points given in Figure 4.5 for the percentage of cadmium desorbed (D) and the predicted values from equation (4-15) was achieved. The K_{cd} value was estimated to be 0.57 $(mole/L)^{-1/2}$. This chelation reaction constant was also compared to the stability constant data for metal complexes on organic ligands (IUPAC, 1979) which showed that the binding constant of cadmium on pyridine (imine ligand) and sterotonin (amine ligand) were $10^{1.36}$ and $10^{3.6}$ $(mole/L)^{-1/2}$ respectively. Therefore, the value for estimated K_{cd} indicated that the cadmium did not bind very strongly to imino groups on chitosan. This low binding constant facilitated the desorption process as the hydrogen ions easily displaced the cadmium ions to accomplish the neutralization reaction. However, hydrogen ions were still required for desorption because water alone could not desorb the bound cadmium.

Another approach for the calculation of K_{cd} was considered by using the low cadmium concentration adsorption isotherm data for 2.5 wt % crosslinked chitosan beads (Figure 2.10). In Figure 2.10, q_{Cd} is equal to 30.66 mg Cd^{+2}/g chitosan (0.27 mmole/g

chitosan) at an equilibrium cadmium concentration of 234.4 mg Cd^{+2}/L (2.09 mmole Cd^{+2}/L). According to equation (4-12), when the pH is greater than or equal to 7.0, the product of the $K_a' C_{ae}$ will be much smaller than the product of $K_{Cd}C_e^{1/2}$. The value of K_{Cd} was determined by setting C_e, Q_M and q_{Cd} equal to 2.09 mmole/L, 6.2 mmole/g , and 0.27 mmole/g respectively in equation (4.12). The K_{cd} value estimated at pH 7.0 was 2.12 $(mole/L)^{-1/2}$ which is higher than the K_{cd} value of 0.57 $(mole/L)^{-1/2}$ estimated by equation (4.15) . However, the values of K_{Cd} estimated by both methods are in general much smaller than the value of K_a' . The value of K_{cd} is not sensitive to the prediction of the percentage of cadmium desorbed by Langmuir-Freundlich equation, since the K_a' value was three orders of magnitude bigger than the value of K_{cd}. Thus, the K_a' value (pK_a value) determines how adsorbed cadmium ions are displaced by hydrogen ions. In other words, the value of the K_a' is the limiting parameter for the predicting desorption profile.

At pH ranging from 1 to 8, the percentage of cadmium desorbed was predicted using equation (4-15). The experimental and the predicted percentages of cadmium desorbed are plotted in Figure 4.5 as a function of pH. In Figure 4.5, the majority of the adsorbed cadmium ions were desorbed at pH ranging from 3.0 to 5.5. As mentioned previously in Figure 4.6, the titration curve has two equivalent points at pH of 2.5 and 3.9. Since the experimentally occurred percentage of cadmium desorbed was significant even at pH values above 4.0, the first equivalent point at pH 3.9 may determine the actual

pK_a required for desorption. Therefore, for comparison, the predicted desorption profile assuming pK_a equal to 3.9 is also provided in Figure 4.5.

The experimental data for three repeat runs is scattered in the pH range from 4.5 to 6.0, as shown in Figure 4.5. Equation (4.15) does not accurately predict the behavior of desorption in this pH range. At pH ≥5.0, the desorption process may be more complex than the model suggests. The ion exchange behavior can not fully predict the chelation reaction.

CHAPTER 5

SUMMARY AND CONCLUSIONS

Chitosan is nature's most abundant biopolymer next to cellulose. It is well known that chitosan is a selective adsorbent for heavy metal ions. However, the chitosan raw material needs to be modified for use in low pH environments. To address this need, chemically modified porous chitosan beads were synthesized.

In order to fabricate porous chitosan beads, chitosan in acetic acid solution was cast into spherical gel beads of 3 mm diameter and precipitated to a gel in 2 M NaOH solution. Two chemical modifications of chitosan were considered. First, the linear chitosan chains within gel beads were heterogeneously crosslinked by glutaric dialdehyde solution. Second, partially N- acylated chitosan containing C_9 hydrocarbon side chains was formed by reacting nonanoyl chloride with chitosan in acetic acid solution. 7 % of the amine groups were N-acylated. N-acylated, crosslinked chitosan gel beads were formed by the same procedures as the 3 mm chitosan beads. The chitosan gel beads were then freeze dried to form porous beads.

N-acylation, crosslinking, and freeze drying steps must be combined to minimize acid solubility and maximize the internal surface area of the chitosan beads. The hydrocarbon chains on N-acylated, crosslinked chitosan beads increased the hydrophobicity of the biopolymer. However, N-acylation alone was not successful in reducing acid solubility. After acylation, 96.5 % of the chitosan in the uncrosslinked N-acylated chitosan beads dissolved in acetic acid solution after 24 hours.

Crosslinking significantly reduced the solubility of chitosan in dilute acid solution and greatly improved the internal surface area. The solubility of the crosslinked N-acylated chitosan beads decreased drastically from 96.5 % to 0.3 % as the extent of crosslinking increased from 0 to 0.81 mole GA/total mole $-NH_2$. The average internal surface area of uncrosslinked N-acylated chitosan beads was only 42.6 m^2/g. The average internal surface area of the 7 % N-acylated chitosan gel beads crosslinked with 0.81 mole GA/total mole $-NH_2$ was 223.6 ± 10.6 m^2/g after freeze drying. However, the internal surface area of the nonacylated chitosan beads was 192.4 m^2/g crosslinked and freeze dried under the same conditions.

A diffusion-limited modified shrinking core model was developed to describe the formation of the crosslinked layer within the gel bead. By applying this model to the crosslinking kinetics data, the effective diffusivity for glutaric dialdehyde in the gel beads was estimated to be $4.11 \bullet 10^{-8} \pm 8.17 \bullet 10^{-10}$ (1s) cm^2/s. The modified shrinking core model predicted the extent of crosslinking within the gel bead and the depletion of glutaric dialdehyde in the crosslinking bath as a function of time and initial glutaric dialdehyde concentration in the crosslinking bath. Model predictions were consistent with experimental results at a high initial crosslinking bath concentration of 2.5 wt % glutaric dialdehyde. However, the model under predicted the crosslinking rate at a low initial glutaric dialdehyde concentration of 0.75 wt %, suggesting a reaction limited process at lower extents of crosslinking.

The cadmium adsorption isotherms for the freeze-dried 7 % N-acylated and nonacylated chitosan beads crosslinked at three extents of crosslinking were measured.

N-acylation of uncrosslinked chitosan beads improved the saturation adsorption capacity from 169 to 216 mg Cd^{+2}/g-bead. All of the isotherms possessed a similar stepped shape. There was no significant difference in the adsorption capacity at final cadmium ion concentrations ranging from 4 to 200 mg/L. However, at final cadmium ion concentrations higher than 600 mg/L, the adsorption capacity decreased as the extent of crosslinking increased. The saturation adsorption capacity for 7 % N-acylated chitosan beads reduced from 136 to 86 mg Cd^{+2}/L when the extent of crosslinking was increased from 0.29 mole GA/total mole $-NH_2$ to 0.81 mole GA/total mole $-NH_2$, a reduction of 37 %.

On a chitosan basis, the crosslinked gel beads had a higher adsorption capacity than the freeze-dried chitosan beads at the same extent of crosslinking. The saturation cadmium adsorption capacities were 161 and 138 (mg Cd^{+2}/g-bead) respectively for 7 % N-acylated chitosan gel and freeze-dried beads.

There was no correlation between the high internal surface area and cadmium adsorption capacity for chitosan beads. The extent of crosslinking was the determining variable for cadmium adsorption on the chitosan gel beads and freeze-dried chitosan beads. Apparently, the freeze drying step of the bead synthesis process can be omitted without sacrificing the cadmium adsorption capacity. At the same time, the cost of producing the chitosan beads can be significantly reduced.

In order to understand how crosslinking affected the cadmium ion adsorption capacity, the distribution of the adsorbed cadmium within the bead was determined. EDAX and SEM images for crosslinked chitosan beads showed that the majority of the adsorbed cadmium was localized in the outer shell near the surface of the bead. There

was no significant Cd signal within the interior of the bead. A simple saturation adsorption model indicated that the cadmium loaded layer of the bead decreased as the extent of crosslinking increased. However, the saturation cadmium adsorption capacity leveled off to a plateau value of 83 mg Cd per gram of chitosan at higher extents of crosslinking.

Heterogeneous crosslinking was superior to than homogeneous crosslinking in two respects. First, homogeneous crosslinking reduced saturation cadmium adsorption capacity much more significantly than for heterogeneous crosslinking (49.6 mg Cd^{+2}/g vs. 103.3 mg Cd^{+2}/g) at extent of crosslinking of 0.81 mole GA/total mole -NH_2. Second, heterogeneous crosslinking was required for synthesis of crosslinked chitosan beads. The homogeneous crosslinking process was much faster than the diffusion limited heterogeneous crosslinking process. Consequently, it was impossible to prepare homogeneously crosslinked chitosan beads because a rigid crosslinked gel was formed before it could be cast into spherical particles.

To summarize, freeze drying increased the internal surface area of porous beads but decreased the cadmium adsorption capacity for 7 % N-acylated beads. Acylation improved the cadmium adsorption capacity but only at high cadmium concentrations exceeding 1300 mg Cd^{+2}/L. Crosslinking significantly reduced the cadmium adsorption capacity. An optimum extent of crosslinking equal to 0.29 mole GA/total mole -NH_2 increased the internal surface area and rendered the bead insoluble in acid solution while minimizing the reduction in the cadmium adsorption capacity.

The desorption of cadmium from cadmium-adsorbed chitosan beads with dilute nitric acid was tested to evaluate the feasibility of recovering the cadmium and

regenerating the adsorbent. Hydrogen ions were needed to displace the cadmium ions adsorbed on the chitosan beads. Two types of desorption experiments, single stage and multiple stage, were performed using a Carberry spinning basket reactor. In the experiments, 0.5 g of chitosan beads were packed into the hollow impeller basket assembly and contacted with 200 mL of 200 mg /L cadmium ion solution at 150 rpm and 25 °C until the adsorption equilibrium was achieved. After adsorption, different doses of 0.1 N HNO_3 solution were added to the vessel to initiate the desorption process. The cadmium concentration increased sharply during the first 12 hours of desorption following the addition of nitric acid, and then leveled off. At a final pH value of 2.0, 94 % of cadmium desorption was achieved, and 8.3 mmole H^+ per gram of beads was adsorbed to displace the bound cadmium. Equilibrium shake flask experiments were carried out to determine the equilibrium hydrogen and cadmium loading on the chitosan beads at different pH levels. Decreasing the equilibrium pH increased the percentage of cadmium desorbed according to an S-shaped profile, consistent with the ion-exchange mechanism. A Langmuir-Freundlich model proposed that the desorption process is accomplished by displacing adsorbed cadmium ions with hydrogen ions. Based on the high efficiency of the desorption treatment, cadmium recovery and adsorbent regeneration is feasible.

In summary, chemical modifications of acylation and crosslinking improve the material properties of the chitosan beads for waste water treatment applications, but do not improve the adsorption capacity for cadmium ions. The adsorbent can be regenerated by dilute acid treatment, and 100 % cadmium recovery from the chitosan beads is feasible at pH less than 3.0.

Recommendations

Three recommendations for future research are suggested:

1. Use alternative crosslinking reagents such as poly(amine) or poly(imino) functional reagents to increase the density of amine adsorption sites while simultaneously crosslinking the chitosan chains.
2. Many industrial waste water matrices contain several heavy metal ions. Therefore, determine the multi-component heavy metal ion adsorption capacity on the chitosan beads.
3. Modify the bead synthesis process. The freeze drying process does not improve the adsorption capacity. Therefore, consider alternative drying methods that do not reduce the adsorption capacity and are less expensive than freeze drying.

BIBLIOGRAPHY

Aldor, I., Fourest, E., and Volesky, B., 1995. "Desorption of Cadmium from Algal Biosorbent." *The Canadian Journal Of Chemical Engineering*, 73, Aug., 516-522.

Boyd, R.H., and Phillips, P.J., 1993. Network Formation by Non-linear Polymers: Branching and Crosslinking; Gelation. The Science of Polymer Molecules. 1 st edition, Cambridge University Press, 38-50.

Carberry, J.J., 1976. *Chemical and Catalytic Reaction Engineering*, Chemical Engineering Series, McGraw-Hill, Inc.

Coughlin, R.W., Deshaies, M.R., and Davis, E.M., 1990. "Chitosan in Crab Shell Wastes Purifies Electroplating Wastewater." *Environmental Progress.* 9 (1), 35-39.

Delben F., and Muzzarelli, R.A., 1989. "Thermodynamic Study of the Interaction of N-carboxymethyl Chitosan with Divalent Metal Ions," *Carb. Polymers, 11*, 221-232.

Dusek K., and MacKnight, W. J. 1988. "Cross-linking and Structure of Polymer Networks", *ACS Symposium Series 367, Cross-linked Polymers: Chemistry, Properties, and Applications*, 3-27.

Fourest, E., and Roux, J. C., 1992. "Heavy Metal Biosorption By Fungal Mycelial By-roduct: Mechanisms and Influence of pH." *Appl. Microbiol. Biotechnol.*, 37, 399-403.

Godmund, S., Hans, G., and Olav, S. 1989. "Imhomogeneous Polysaccharide Ionic Gels", *Carbohydrate Polymers*, 10, 31-54.

Gregg, S.J., and King, K.S.W. 1982. *Adsorption, Surface Area, and Porosity*, Academic Press.

Hardy, P. M., Nicholls A. G., and Pydon, H.N. 1969. "The Natural of Glutaraldehyde in Aqueous Solution", *Chemical Communications*, 565-566.

Hayes, K.F., and Leckie, J.O., 1987. "Modeling Ionic Strength Effects on Cation Adsorption at Hydrous Oxide/Solution Interfaces." *Journal of Colloid and Interface Science*, 115, 564-572.

Hirano, S., Ohe, Y., and Ono, H. 1976. "Selective N-acylation of Chitosan." *Carb. Res., 47*, 315-320.

Hsien T. Y., and Rorrer, G. L. 1995. "Effects of Acylation and Crosslinking on the Material Properties and Cadmium Ion Adsorption Capacity of Porous Chitosan Beads", *Seperation Science and Technology*, 12 (30), 2455-2475.

Huheey, J.E. 1983. *Inorganic Chemistry, Principles of Structure and Reactivity*, Harper International, pp. 359-381.

Inoue, K., Baba, Y., Yoshizuka, K., Noguchi, H., and Yoshizaki, M. 1988. "Selectivity Series in the Adsorption of Metal Ions on a Resin Prepared by Crosslinking Copper (II) Complexed Chitosan," *Chem. Lett.*, 1281-1284.

Inoue, K., Yamaguchi, T., Iwaski, M., Ohto, K., and Yoshizuka, K., 1995. "Adsorption of Some Platinum Group Metals on Some Complexane Types of Chemically Modified Chitosan." *Separation Science and Technol.*, 30, 12, 2477-2489.

Jha, I.N., Iyengar, L., and Rao, A.V.S., 1988. "Removal of Cadmium Using Chitosan." *J. Environs. Eng.*, 114, 962-974.

Kawahara, J., Ohmori, T., Ohkubo, T., Hattori S., and Kawamura, M. 1992. "The structure of Glutaraldehyde in Aqueous Solution Determined by Ultraviolet Absorption and Light Scattering", *Analytical Biochemistry*, 201, 94-98.

Kawamura, Y., Mitsuhashi, M., Tanibe, H., and Yoshida, H. 1993. "Adsorption of Metal Ions on Polyaminated Highly Porous Chelating Resin," *I & EC Research, 32*, 386-391.

King, C.J., Chairman. 1987. "Separation and Purification: Critical Needs and Opportunities; " *Committee Separation Science and Technology*; National Academy Press: Washington, DC.

Korn, A. H., Fearirheller S. H., and Filachione, E.M. 1972. "Glutaraldehyde: Nature of the Reagent", *J. Mol. Biol.*, 65, 525-529.

Koyama, Y., and Taniguchi, A., 1986. "Studied on Chitin X. Homogeneous Cross-linking of Chitosan for enhanced Cupric Ion Adsorption." *Journal of Applied Polymer Science*. 31, 1951-1954.

Kurita, K., Chikaoka, S., and Koyama, Y., 1988. "Improvement of Adsorption Capacity for Copper (II) Ion by N-Nonanoylation of Chitosan." *Chemistry Letters*, 9-12.

Lankford, P.W., and Torrens, K.D. 1988. "Reducing Wastewater Toxicity." *Chemical Engineering*, 95 (11), 72.

Levenspiel, O., 1984. Unreacted Core Model for Spherical Particles of Unchanging Size. Chemical Reaction Engineering. 2nd edition, 361-368.

Margel S., and Rembaum, A. 1980. " Synthesis and Characterization of Poly(glutaraldehyde). A Potential Reagent for Protein Immobilization and Cell Separation", *Macromolecules*, 13, 19-24.

Maruca, R., 1982. "Interaction of Heavy Metals With Chitin and Chitosan. III. " Chromium. *Journal of Applied Polymer Science*, 27, 4827-4837.

Masri, M.S., Reuter, F.W., and Friedman, M., 1974. "Binding of Metal Cations by Natural Substances." *Journal of Applied Polymer Science*, 18, 675-681.

Masri, M.S., Randall V.G., and Pittman, A.G., 1978. "Removal of Metallic Ions by Partially Crosslinked Polyamine Polymers." *ACS Polym. Prepr.* 19, 483-488.

McKay, G., Blair, H.S., and Findon, A. 1989. "Equilibrium Studies for the Sorption of Metal Ions onto Chitosan," *Indian J. Chem., 28A*, 356-360.

Monsan, P.,,Puzo, G., and Mazarguil, H. 1975. *Biochimie*, 57, 1281-1292.

Muzzarelli, R.A.A., and Tubertini, O. 1969. "Chitin and Chitosan as Chromatographic Supports And Adsorbents For Collection Of Metal Ions From Organic And Aqueous Solutions And Sea-Water." *Talanta*, 16, 1571-1577.

Muzzarelli, R.A.A., and Raith, G., Tubertini, O. 1970. "Separation of Trace Elements From Sea Water, Brine And Sodium And Magnesium Salt Solutions By Chromatography On Chitosan." *J. Chromatog.*, 47, 414-420.

Muzzarelli, R.A.A. 1971. "Selective Collection of Trace Metal Ions By Precipitation Of Chitosan And New Derivations Of Chitosan." *Anal. Chim. Acta.*, 54, 133-142.

Muzzarelli, R.A.A. 1973. *Natural Chelating Polymers*, Pergamon Press.

Muzzarelli, R.A.A., and Rocchetti, R., 1974. "The Use of Chitosan Columns For the Removal Of Mercury From Eaters." *J. Chromatog.*, 96, 115-121.

Muzzarelli, R.A.A. *Chitin,* Pergamon Press, 1977.

Nishimura, K., Nishimura, S., Seo, H., Nishi, N., Tokura, S., and Azuma, I., 1986. "Macrophage Activation With Multi-Porous Beads Prepared From Partially Deacetylated Chitin." *Journal of Biomedical Materials Research.*, 20, 1359-1372.

Perrin, D.D. 1979. *Stability Constants of Metal-ion Complexes: Part B Organic Ligands* (IUPAC), Pergamon Press.

Randall, J.M., Randall, V.G., McDonald, G.M., Young, R.N., and Masri, M.S., 1979. "Removal of Trace Quantities of Nickel from Solution." *Journal of Applied Polymer Science*. 23, 727-732.

Richards F. M., and Knowles, J. R. 1968. "Glurtaraldehyde as a Protein Cross-linking Reagent", *J. Mol. Biol.* 37, 231-233.

Roberts, G.A.F., and Taylor, K.E., 1989. "The Formation of Gels by Reaction of Chitosan with Glutaraldehyde." *Makromol. Chem.* 190, 951-960.

Rorrer, G.L., Hsien, T.Y., and Way, J.D., 1993. "Synthesis of Porous-Magnetic Chitosan Beads for Removal of Cadmium Ions from Waste Water." *I & EC Research*, 32, 2170-2178.

Rozzlle, L.T., 1987. *J.Am. Water Works Assn.*, 10, 53-59.

Ruthven, D.M., 1984. "Langmuir-Freundlich Equations." *Principles of Adsorption & Adsorption Processes*, John Wiley & Sons, Inc., 108.

Sandford, P.A., and Hutchings, G.P. 1987. "Chitosan- A Natural, Cationic Biopolymer: Commerical Applications." *Industrial Polysaccharides: Genetic Engineering, Structure/Property Relations and Applications.* ed. M. Yalpani, Amsterdam: Elsevier., 363-375.

Schultz, M.F., 1987. "Adsorption and Desorption of Metals On Ferrihydrite: Reversivility of Reaction and Sorption Properties of the Regenerated Solid." *Environ. Sci. Technol.* 21, 863-869.

Snoeyink, V., and Jenkins, D., 1982. *Water Chemistry.* 86-120.

Sposito, G. 1984. *The Surface Chemistry of Soils*, Oxford Univ. Press, New York.

Trujlllo, E.M., Jeffers. T.H., Ferguson, C., and Stevenson, H.Q. 1991. "Mathematically Modeling the Removal of Heavy Metals from Wastewater Using Immobilized Biomass." *Environ. Sci. Technol.*, 25(9), 1559-1565.

Tsuchiya, K. 1969. "Causation of itai-itai disease-an introduction review." *Keio J. Med.*, 18,181-211.

Udaybhaskar, P., Iyengar, L., and Prabhakara,R., 1990. "Hexavalent Chromium Interaction with Chitosan." *Journal of Applied Polymer Science.*, 39, 739-747.

Volesky, B. 1987. "Biosorbents for Metal Recovery, *TIBTECH, 5*, 95-101.

Weber, W., Jr; and Morris, J.C., 1963. "Kinetics of Adsorption on Carbon from Solution." *J. San. Eng. Div., ASCE, 89, SA2, 31-59.*

Wilke C. R., and Chang, P. 1955. *A.I.Ch.E. J.*, 1, 264.

Yang, T.C., and Zall, R.R., 1984. "Adsorption of Metals by Natural Polymers Generated from Seafood Processing Wastes." *Ind. Eng. Chem. Prod. Res. Dev.*, 23, 168-172.

Yen, S.S., Rembaum, A., and Landel, R.F., 1981. "Functional Magnetic Microspheres." *U.S.A. Patent 4,285,819.*

Yoo, R.S., 1987. *J.Am. Water Works Assn.*, 10, 34-38.

Yoshida, H., Kishimoto, N., and Kataoka, T. 1994. "Adsorption of Strong Acid on Polyaminated Highly Porous Chitosan: Equilibris." *Ind. Eng. Chem. Res.*, 33, 854-859.

APPENDICES

Appendix A

Experimental Procedures

Appendix A-1 Preparation of 7 % N-acylated Chitosan

1. Place 3.75 g of chitosan powder and 70 mL of 4.179 wt % acetic acid solution in a 250 mL beaker.
2. Mix the chitosan solution at 500 rpm for 20 minutes.
3. Store the chitosan solution in an orbital shaker at 25 °C and 120 rpm for 24 hours.
4. Add 70 mL of pure pyridine to the chitosan solution and manually stir for a while.
5. Place the chitosan solution in an ice bath and gradually add 0.28 mL of nonannoyl chloride.
6. Stir the acylated chitosan solution for 1 hour at 25 °C.
7. Place the acylated chitosan solution in an orbital shaker at 25 °C and 120 rpm for 48 hours.
8. Pour the acylated chitosan solution into a 1000 mL beaker and mix with 20 mL of ethyl acetate solution for 20 minutes.
9. Add 480 mL of acetone/water solution (7/1 v/v) to the acylated chitosan solution and manually stir for a while.
10. Repeat step 9 but use a fresh acetone/water solution.
11. Separate the white precipitate from the acetone/water solution and store in a 250 mL beaker.
12. Place the white precipitate in a hood at 25 °C for 20 minutes.

Appendix A-2 Gel Bead Casting

1. Arrange the tubes and deliver the chitosan solution or acylated chitosan solution to a spinnerette by a peristaltic pump.
2. Set the flowrate of the peristaltic pump to 0.95 mL/min.
3. Add 500 mL of 2 N NaOH solution into a 1000 mL beaker for the precipitation bath of chitosan solution.
4. Add 500 mL of 1 N methanolic NaOH solution (1/1 v/v) into a 1000 mL beaker for the precipitation bath of acylated chitosan solution.
5. Place the precipitation bath into an isothermal tank and keep at 25 °C.
6. Wet chitosan or acylated chitosan gel beads will be formed when the chitosan dopes have fallen down into the precipitation bath.
7. Separate the gel beads from the precipitation bath every 4 hours and place the gel beads in distilled water.
8. Wash the gel beads with distilled water to remove the remaining NaOH solution.
9. Decan the solution and collect the gel beads.

Appendix A-3 Crosslinking Experiments

1. Place 6.4 g of gel beads and 9.5 mL of GA solution (0.125 wt % to 5.0 wt %) to a 250 mL beaker.
2. Store the solution in an orbital shaker at 120 rpm and 27 °C.
3. Remove the beaker from the shaker at different crosslinking times (1, 2, 4, 8, 12, 24,

36, 48 hours) for crosslinking kinetics measurement.

4. Remove the beaker and withdraw 0.6 μL of glutaric dialdehyde from the beaker at desired time intervals ranging from 1 minute to a couple hours for the glutaric dialdehyde diffusivity estimation in the gel beads.
5. Remove the beaker from the shaker after 48 hours of crosslinking for final GA concentration analysis.
6. Separate the glutaric dialdehyde solution from the gel beads by filtration and store it in 20 mL vials for GC analysis.

Appendix A-4 Glutaric Dialdehyde Analysis by Gas Chromatography

GA Concentration Analysis by HP 5890 Series II Gas Chromatography

Start-up

1. Turn on the power switch on the right hand side of the HP 5890 series II GC unit and start the program on the HP Vectra 486/33N computer.
2. Open the gas cylinder valves, regulator, and final regulator at the auxiliary flow panel on the left side of GC unit. Set the carrier regulator to 60 psi.
3. Place the bubble flow meter for flowrate measurement.
4. Press the "Flow" and "B" pads to monitor the flowrate of channel B.
5. Open the total flow valve (split) and increase the flowrate of carrier to the desired value.
6. Plug the bubble flow meter to the split/splitless purge outlet.

7. Press the 'Time" pad three times to reach the stopwatch displays function.
8. Measure the total flowrate using the bubble flow meter and stopwatch display
9. Adjust the total flowrate to the desired value by repeating step 8.
10. Remove the bubble flow meter and connect the flame ionization detector adapter to the bubble flow meter.
11. Place the adapter of the bubble meter to the port of the flame ionization detector and measure the flowrate of the column by the flowrate meter and stopwatch.
12. Adjust the column head pressure valve to obtain the desired flowrate through the column.
13. Fully open the auxiliary gas valve (AUX) for detector B
14. Adjust the flowrate of AUX by tuning the valve knob and measure the flowrate by flow meter and stopwatch.
15. Fully open the hydrogen valve.
16. Adjust the flowrate of hydrogen by tuning the final stage regulator and measuring the flowrate by the flow meter and stopwatch.
17. Same procedures for hydrogen valve adjustment.
18. Remove the bubble flow meter and start the FID by pressing the FID ignition.
19. Change the channel to channel A by pressing the "low" and "A" pads.
20. Open the carrier flow valve to 2-4 psi to prevent the coating from thermally deteriorating.
21. Open the reference gas valve three turns to prevent the burn-out of the thermal conductivity detector (TCD).
22. Open the Windows operation system and execute the "Hp Chem" program.

23. Choose the 'Load" function in the "method" menu.
24. Choose the "glutar" file to start the GC unit and display the operation information on the screen.
25. Check the accuracy of the "temperature program", "enable detector", "signal", "channel of data acquisition", and "analysis run time" information in the "instruments" menu.
26. Wait until the run status window is green and the "Ready" signal is on the screen
27. Rinse the 10 µL syringe with HPLC grade water for analysis.

Standard and Sample Solutions Analysis

1. Prepare different concentration of glutaric dialdehyde solutions for standard solution
2. Choose "sample info" in the "Run Control" menu to check the accurate file directory, and filename.
3. Remove any bubbles from the syringe during the loading of the 0.6 µL of standard solution.
4. Inject the standard solution into the injection port of the GC unit and press the "Enter" pad at the same time of injection then remove the needle of the syringe from the injection port.
5. Check that the run status on the screen is blue and the display status reads "run in progress".
6. Clean the syringe using HPLC grade water.
7. Adjust the attenuation of the chromatogram on the display plot.

8. Choose "Specify Report" in the "Data Analysis" menu and click on the item "Printer" to choose "Combined Chromatogram and Report on Same Page". Click "OK" for the printout.
9. Repeat the previous procedures for different glutaric dialdehyde concentrations to obtain a calibration curve by plotting the concentration of glutaric dialdehyde versus the area below the peak on the chromatograms.
10. Repeat the previous procedures for different glutaric dialdehyde solutions after crosslinking process.

Shut Down

1. Choose "Temperature" in the "Instruments" menu.
2. Adjust the set temperature of the oven to 25 °C and turn off the detector and injector heater in the zone temperature window.
3. Turn off the TCD and FID detectors in the "Detector" function of the "Instruments" menu.
4. Shut off the REF valve to the TCD detector and turn off the air, hydrogen, and auxiliary gas of the FID detector.
5. Press the "Flow" and "B" pads to observe the flowrate of the channel while decreasing the total flowrate of channel B.
6. Wait until the oven temperature is 25 ° C.
7. Turn off the carrier flow valve in channel A.
8. Choose "Load" and "End.mth" in the "Method" menu to shut off the unit.

9. Choose "Exit" in "Run Control" menu to leave the analysis program.

10. Quit Windows and shut off the PC.

HP 5890 series II Operation Conditions for GA Analysis

Column: HP-FFAP (10 m X 0.53 mm ID X 1.0 μm coating) capillary column

Carrier gas: helium

Detector: flame ionization detector (FID)

Total flowrate: 200 mL/min

Column flowrate: 10 mL/min

Split ratio: 20:1

Septum purge flowrate: 4-5 mL/min

Auxiliary gas: nitrogen

Auxiliary gas flowrate: 30 mL/min

Auxiliary gas + hydrogen flowrate: 60 mL/min

Auxiliary gas + hydrogen gas + air flowrate: 400 mL/min

Injector temperature: 150 °C

Detector temperature: 155 °C

Oven temperature: 100 °C

Analysis time: 4 min

Controlling program: HP 3365 series II Chemstation

Calibration Data

Calibration data I: Response factor = 537000 (counter-sec/wt%)

Table A-1 The first set of calibration data for GC analysis

GC Calibration		
Parameters		
Temperature :	100	C for oven
	150	C for inlet
	155	C for detector
Amount of injection:	0.6	uL
Analysis time:	4	min
GA concentration	Area	
(wt%)	(counts-sec)	
0.125	68018	
0.125	63428	
0.125	63663	
0.125	65051	
0.125	72809	
0.125	60587	
0.125	65623	
0.25	123542	
0.25	122296	
0.25	129525	
0.75	408352	
0.75	389772	
0.75	429988	
1.25	767245	
1.25	782225	
1.25	838811	
1.25	886943	
1.25	823234	
2.5	1344938	
2.5	1380251	
2.5	1303366	
3.75	1921591	
5	2802503	
5	2586664	
5	2495094	
5	2737434	

Calibration data II: Response factor = 653107 (counter-sec/wt%)

Table A-2 The second set of calibration data for GC analysis

GC Calibration		
Parameters		
Temperature :	100	C for oven
	150	C for inlet
	155	C for detector
Amount of injection:	0.6	uL
Analysis time:	4	min
GA concentration	Area	
(wt%)	(counts-sec)	
0.125	96853	
0.125	109938	
0.125	100328	
0.25	198652	
0.25	189652	
0.25	185207	
0.75	458062	
0.75	458819	
0.75	460254	
1.25	875413	
1.25	881235	
1.25	872358	
2.5	1896347	
2.5	1952013	
2.5	1856324	
3.75	2441258	
3.75	2398578	
3.75	2336513	
5	3152892	
5	3125482	
5	3206512	

Calibration Curve I: Response factor = 537000 (counter-sec/wt%)

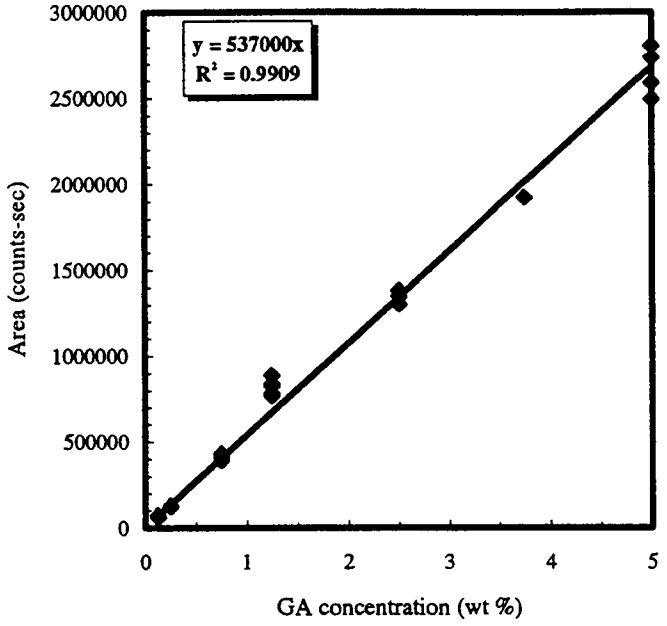

Figure A.1 The first calibration curve for glutaric daildehyde

Calibration Curve II: Response factor = 653107 (counts-sec/wt %)

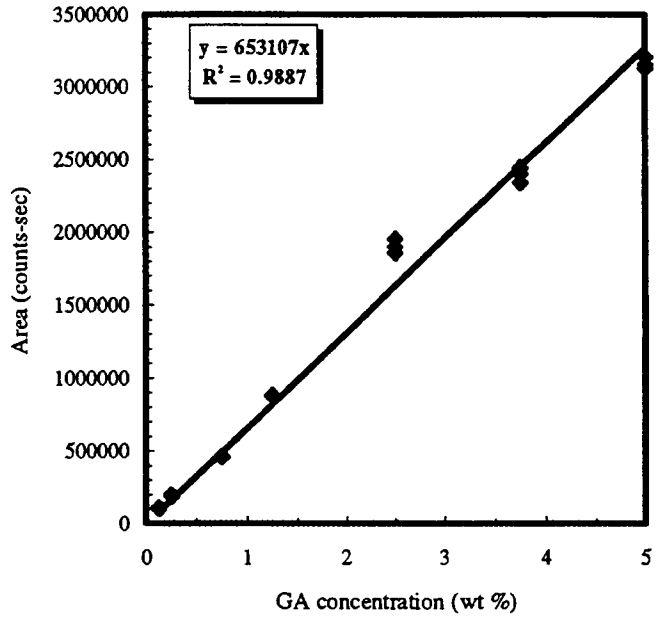

Figure A.2 The second calibration curve for glutaric dialdehyde

Sample Calculation for C_A and X_T

$$C_A\ (\text{wt\%}) = \frac{\text{area from the retention time of 2.7 min for GC analysis (counts - sec)}}{\text{Response Factor (counts - sec / wt \%)}}$$

$$C_A\left(\frac{\text{mmole GA}}{\text{cm}^3}\right) = C_A\left(\frac{\text{g GA}}{100\ \text{mL}}\right)\ \frac{1\ (\text{mole GA})}{100.2\ (\text{g GA})}\ \frac{1000\ (\text{mmole GA})}{1\ (\text{mole GA})}$$

$$X_T = \frac{(C_{A0} - C_A)\ V_C}{m_b\ x_B\ Y_B}$$

data: at t= 48 hours, $C_{A0} = 2.5$ wt %, $C_A = 0.013$ wt %, and $x_B = 0.0531$

$$X_T\left(\frac{\text{mmole GA crosslink}}{\text{total moole GA}}\right) = \frac{\frac{(2.5 - 0.013)\ \text{g GA}}{100\ \text{mL}}\ 9.6\ \text{mL}\ \frac{1\ \text{mole GA}}{100.2\ \text{g GA}}\ \frac{1000\ \text{mmoleGA}}{1\ \text{mole GA}}}{6.4\ \text{g gel beads}\ \frac{0.053\ \text{g chitosan}}{1\ \text{g gel beads}}\ \frac{5.769\ \text{mmole NH}_2}{1\ \text{g chitosan}}}$$

Appendix A-5 Gravimetric Analysis of Crosslinked Gel Beads

Sampling Procedure

1. If weight increases of the gel beads after different crosslinking times are desired, separate the gel beads from glutaric dialdehyde solution by filtration at different crosslinking times (1, 2, 4, 8, 12, 24, 36, 48 hours).
2. If the final weight increases of the gel beads after crosslinking are desired, separate the gel beads from glutaric dialdehyde solution by filtration after 48 hours of

crosslinking.

3. Place the gel beads in a petri-dish to be air-dried at 25 °C for 24 hours.
4. Measure the weight of the air-dried crosslinked gel beads using a electronic balance.
5. Dry the air-dried gel beads in an oven at 85 °C for 1, 4, and 24 hours.
6. Measure the weight of the gel beads at different oven drying time.

Sample Calculation for X_R

$$X_R = \frac{(W_{A0} - W_A)}{m_b \, x_B \, Y_B \, M_A}$$

data: at 48 hours, $W_A = 0.5199$ g , $W_{A0} = 0.4499$ g, and $x_b = 0.0531$

$$X_R \left(\frac{\text{mole GA retent}}{\text{total mole } NH_2}\right) = \frac{(0.5199 - 0.4499) \text{ g retent GA}}{6.4 \text{ g gel beads} \; \frac{0.0531 \text{ g chitosan}}{1 \text{ g gel beads}} \; \frac{5.769 \text{ mmole } NH_2}{1 \text{ g chitosan}} \; \frac{86 \text{ g retent GA}}{1 \text{ mole retent GA}}}$$

Appendix A-6 Homogeneous Crosslinking of Chitosan

1. Place 3.75 g of chitosan powder and 70 mL of 4.179 wt % acetic acid solution in a 250 mL beaker.
2. Mix the chitosan solution at 500 rpm for 20 minutes.
3. Prepare a 2.5 wt % glutaric dialdehyde solution by dilution of a Aldrich 25 wt % glutaric dialdehyde solution.
4. Weight 6.4 g of chitosan solution and place it in a 250 mL beaker.
5. Add 9.6 mL of 2.5 wt % glutaric dialdehyde aqueous solution to the chitosan solution.
6. Manually stir the crosslinking mixture until a firm gel structure is formed.

Appendix A-7 Bead Characterization Measurements

Chitosan Content (wt %) in Gel Bead

1. Place 3.75 g of chitosan powder and 70 mL of 4.179 wt % acetic acid solution in a 250 mL beaker.
2. Mix the chitosan solution at 500 rpm for 20 minutes.
3. Store the chitosan solution in an orbital shaker at 25 °C and 120 rpm for 72 hours.
4. Arrange the tubes and deliver the chitosan solution to a spinnerette using a peristaltic pump and form the gel beads in the precipitation bath.
5. Wash the gel beads with distilled water to remove the remaining NaOH solution.
6. Decan the solution and collect the gel beads.
7. Weight the gel beads.
8. The chitosan content in the gel beads is calculated by

$$x_B\ (\text{wt}\ \%) = \frac{3.75\ \text{g chitosan}}{\text{total weight of gel beads}}$$

9. This calculation is based on the assumption that all of the chitosan solution forms the gel beads in the precipitation bath.

Density of Gel Bead

1. Place 10 mL of distilled water in a graduated cylinder.
2. Weight 10.00 g of gel beads and add then into the graduate cylinder.
3. Measure the volume increase after the addition of gel beads either by scales of a graduated cylinder or a pipette.

4. The density of gel beads is evaluated by

$$\rho_b\ (g/cm^3) = \frac{\text{amount of gel beads addrd into the graduated cylinder (g)}}{\text{Increse in volume after the gel beads were added into the water (mL)}}$$

data:

Amount of gel beads: 10.00 g

Initial water volume: 10 mL

Final water volume: 19.2 mL

$$\rho_b\ (g/cm^3) = \frac{10.00\ (g)}{19.2\ -\ 10.00\ (mL)} = 10.9\ (g/cm^3)$$

Particle Size

1. Randomly pick 20 to 50 beads.
2. Measure the individual diameter of each gel bead by using a Vernier digital caliper.
3. Turn on the Vernier caliper and set the measurement unit to cm.
4. Measure every bead at least four times to ensure there is no significant difference between the length and width of the bead.
5. If there is no significant difference between the length and width of the bead, record the diameter.
6. If there is significant difference between the length and width of the bead, record this length and width
7. Calculate the mean diameter and standard deviation of the mean diameter of the sample beads.

ASAP 2000 Accelerated Surface Area and Porosimetry System for BET Analysis

1. Turn on the power switch at the back of the analyzer, open the valves and regulators for the He, Ar, and N_2 cylinders. Turn on the molecular drag pump.
2. Close the gas inlet valves on the back of the ASAP 2000 analyzer.
3. Fill up the cold trap dewar with liquid N_2 to 3 inches from the dewar mouth.
4. Place the dewar back to the original dewar position.
5. Execute "RUN20" to start the operation program.
6. Choose "F8" from the main menu display, then choose "F3" for manual control.
7. Use "F3" to activate solenoid valves at position 1, 2, 4, 5, 6, and 7 on the diagram.
8. Wait until the pressure display on the control panel in front of the analyzer is stable.
9. Use "F3" to shut off the solenoid valves 4, 5 and 6.
10. Check the status of the highlighted part of the computer screen to be idle.
11. Press "ESC" to go back to the main function menu.
12. Open the gas inlet valve of nitrogen on the back of ASAP system.
13. Weight the sample tube and place a certain amount of the beads into the sample tube. Close the tube by using a frit stopper.
14. Disconnect one of the degassing port and place a connector nut, ferrule, and O-ring on the sample tube.
15. Insert the sample tube into the degassing port.
16. Wrap the sample tube with a heating mantle and switch the heating "on" .
17. Set the heating temperature. (70 °C)

18. Set a auto degas mode and then press "load", 'left", "begin" to start the degas process.
19. Wait until the pressure in the degassing port is stable and reach a very small value.
20. Check the degassing pressure by pressing "check", "left", begin" to ensure the degassing process is finished.
21. Stop the degassed sample by pressing "unload", "left", "begin".
22. Remove the heating mantle and wait until the sample tube reaches the room temperature.
23. Unscrew the connector nut. Weigh the sample tube and then calculate the sample weight.
24. Put the plug and connector assembly back to the degassing port.
25. After weight measurement, immediately connect the sample tube into the analysis port to avoid the pressure leakage from the sample tube.
26. Fill the analysis dewar with liquid nitrogen with a level of 3 inches from the dewar mouth.
27. Place the analysis on the elevator and cover the dewar mouth with a foam sheet.
28. Cover the sample tube by using an isothermal jacket.
29. Remove the Foam sheet on the dewar mouth and start the analysis by pressing "F3" in the main function menu.
30. Choose "F3" to add sample information.
31. Complete the following items on first page of the screen.

    Sample No.:

    Sample ID:

Submitter ID:

Operator ID:

Report title:

Sample weight:

Type of data:

32. Press "PgDn" to reach the next page of sample information.

33. Complete the following items on first page of the screen.

Analysis gas: nitrogen

Analysis bath temp.: 87.3 °K

Fast evacuation: No

Preliminary evac. time: 0.5 hr

Leak test: yes (Press "F3" for switch)

Measure free space: yes

Equil. interval: 45 sec

Crossover pressure: 5.0 mm Hg

P/Po tolerance: 5.0 % 5.0 mm Hg

Leak interval: 120 and 180 sec

Measure Po: Yes

Po interval: 120 min

Free space evac. time: 0.5 h

Dose amount: 1.5 cc/g STP

Min. equil. time: 0 h

34. Press "PgDn" to reach the next page of sample information.

35. Complete the following items on first page of the screen.

    Use standard pressure table: yes

    No of surface area points: 5

    No of micropore points: 5

    No of adsorption points: 20

    No of desorption points: 20

    Total pore volume: yes

36. Press "PgDn" to reach the next page of sample information.

37. Complete the following items on first page of the screen.

    Print analog log.: yes

    Plot isotherm: yes

    Report surface area: yes

    Report BJH ads.: yes

    Report BJH des.: Yes

    Print summary: yes

38. Press "ESC' to go back to the main function menu.

39. Press "F7" to start run screen.

40. Type 1 in the unit no. of the start run screen and then press "enter" .

41. Check the sample information listed on the screen. Press "PgDn" to start the run.

42. Press "F8" then "F4" to check the run status.

43. After the result is printed from a printer, follow the similar steps 23,24 to clean the analysis port and sample tube.

44. Close the gas inlet valve.

45. Swift off the molecular drag pump.
46. Press "F9" and then "F10" to exit to the DOS system.
47. Turn off the computer and monitor.
48. Turn off the power of ASAP unit.

Differential Crushing Strength

1. Place 12 beads within the column on the base plate.
2. Weight the plunger set by including the plunger and the top plate of the plunger.
3. Slowly load the plunger set into the column on the base plate.
4. Mark the position of the plunger on the column when the plunger reaches the external surface of the 12 beads.
5. Gradually place different weights on the top plate of the plunger.
6. Record the weight applied on the plunger and mark the position change of the plunger after 5 minute since weight was applied.
7. Stop the addition of weight to the top plate of plunger if the position change of plunger is above 0.5 mm.
8. Calculate the crushing strength of the beads by

$$\textit{Crushing}\ \text{Strength}\ ,\ \Delta P\left(\frac{\text{Nt}}{\text{m}^2}\right) = \frac{\text{total weight applied before the limit of plunger movement} \cdot \text{G (Nt)}}{\text{cross surface of the column on the base plate } (\text{m}^2)}$$

Data:

Weight of the plunger set: 167.1 g

Total weight applied before the limit of plunger movement: 667.1 g

Inner diameter of the column: 1.23 cm

$$\Delta P\ (\text{psi}) = \frac{667.1\ (\text{g})\ \frac{1\ (\text{Kg})}{1000\ (\text{g})}\ 9.8\ (\frac{\text{m}}{\text{sec}^2})}{\frac{\pi\ (\ 1.23\ (\text{cm})\ \frac{1\ (\text{m})}{100\ (\text{cm})}\ )^2}{4}} \cdot \frac{14.7\ (\text{psi})}{1.0133\ \text{E}\ +05\ (\frac{\text{Nt}}{\text{m}^2})} = 1.99\ (\text{psi})$$

Appendix A-8 Cadmium Ion Adsorption Capacity

Batch Adsorption Experiment

1. Place 0.040 g of chitosan beads into a 125 mL Erlenmeyer flask.
2. Add 40 mL of different concentration of cadmium solution to the flask.
3. Use the vacuum to remove the remaining gas staying in the porous structure of the chitosan beads.
4. After all the chitosan beads have fallen down to the bottom of the flask, the flask is stored in a shaker at 25 °C and 120 rpm for 60 hours.
6. Separate the wet chitosan beads and store the filtered cadmium solution in vials for IC analysis.
7. Vacuum filter the cadmium solution if there is any debris in the previous filtered cadmium solution.

Cadmium Ion Concentration Measurement

DIONEX DX-300 Series Ion Chromatography Operation

Start-up

1. Degas the eluant solution for 40 minutes by delivering the helium gas to the eluant solution tank.
2. Prepare 1 L of post column solution and store it in the post column tank.
3. Open the nitrogen gas cylinder valve and adjust the regulator to 80 psi.
4. Press the "On" pad on the right hand side corner of the front panel at the bottom drawer of the dual-piston gradient high pressure pump.
5. Check the flowrate of eluant solution to be 1.0 mL/min.
6. Start the PeakSimple II program.
7. Prime the pump by connecting a syringe to the seal of the pump head at the left hand side corner of the front panel at the bottom drawer of the dual-piston gradient high pressure pump to remove any remaining gas in the carrier solution.
8. Check the back pressure from the pressure display window on the front panel at the bottom drawer of the dual-piston gradient high pressure pump.
9. Turn on the UV/VIS variable length detector and set the wavelength to 520 nm and the absorbance to 0.1 AU.
10. Wait until the reading of the UV/VIS variable length detector is stable.
11. Turn on reagent 1 using the Reagent delivery module panel on the right hand side corner of the top drawer of the IC system.

12. Check the reaction coil inside the drawer to be orange and the module pressure on the front panel to be 80 psi.
13. Prime the pump if there is any noise appearing from the dual-piston gradient high pressure pump.
14. Inject 100 μL of eluant solution into the automatic sample injector on the left hand side of the IC system.
15. Press the 'Inject" pad next to the "On" pad (for location, see step 4). The injector has already been set to switch on at 0.1 minute and then switch off at 1.0 min.
16. Check the reading of the UV/VIS variable length detector to be stable to avoid any interference of remaining sample solution.
17. Rinse the 100 μL syringe with HPLC grade water for analysis.

Standard and Sample Solution Analysis

1. Prepare different concentration of cadmium solutions for standard solution.
2. Prepare different concentration of cobalt solutions for internal standard solution.
3. Adjust the parameters in the PeakSimple II program.
3. Choose "path" in the "Controls" menu and type c:\peak2\ data.
4. Choose "channels" in the "Controls" menu and then choose the "Details" function to type the description and end time for this present running.
5. Save the present run by choosing the "PostRun" function in the 'channels" menu.
6. Inject 100 μL of standard or sample solution into the automatic sample injector on the left hand side of the IC system.

7. Press the 'Inject" pad next to the "On" (for location, see step 4 on start-up procedure) while at the same time pressing the "+" key on the keyboard.
8. Check the "Running" status on the screen.
9. Choose "results" in the "Analysis" menu and set channel 2 for result display.
10. Choose "print" in the "Analysis" menu to choose type of print header condition, print chromatogram format, and print report format.
11. Receive the print of present results from the printer.
12. Clean the syringe by HPLC grade water.
13. Repeat the previous procedures for different cadmium or cobalt concentrations.
14. Prepare calibration curves of the cadmium and cobalt ions for the sample analysis.

Shut Down

1. Turn off the reagent 1 using the Reagent delivery module panel on the right hand side corner of the top drawer of the IC system.
2. Wait until all the back pressure is released and the reading of the module pressure is zero.
3. Turn off the UV/VIS variable length detector and set the absorbance value to its lowest level.
4. Press the "Off" pad on the right hand side corner of the front panel at the bottom drawer of the dual-piston gradient high pressure pump.
5. Rinse the pump head by flushing distilled water into the drainage lines of the pump head inside the bottom drawer.

6. Open the post column tank and remove the remaining post column reagent. Refill the tank with distilled water.
7. Turn off the nitrogen gas cylinder.
8. Choose "yes" in the "Quit" menu to skip the PeakSimple II program.

Maintenance

1. Prepare fresh eluant solution every 3 weeks.
2. Check the leakage of the reagent carrier line and column connections.
3. Add 0.1 mL of grease to the dual-piston gradient high pressure pump every 3-6 months.
4. Check the display on the front panel of the IC system.
5. Flush the guard and analysis column every week by following steps 3-9 of the start-up procedure and shut down procedures.

DIONEX DX-300 Series Operation Conditions for IC Analysis

Columns: Ion Pac CS-5 (25.4 cm packing X 4 mm ID) analysis column
Ion Pac CG-5 (4.5 cm X 4 mm ID) guard column

Detector: variable wavelength detector -II

Absorbance: 0.1 AU

Wavelength: 520 nm

Total flowrate: 1.0 mL/min

Auxiliary gas: nitrogen

Reagent delivery module pressure: 80 psi for reagent 1

Sample Injector time: 0.1 min

Analysis time: 10 min

Controlling program: PeakSimple data system for chromatography

Sample Calculations for C_o and C_f

$$C_o \text{ or } C_f = \frac{\text{Area of Cd}}{\text{Area of Co}} \bullet \text{Reponse factor} \bullet \frac{\text{amont of Co}}{\text{total volume of injection}} \bullet \text{dilute factor}$$

data: Area of Cd: 2000 (μV-Sec)

Area of Co: 1500 (μV-Sec)

Response factor : 9.44 (μV-Sec Co * μg Cd / μV-Sec Cd *μg Co)

amount of Co: 10.25 μg

total volume of injection: 1.0 mL

dilute factor: 2

$$C_f = \frac{2000\ \mu v\text{-}sec}{1500\ \mu v\text{-}sec} \bullet 9.44\ \frac{\mu v\text{-}sec * \mu g\ Cd}{\mu v\text{-}sec * \mu g\ Co} \bullet \frac{10.25\ \mu g\ Co}{1.0\ mL} \bullet 2$$

$$= 258\ \frac{\mu g\ Cd}{mL}\ (ppm)$$

Calibration Data

Response factor = 10.05 (μV-Sec Co * μg Cd / μV-Sec Cd *μg Co)

Table A-3 The first set of calibration data for IC analysis

	IC Calibration		
	Parameters		
	Temperature :	25 C	
	Amount of injection:	100 uL	
	Analysis time:	10 min.	
Cobalt		**Cadmium**	
Concentration	Area	Concentration	Area
(ug)	(uV-sec)	(ug)	(uV-sec)
0.00	0.00	1.39	3882.92
0.21	4609.34	13.85	40872.56
2.05	55626.62	27.30	76079.88
		45.20	117246.12
		64.50	182871.89
		88.00	235605.86
		112.00	309171.05
		151.20	399566.16

Response factor = 9.44 (μV-Sec Co * μg Cd / μV-Sec Cd *μg Co)

Table A-4 The second set of calibration data for IC analysis

	IC Calibration		
	Parameters		
	Temperature :	25 C	
	Amount of injection:	100 uL	
	Analysis time:	10 min.	
Cobalt		**Cadmium**	
Concentration	Area	Concentration	Area
(ug)	(uV-sec)	(ug)	(uV-sec)
0	0	13.8	30582.32
0.205	4609.34	27.3	67344.36
2.05	45889.25	45.2	106549.68
		88	236976.63
		102.6	238478.28
		134.4	301336.84
		151.2	364171.12
		200	471298.15

Calibration Curves:

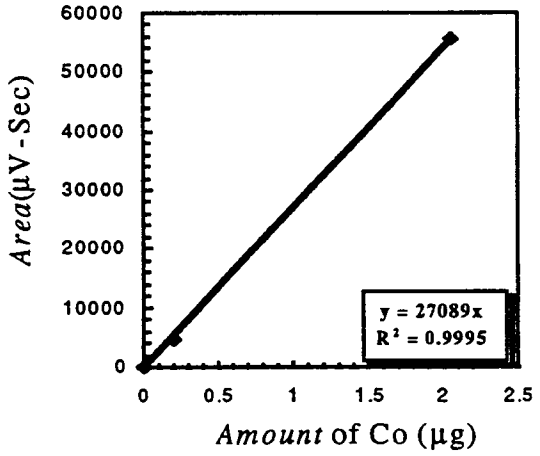

Figure A.3 The first calibration curve for cobalt

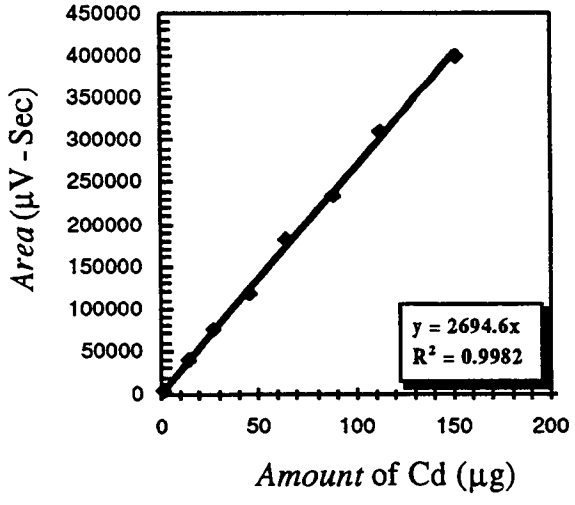

Figure A.4 The first calibration curve for cadmium

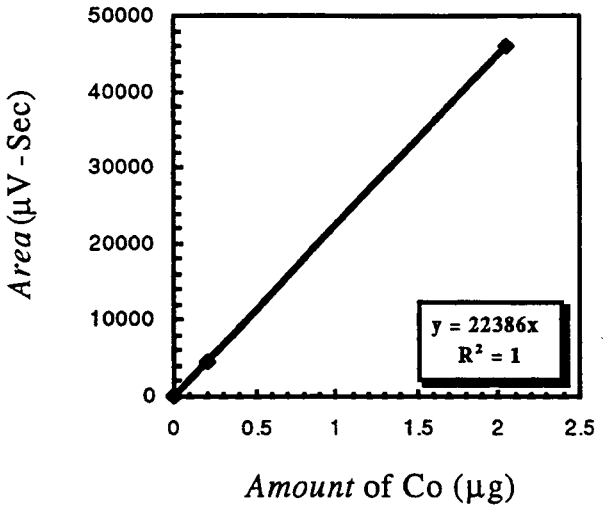

Figure A.5 The second calibration curve for cobalt

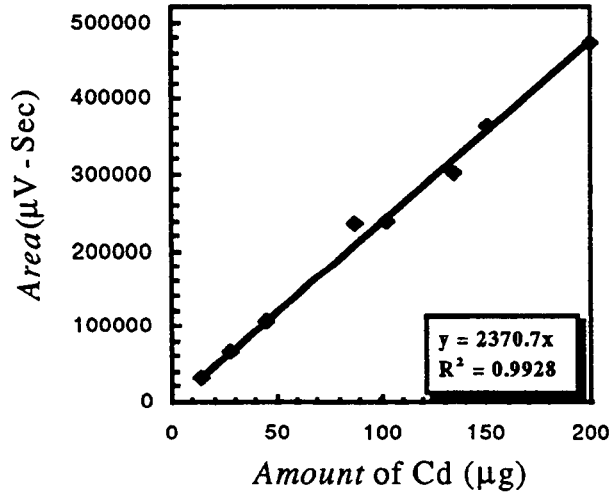

Figure A.6 The second calibration curve for cadmium

Appendix A-9 EDAX Sample Preparation

1. Place 0.040 g of freeze-dried chitosan beads into a 125 mL Erlenmeyer flask.
2. Prepare a 1026 mg Cd^{+2}/L initial concentration of aqueous cadmium solution.
3. Add 40 mL of cadmium solution to the flask.
4. Use a vacuum to remove the remaining gas staying in the porous structure of the chitosan beads.
5. After all the chitosan beads have fallen down to the bottom of the flask, the flask is stored in a shaker for 60 hours of agitation.
6. Filter the wet chitosan beads until no water is remaining on the outer surface.
7. Store a few cadmium adsorbed chitosan beads in a 300 mL freeze-dried flask and immediately immerse the flask into liquid nitrogen.
8. Fracture the frozen chitosan beads by using a razor blade and store the fractured beads in a hood at 25 °C for 48 hours.
9. Fix the fractured air-dried chitosan beads in a stand and sputter coat them with carbon for EDAX analysis.

Appendix A-10 Single Stage Adsorption\Desorption Experiments

1. Place 0.50 g of crosslinked chitosan beads into the hollow impeller basket.
2. Arrange the hollow impeller basket assembly.
3. Add 200 mL of 200 mg/L cadmium ion solution to the 250 mL vessel.
4. Place the hollow impeller into the vessel and arrange the head plate assembly.
5. Plug the pH and ATC probes through the head plate and then immerse into

thecadmium solution.

6. Start the pH recording program by typing "pH" in directory c:\
7. Place the spinning basket reactor into the isothermal tank and set the temperature to 25 ° C.
8. Connect the shaft of the impeller to the motor head and set the rotating speed to 150 rpm.
9. Discharge 0.5 mL of cadmium solution from the vessel by using a 250 μL syringe at certain periods of adsorption time. Store the cadmium solution in a 2 mL vial for cadmium concentration analysis.
10. Wait until the cadmium adsorption on the chitosan beads is finished (around 48 to 51 hours).
11. Use a pipet to add different amounts of 0.1 N nitric acid into the cadmium solution through a hole in the head plate assembly.
12. Discharge 0.5 mL of cadmium solution from the vessel by using a 250 μL syringe at certain periods of desorption time. Store the cadmium solution in a 2 mL vial for cadmium concentration analysis.
13. Wait until the pH value of the cadmium solution reaches equilibrium.
14. Stop the mixer and the pH recording program.
15. Remove the pH and ATC probe from the top plate and rinse with distilled water to remove any remaining cadmium solution.
16. Store the pH probe in a Ag/AgCl solution and cover the head of the ATC probe by using its plastic head cover.
17. Release the head plate assembly and remove the hollow impeller basket assembly.

18. Store the wet, swelled chitosan beads in a 20 mL vial for freeze drying.

Appendix A-11 Equilibrium Desorption Measurements

1. Place 0.10 g of chitosan beads into a 125 mL Erlenmeyer flask.
2. Add 40 mL of 200 mg/L cadmium ion solution to the flask.
3. Use a vacuum to remove the remaining gas residing in the porous structure of the chitosan beads.
4. After all the chitosan beads have fallen down to the bottom of the flask, place the flask in a shaker at 25 °C and 120 rpm for 51 hours.
5. Discharge 0.5 mL of cadmium solution from the vessel by using a 250 μL syringe after 51 hours of adsorption. Store the cadmium solution in a 2 mL vial for cadmium concentration analysis.
6. Measure the pH value of the cadmium solution after 51 hours of adsorption.
7. Add different concentrations and different amounts of nitric acid solution into the flask to adjust the pH of the cadmium solution.
8. Wait 140 hours for cadmium desorption.
9. Discharge 0.5 mL of cadmium solution from the vessel by using a 250 μL syringe after 140 hours of desorption. Store the cadmium solution in a 2 mL vial for cadmium concentration analysis.
10. Measure the pH value of the cadmium solution.

Appendix B

Calculations for Crosslinking Study

Appendix B-1 Calculations for D_o

Wilke and Chang Correlation $$\frac{D_{AB}\,\mu_B}{T} = \frac{7.4 \cdot 10^{-8}\,(\Phi_B\,M_B)^{1/2}}{V_A^{0.6}}$$

where D_{AB} is the mass diffusivity of A (GA) diffusing through liquid solvent B (water) (cm^2/s), μ_B is the viscosity of the solution (centipoises), T is the absolute temperature (K), M_B is the molecular weight of solvent (g/mole), V_A is the molar volume of the solute at normal boiling point (cm^3/g mole), Φ_B is the associate parameter for solvent B.

Data:

A: glutaric dialdehyde, $CHO(CH_2)_3CHO$

B: water, H_2O

μ_B: 0.894 centipoises

T: 298 °K

M_B: 18 g/mole

V_A: $5V_C + 8V_H + 2V_O$, 118.4 cm^3/g mole

Φ_B: 2.26

$$D_{AB} = \frac{7.4 \cdot 10^{-8}\,(2.26 \cdot 18)^{1/2}}{(118.4)^{0.6}}\,\frac{298}{0.894}$$

$$= 8.969 \cdot 10^{-6}\ (cm^2/s)$$

Appendix B-2 Results of Statistical Analysis for Calculation of D_e

Table B-1 The results of statistical analysis for calculation of D_e

Regression Output:	
Constant	9.13 E -04
Std Err of Y Est.	9.33 E -04
R Squared	9.90 E -01
No. of Observations	2.70 E +01
Degree of Freedom	2.50 E +01
X Coefficient	8.14 E -06
Std Err of Coefficient	1.62 E -07
D_{Ac} = 4.11 E -08 cm^2/sec	

Table B-2 Numerical implementation of crosslinked model

Crosslinking of 7 % N-acylated 3 mm Chitosan Gel Bedas					file:hslenty\xlink\NREAT75.XLS				
Constant Process Parameters:					Date:				
Temperature:	27	C			Magnetite:	0.00	wt %		
Shaker Speed:	120	rpm			MW,A:	100	g GA/100 mL		
Mb,gel:	6.4	g			MW,B:	161.2	g glucosamine unit/g-chitosan		
Density:	1.06	g gel/cm^3			CA0:	0.75	g GA/100 mL		
R:	0.15	cm			wt. chitosan:	3.75			
Vc:	9.6	mL			wt. gel beads:	68.18	g gel beads		
YB:	5.769	mmole NH2/g-chitosan			x,chit:	0.055	g-chitosan/g gel		
% N-acylation:	0.07	mole NH2/total mole NH2			Beta:	4	mole GA reacted/mole NH2 reacted		
X-linking Time		CA	CA	XT	X	F(X)	CA dt	Sum (CA dt)	F(X),predicted
sec	hour	g GA/100 mL	mmole/cm^3	mole GA/total NH2	mole NH2 react/total NH2		mmole/cm^3 sec		
0	0.000	2.500	0.250	0.000	0.000	0.00E+00		0.00E+00	
30	0.008	2.356	0.235	0.068	0.017	9.73E-05	7.27E+00	7.27E+00	9.73E-04
60	0.017	2.184	0.218	0.149	0.037	4.73E-04	6.80E+00	1.41E+01	1.03E-03
120	0.033	2.145	0.214	0.168	0.042	5.98E-04	1.30E+01	2.70E+01	1.13E-03
180	0.050	1.890	0.189	0.288	0.072	1.79E-03	1.21E+01	3.91E+01	1.23E-03
300	0.083	1.852	0.185	0.306	0.077	2.02E-03	2.24E+01	6.15E+01	1.42E-03
600	0.167	1.815	0.181	0.324	0.081	2.27E-03	5.49E+01	1.16E+02	1.86E-03
900	0.250	1.769	0.177	0.346	0.086	2.59E-03	5.37E+01	1.70E+02	2.30E-03
1200	0.333	1.713	0.171	0.372	0.093	3.01E-03	5.21E+01	2.22E+02	2.73E-03
1500	0.417	1.675	0.167	0.390	0.098	3.31E-03	5.07E+01	2.73E+02	3.14E-03
1800	0.500	1.638	0.163	0.408	0.102	3.63E-03	4.96E+01	3.23E+02	3.54E-03
2400	0.667	1.626	0.162	0.413	0.103	3.73E-03	9.77E+01	4.20E+02	4.34E-03
3000	0.833	1.618	0.161	0.417	0.104	3.80E-03	9.71E+01	5.17E+02	5.13E-03
3600	1.000	1.520	0.152	0.463	0.116	4.72E-03	9.40E+01	6.11E+02	5.90E-03
4200	1.167	1.399	0.140	0.520	0.130	6.00E-03	8.74E+01	6.99E+02	6.61E-03
4800	1.333	1.327	0.132	0.555	0.139	6.84E-03	8.16E+01	7.80E+02	7.28E-03
5400	1.500	1.286	0.128	0.574	0.143	7.34E-03	7.82E+01	8.59E+02	7.92E-03
6000	1.667	1.224	0.122	0.603	0.151	8.14E-03	7.51E+01	9.34E+02	8.53E-03
6600	1.833	1.147	0.114	0.640	0.160	9.19E-03	7.10E+01	1.00E+03	9.11E-03
7200	2.000	1.023	0.102	0.698	0.175	1.10E-02	6.50E+01	1.07E+03	9.64E-03
9000	2.500	0.923	0.092	0.746	0.186	1.27E-02	1.75E+02	1.24E+03	1.10E-02
10800	3.000	0.882	0.088	0.765	0.191	1.34E-02	1.62E+02	1.41E+03	1.24E-02
12600	3.500	0.779	0.078	0.814	0.203	1.52E-02	1.49E+02	1.56E+03	1.36E-02
14400	4.000	0.705	0.070	0.849	0.212	1.66E-02	1.33E+02	1.69E+03	1.47E-02
43200	12.000	0.284	0.028	1.048	0.262	2.60E-02	1.42E+03	3.11E+03	2.63E-02
86400	24.000	0.057	0.006	1.155	0.289	3.21E-02	7.35E+02	3.85E+03	3.23E-02
172800	48.000	0.014	0.001	1.175	0.294	3.33E-02	3.06E+02	4.15E+03	3.48E-02

Appendix B-3 Computer Program

```
   CLS
REM    Rev. 12/21/95
REM    XLINK-1.BAS
REM    CROSSLINKING MODEL I:  DIFFUSION LIMITED
REM
REM    MODEL INPUT PARAMETERS
REM
      VC = 9.6 'cm^3 crosslinking bath
      MB = 6.4 'g gel bead
      XB = .0529  'g chitosan/g gel bead
      YB = 5.769 'mmole -NH2/g chitosan
      BETA = 3 ' mmole GA consumed to form crosslink/mmole -NH2 consumed
      DAE = 4.11E-08'cm^2/sec for glutaraldehyde in crosslinked gel layer
      R = .15  'cm radius of bead
      DENSB = 1.06'g gel bead/cm^3 gel bead
REM
REM    INTEGRATION CONTROL AND PRINTOUT PARAMETERS
REM
      INPUT "tmax (hr) = ", T1MAX
      INPUT "dt (hr) = ", DT1
      INPUT "Print interval (hr) = ", DK
REM    INPUT "Enter output filename: ", FILE1$
REM    OPEN "O", 1, FILE1$
      PRINT
```

Computer Program (continued)

```
  TMAX = T1MAX * 3600
     DT = DT1 * 3600
     N = INT(TMAX / DT)
REM
REM    USE ANALYTICAL SOLUTION FOR CA = CAO TO ADJUST INITIAL CONDITION
REM
     CAO = .2495 'mmole glutaraldehyde/cm^3
     X = .001
     T = XB * DENSB * YB * BETA * R ^ 2 / (6 * DAE * CAO) * (1 - 3 * (1 - X) ^ (.6667) + 2 * (1 - X))
     RC = R * (1 - X) ^ .333
     CA = CAO - X * BETA * MB * XB * YB / VC
     T1 = T / 3600
     PRINT USING "###.#######  #.####  #.####   #.####"; T1; CA; X; RC
REM    PRINT #1, T1, CA, X
REM
REM    SOLUTION OF DIFFERENTIAL EQUATION FOR RC BY 4TH-ORDER RUNGE-KUTTA METHOD
REM
     K = DK' set print counter
     FOR I = 1 TO N + 1
     IF I * DT / 3600 > K THEN PRINT USING "###.#######  #.####  #.####   #.####"; T1; CA; X; RC
REM    IF I * DT / 3600 > K THEN PRINT #1, T1, CA, X
     IF I * DT / 3600 > K THEN K = K + DK
     T = T + DT
     T1 = T / 3600
     F11 = -DAE * CA / (XB * DENSB * YB * BETA * (1 / RC - 1 / R) * RC ^ 2)
     F12 = -DAE * CA / (XB * DENSB * YB * BETA * (1 / (RC + .5 * F11 * DT) - 1 / R) * (RC + .5 * F11 * DT) ^ 2)
```

Computer Program (continued)

```
    F13 = -DAE * CA / (XB * DENSB * YB * BETA * (1 / (RC + .5 * F12 * DT) - 1 / R) * (RC + .5 * F12 * DT) ^ 2)
      F14 = -DAE * CA / (XB * DENSB * YB * BETA * (1 / (RC + F13 * DT) - 1 / R) * (RC + F13 * DT) ^ 2)
      RC = RC + (F11 + 2 * F12 + 2 * F13 + F14) * DT / 6
      X = 1 - (RC / R) ^ 3
      CA = CAO - X * BETA * MB * XB * YB / VC
      NEXT I
REM   CLOSE
      END
```

Appendix B-4 Reaction Control for Crosslinking Study

At short crosslinking times when only a small fraction of NH_2 in the gel bead is crosslinked, the rate equation for the crosslinking reaction can be expressed as

$$-R_A = k C_A C_B \approx k C_A C_{B0} = k C_A \rho_b x_B Y_B = k' C_A \qquad \text{(B-1)}$$

where k' is a lumped parameter to be equal to $\rho_b x_B Y_B$. The material balance for GA in the crosslinking bath is

$$R_A V_C = \frac{d(V_C C_A)}{dt} \qquad \text{(B-2)}$$

Substitution of equation (B-1) into the equation (B-2) yields

$$\frac{d C_A}{dt} = - k' C_A \qquad \text{(B-3)}$$

The integral equation is

$$C_A = C_{A0} e^{-k't} \qquad \text{(B-4)}$$

The k' value can be evaluated from the least-squares of lnC_A versus t data at short crosslinking times when the thickness of crosslinked shell is small and $C_B \approx C_{B0}$. The lumped rate constant k' was estimated from the least-squares slope of the data at very short times of 0 to 0.05 hour. The value for k' is 5.12 hr^{-1}, with a regression coefficient of 0.94

The Thiele Modulus for the thin crosslinked shell can be expressed as

$$\phi = l \sqrt{\frac{k'}{D_{Ae}}} \qquad \text{(B-5)}$$

where $l = R - r_c$

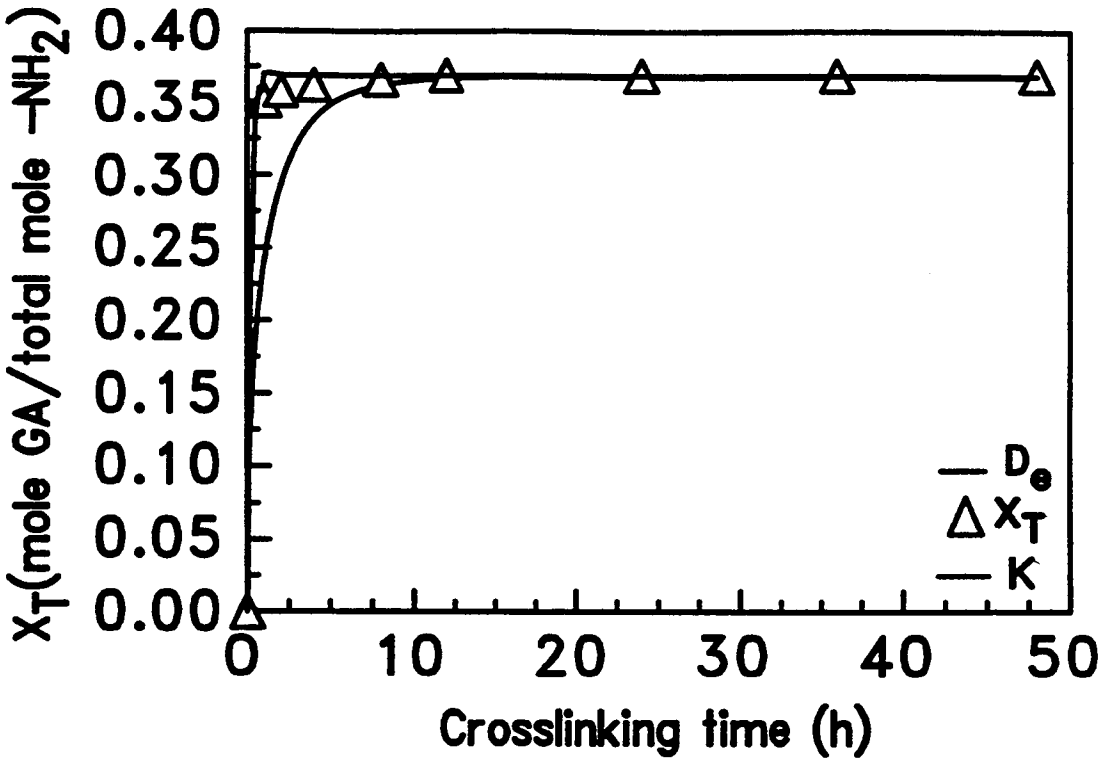

Figure B.1 The extent of crosslinking versus crosslinking time for N-acylated chitosan gel beads crosslinked with 0.75 wt % GA

Appendix C

Effect of Cadmium Loading on BET Surface Area and Pore Size Distribution

Table C-1 The BET surafec area comparisons for 1mm crosslinked, 3 mm uncrosslinked, and crosslinked chitosan beads before and after cadmium loading

Citosan Sample	Data Filename	BET Surface Area (m^2/g)			Reduction of BET Sueface Area (%)	Cadmium Capacity (mg Cd^{+2}/g)
		Before	Control	After		
3 mm crosslinked bead (CHI-B-X-3)	29, 32, 33	216	205	180	17	161
3 mm uncrosslinked bead (CHI-B-1)	57, 65,58	55	53	42	24	151
1 mm crosslinked bead (CHI-B-X-1)	42, 46, 41	234	169	134	43	174

Table C-2 The BJH adsorption pore distribution for crosslinked 3 mm beads

Sample: Crosslinked 3 mm Beads, Batch # CHI-B-X-3, 3/18/93

ASAP 2000 V2.03

SAMPLE DIRECTORY/NUMBER: DATA1 /29

SAMPLE ID: Beads

SUBMITTER: HsienTY

OPERATOR: HsienTY SAMPLE WT: 0.2123 g

UNIT NUMBER: 1 FREE SPACE: 56.2515 cc

ANALYSIS GAS: Nitrogen EQUIL INTRVL: 5 sec

BJH ADSORPTION PORE DISTRIBUTION REPORT

PORE RANGE (A)	AVERAGE DIAMETER (A)	INCREMENTAL PORE VOLUME (cc/g)	CUMULATIVE PORE VOLUME (cc/g)	INCREMENTAL PORE AREA (sq. m/g)	CUMULATIVE PORE AREA (sq. m/g)	DIFFERENTIAL PORE VOLUME f(D) (cc/g)	f(D)dlogD (cc/g)	D*f(D)dlogD (cc/g)	INTEGRAL D*f(D)dlogD (cc/g)	D,av (A)
1121										
1046.9	1081.4	0.036131	0.036131	1.336	1.336	1.216515079				
873.8	944.4	0.069218	0.105349	2.932	4.268	0.881834806	0.08235306	79.08775734	79.08775734	750.72148
703	769.5	0.069465	0.174814	3.611	7.879	0.735416214	0.07638011	60.21807842	139.3058358	796.88032
592.1	637.8	0.051969	0.226783	3.259	11.138	0.697006653	0.05340091	34.57976155	173.8855973	766.74882
492.3	532.8	0.051651	0.278434	3.878	15.016	0.644306803	0.05376335	29.15048711	203.0360844	729.20722
396.5	433.8	0.051775	0.330209	4.774	19.79	0.550876143	0.05616562	24.96000023	227.9960846	690.45993
320.4	350	0.051622	0.381831	5.899	25.69	0.557770052	0.05130298	18.38955389	246.3856385	645.27406
253.6	278.9	0.051762	0.433593	7.424	33.114	0.509753192	0.05419989	15.55536964	261.9410082	604.11724
212.9	229.5	0.034088	0.467681	5.941	39.055	0.448682246	0.03640789	8.492140212	270.4331484	578.24275
161.3	179.6	0.049997	0.517677	11.135	50.19	0.41476243	0.05204037	9.736753092	280.1699015	541.20601
130.7	142.5	0.033503	0.55118	9.402	59.592	0.366718996	0.03569759	5.211848833	285.3817503	517.76507
104.8	114.6	0.030565	0.581745	10.666	70.257	0.31866988	0.0328693	3.870359934	289.2521103	497.2146
81.4	89.8	0.031096	0.612841	13.85	84.107	0.283368733	0.03303292	3.075364741	292.327475	477.00378
61.3	68.1	0.029595	0.642436	17.371	101.479	0.240289506	0.0322479	2.300887911	294.6283629	458.61123
47	52	0.024626	0.667061	18.949	120.428	0.213457364	0.02617271	1.417252413	296.0456153	443.80591
36.1	39.8	0.022836	0.689897	22.931	143.358	0.199283264	0.02364811	0.982578957	297.0281943	430.53991
29.9	32.3	0.015307	0.705204	18.968	162.327	0.18704479	0.01580777	0.521656541	297.5498508	421.93443
24.4	26.4	0.017011	0.722216	25.732	188.058	0.192702056	0.01676228	0.455096022	298.0049468	412.62579
19.3	21.1	0.019854	0.74207	37.689	225.747	0.194967192	0.01973867	0.43128989	298.4362367	402.16723

Table C-3 The BJH desorption pore distribution report for 3 mm crosslinked chitosan beads

ASAP 2000 V2.03										
SAMPLE DIRECTORY/NUMBER: DATA1 /29										
SAMPLE ID: Beads										
SUBMITTER: HsienTY										
OPERATOR: HsienTY		SAMPLE WT: 0.2123 g								
UNIT NUMBER: 1		FREE SPACE: 56.2515 cc								
ANALYSIS GAS: Nitrogen		EQUIL INTRVL: 5 sec								
BJH DESORPTION PORE DISTRIBUTION REPORT										
PORE RANGE	AVERAGE	INCREMENTAL	CUMULATIVE	INCREMENTAL	CUMULATIVE	DIFFERENTIAL			INTEGRAL	
(A)	DIAMETER	PORE VOLUME	PORE VOLUME	PORE AREA	PORE AREA	PORE VOLUME f(D)	f(D)dlogD	D*f(D)dlogD	D*f(D)dlogD	D,av
	(A)	(cc/g)	(cc/g)	(sq. m/g)	(sq. m/g)	(cc/g)	(cc/g)	(cc/g)	(cc/g)	(A)
899.8										
840.4	868	0.006898	0.006898	0.318	0.318	0.232569547				
786.3	811.5	0.011342	0.01824	0.559	0.877	0.392487059	0.009031	7.345665129	7.345665129	402.7229
653.7	707.5	0.036747	0.054987	2.077	2.954	0.458136091	0.034114	24.56218975	31.90785488	580.28
457.1	520.5	0.098998	0.153985	7.609	10.563	0.637186996	0.085089	47.25825035	79.16610522	514.1157
348.2	387.5	0.095489	0.249474	9.856	20.419	0.807979496	0.085397	34.38496578	113.551071	455.1619
267.3	296.8	0.095472	0.344946	12.869	33.288	0.831421751	0.094126	28.96729656	142.5183676	413.1614
230.8	246.2	0.050346	0.395292	8.179	41.466	0.789578254	0.05168	12.87091313	155.3892807	393.1
156.3	178.7	0.11161	0.506902	24.978	66.444	0.659334194	0.122634	23.73574306	179.1250238	353.3721
125.3	137.1	0.049218	0.55612	14.36	80.804	0.512645276	0.05626	7.921358441	187.0463822	336.3418
96.9	107.1	0.045822	0.601942	17.11	97.913	0.410491004	0.051524	5.724272233	192.7706544	320.2479
75.1	82.9	0.034432	0.636374	16.613	114.527	0.311084256	0.039933	3.434268988	196.2049234	308.317
54.5	61.1	0.033448	0.669822	21.883	136.41	0.240212403	0.038382	2.487167864	198.6920913	296.6342
42	46.4	0.020594	0.690416	17.749	154.158	0.182010671	0.023887	1.152532397	199.8446237	289.4554
33.1	36.3	0.017217	0.707633	18.966	173.125	0.166474416	0.01802	0.676665638	200.5212893	283.369
27.5	29.7	0.011633	0.719267	15.692	188.816	0.144530178	0.012517	0.379271282	200.9005606	279.3129
22.5	24.4	0.012255	0.731521	20.095	208.911	0.140607863	0.012425	0.31062288	201.2111835	275.0587
17.2	19	0.016909	0.74843	35.614	244.525	0.144949935	0.016656	0.330616436	201.5417999	269.2861

Table C-4 The control experiment of BJH desorption pore distribution for 3 mm crosslinked chitosan beads

ASAP 2000 V2.03										
SAMPLE DIRECTORY/NUMBER: DATA1 /32										
SAMPLE ID: 3 mm Bead, 60 hours										
SUBMITTER: HsienTY										
OPERATOR: HsienTY		SAMPLE WT: 0.1730 g								
UNIT NUMBER: 1		FREE SPACE: 55.8197 cc								
ANALYSIS GAS: Nitrogen		EQUIL INTRVL: 5 sec								
BJH DESORPTION PORE DISTRIBUTION REPORT										
PORE RANGE	AVERAGE	INCREMENTAL	CUMULATIVE	INCREMENTAL	CUMULATIVE	DIFFERENTIAL			INTEGRAL	
(A)	DIAMETER	PORE VOLUME	PORE VOLUME	PORE AREA	PORE AREA	PORE VOLUME f(D)	f(D)dlogD	D*f(D)dlogD	D*f(D)dlogD	D,av
	(A)	(cc/g)	(cc/g)	(sq. m/g)	(sq. m/g)	(cc/g)	(cc/g)	(cc/g)	(cc/g)	(A)
987.9										
790.3	899.1	0.011322	0.011322	0.504	0.504	0.116816785				
713	747.5	0.014256	0.025578	0.763	1.266	0.31890868	0.009739	7.32031812	7.320318118	286.1959
636.1	670	0.020499	0.046078	1.224	2.49	0.413605529	0.0181532	12.2452521	19.56557019	424.6185
499.8	551.2	0.061289	0.107367	4.447	6.938	0.585214371	0.0523028	29.7053619	49.27093209	458.902
371.7	416.5	0.093808	0.201174	9.01	15.947	0.729426967	0.0845339	36.8356312	86.10656332	428.0203
271.5	305.6	0.107791	0.308966	14.111	30.058	0.790132277	0.1036512	33.3342285	119.4407918	386.5823
226.7	244.8	0.057646	0.366612	9.419	39.477	0.736047512	0.0597639	14.8871909	134.3279827	366.4037
145.7	168.2	0.121575	0.488187	28.909	68.386	0.633229614	0.1314451	24.4750786	158.8030614	325.2915
118.7	129.2	0.040975	0.529162	12.683	81.069	0.460347571	0.048669	6.43404371	165.2371051	312.2618
93.8	103	0.038888	0.56805	15.098	96.166	0.380330622	0.0429788	4.56649556	169.8036006	298.9237
74.3	81.5	0.029636	0.597685	14.546	110.712	0.292795392	0.0340649	2.86315455	172.6667552	288.8926
56	62.3	0.028252	0.625937	18.148	128.861	0.230063673	0.0321038	2.09155946	174.7583146	279.1947
43.4	47.9	0.020121	0.646059	16.814	145.674	0.181773347	0.0227948	1.13290297	175.8912176	272.2526
34.3	37.6	0.016365	0.662423	17.432	163.106	0.160124296	0.0174702	0.67871801	176.5699356	266.5516
28	30.4	0.012214	0.674637	16.08	179.187	0.138581144	0.0131634	0.41003881	176.9799744	262.3336
22.9	24.8	0.011505	0.686143	18.544	197.73	0.131764362	0.0118036	0.30040237	177.2803768	258.3723
17.5	19.3	0.016985	0.703128	35.252	232.982	0.145422716	0.0161874	0.32698487	177.6073616	252.5961

Table C-5 The control experiment of BJH adsorption pore distribution for 3 mm crosslinked chitosan beads

Sample: Crosslinked 3 mm Beads, Batch # CHI-B-X-3, 3/18/93					
Adsorption in water for 60 hrs followed by freeze drying (Control Experiment)					
ASAP 2000 V2.03					
SAMPLE DIRECTORY/NUMBER: DATA1 /32					
SAMPLE ID: 3 mm Beads, 60 hours					
SUBMITTER: HsienTY					
OPERATOR: HsienTY		SAMPLE WT: 0.1730 g			
UNIT NUMBER: 1		FREE SPACE: 55.8197 cc			
ANALYSIS GAS: Nitrogen		EQUIL INTRVL: 5 sec			
BJH ADSORPTION PORE DISTRIBUTION REPORT					
PORE RANGE (A)	AVERAGE DIAMETER (A)	INCREMENTAL PORE VOLUME (cc/g)	CUMULATIVE PORE VOLUME (cc/g)	INCREMENTAL PORE AREA (sq. m/g)	CUMULATIVE PORE AREA (sq. m/g)
1458.7					
1047.7	1253.2	0.014787	0.014787	0.472	0.472
869.3	941.6	0.06592	0.080707	2.8	3.272
704	768.9	0.06427	0.144977	3.343	6.616
607.5	648.4	0.041985	0.186962	2.59	9.206
484.7	531.9	0.062532	0.249494	4.702	13.908
374.8	415.3	0.064113	0.313607	6.175	20.083
311.9	337.3	0.042672	0.356279	5.06	25.143
257.5	279.2	0.041547	0.397825	5.952	31.095
208	227.2	0.041278	0.439103	7.267	38.362
163.9	180.4	0.041092	0.480196	9.113	47.476
126.6	140.1	0.039355	0.519551	11.235	58.711
108.8	116.2	0.019858	0.539409	6.834	65.544
83.5	92.4	0.03159	0.570999	13.669	79.214
61.9	69.1	0.030741	0.60174	17.795	97.009
45.5	50.8	0.02749	0.629229	21.658	118.667
36.5	39.8	0.017566	0.646796	17.648	136.315
30.2	32.6	0.014446	0.661242	17.733	154.048
24.6	26.7	0.015623	0.676865	23.436	177.484
19.5	21.2	0.018827	0.695692	35.444	212.928

Table C-6 The BJH desorption pore distribution report for 3 mm cadmium-loaded crosslinked chitosan beads

ASAP 2000 V2.03										
SAMPLE DIRECTORY/NUMBER: DATA1 /33										
SAMPLE ID: Beads with Cd										
SUBMITTER: HsienTY										
OPERATOR: HsienTY		SAMPLE WT: 0.1751 g								
UNIT NUMBER: 1		FREE SPACE: 55.7953 cc								
ANALYSIS GAS: Nitrogen		EQUIL INTRVL: 5 sec								
BJH DESORPTION PORE DISTRIBUTION REPORT										
PORE RANGE	AVERAGE	INCREMENTAL	CUMULATIVE	INCREMENTAL	CUMULATIVE	DIFFERENTIAL			INTEGRAL	
(A)	DIAMETER	PORE VOLUME	PORE VOLUME	PORE AREA	PORE AREA	PORE VOLUME f(D)	f(D)dlogD	D*f(D)dlogD	D*f(D)dlogD	D,av
	(A)	(cc/g)	(cc/g)	(sq. m/g)	(sq. m/g)	(cc/g)	(cc/g)	(cc/g)	(cc/g)	(A)
1024.3										
915.3	969.8	0.013537	0.013537	0.558	0.558	0.27703586				
790.9	843.8	0.020415	0.033952	0.968	1.526	0.321790555	0.0189953	16.2049236	16.2049236	477.2892
596.1	665.8	0.057966	0.091918	3.483	5.009	0.472026399	0.0487413	33.8021158	50.0070393	544.0397
442.5	496.2	0.0794	0.171318	6.401	11.409	0.613573513	0.0702415	36.4764047	86.483444	504.8124
377.6	404.7	0.0478	0.219118	4.724	16.134	0.693947521	0.0450319	18.4653172	104.948761	478.96
268.8	304.5	0.100529	0.319647	13.206	29.339	0.681078229	0.1014788	32.7979389	137.7467	430.9338
222.1	240.8	0.0532	0.372847	8.839	38.178	0.641886425	0.0548241	13.4565808	151.203281	405.5371
169.5	188.4	0.063004	0.435851	13.38	51.558	0.536757659	0.0691739	13.5442589	164.74754	377.9905
128.7	143.1	0.053303	0.489154	14.898	66.456	0.445710218	0.0587472	8.75921265	173.506752	354.7078
97.2	108.2	0.041568	0.530722	15.365	81.82	0.340966466	0.0479528	5.41626592	178.923018	337.1313
72.7	81.1	0.032616	0.563338	16.092	97.913	0.258586542	0.0378114	3.21207557	182.135094	323.3141
54.7	60.9	0.024737	0.588075	16.261	114.173	0.20022326	0.0283423	1.80540494	183.940499	312.7841
42.6	46.9	0.017507	0.605582	14.932	129.105	0.16123933	0.0196234	0.95467808	184.895177	305.3182
34.3	37.4	0.013612	0.619194	14.563	143.668	0.144630832	0.0143936	0.55343232	185.448609	299.5
28.1	30.5	0.010589	0.629783	13.9	157.569	0.122292055	0.0115561	0.36055134	185.809161	295.0368
23	24.9	0.010326	0.640109	16.561	174.13	0.118719016	0.0104814	0.26779948	186.07696	290.6957
17.6	19.3	0.015156	0.655265	31.332	205.462	0.130413269	0.0144765	0.29387245	186.370832	284.4206

Table C-7 The BJH adsorption pore distribution report for 3 mm cadmium-loaded crosslinked chitosan beads

Sample: Crosslinked 3 mm Beads, Batch # CHI-B-X-3, 3/18/93					
Adsorption with 1026 ppm Cd (0.1 g bead/100 mL) for 60 hrs, followed by freeze drying					
ASAP 2000 V2.03					
SAMPLE DIRECTORY/NUMBER: DATA1 /33					
SAMPLE ID: Beads with Cd					
SUBMITTER: HsienTY					
OPERATOR: HsienTY			SAMPLE WT: 0.1751 g		
UNIT NUMBER: 1			FREE SPACE: 55.7953 cc		
ANALYSIS GAS: Nitrogen			EQUIL INTRVL: 5 sec		
BJH ADSORPTION PORE DISTRIBUTION REPORT					
PORE RANGE	AVERAGE	INCREMENTAL	CUMULATIVE	INCREMENTAL	CUMULATIVE
(A)	DIAMETER	PORE VOLUME	PORE VOLUME	PORE AREA	PORE AREA
	(A)	(cc/g)	(cc/g)	(sq. m/g)	(sq. m/g)
1158.3					
994.9	1076.6	0.041418	0.041418	1.539	1.539
829	896.6	0.040303	0.081721	1.798	3.337
696.2	750.7	0.040766	0.122487	2.172	5.509
576.5	624.8	0.040748	0.163235	2.609	8.118
476.3	516.5	0.041073	0.204309	3.181	11.299
388.1	422.9	0.042026	0.246335	3.976	15.274
308.8	339	0.041543	0.287878	4.901	20.175
273.6	288.9	0.020957	0.308834	2.901	23.077
219.7	240.4	0.037439	0.346274	6.229	29.305
172.5	190.1	0.036908	0.383181	7.767	37.072
134.8	148.7	0.033977	0.417159	9.139	46.211
101.8	113.3	0.033725	0.450884	11.907	58.118
83.1	90.4	0.020958	0.471842	9.277	67.395
58.8	66.3	0.031714	0.503555	19.133	86.528
45.6	50.3	0.019891	0.523447	15.83	102.358
36.6	39.9	0.016149	0.539596	16.186	118.544
30.2	32.6	0.013174	0.55277	16.165	134.709
24.6	26.7	0.014086	0.566855	21.141	155.85
19.4	21.2	0.017079	0.583934	32.191	188.041

Table C-8 The BJH desorption pore distribution report for 3 mm uncrosslinked chitosan beads

Sample: Uncrosslinked 3 mm Beads, Batch # CHI-B-1, 2/23/93

ASAP 2000 V2.03

SAMPLE DIRECTORY/NUMBER: DATA1 /28

SAMPLE ID: 3 mm Bead uncrosslinked

SUBMITTER: HsienTY

OPERATOR: HsienTY SAMPLE WT: 0.1710 g

UNIT NUMBER: 1 FREE SPACE: 63.4428 cc

ANALYSIS GAS: Nitrogen EQUIL INTRVL: 5 sec

BJH DESORPTION PORE DISTRIBUTION REPORT

PORE RANGE (A)	AVERAGE DIAMETER (A)	INCREMENTAL PORE VOLUME (cc/g)	CUMULATIVE PORE VOLUME (cc/g)	INCREMENTAL PORE AREA (sq. m/g)	CUMULATIVE PORE AREA (sq. m/g)	DIFFERENTIAL PORE VOLUME f(D) (cc/g)	f(D)dlogD (cc/g)	D*f(D)dlogD (cc/g)	INTEGRAL D*f(D)dlogD (cc/g)	D,av (A)
1556.1										
1148.4	1290.9	0.0186	0.0186	0.576	0.576	0.140968555				
894.9	989.8	0.017942	0.036542	0.725	1.301	0.165640873	0.016606	16.96527839	16.96527839	464.2679
711.2	781.7	0.01762	0.054162	0.902	2.203	0.17658361	0.017074	13.71131725	30.67659564	566.3859
566.3	621.9	0.016676	0.070838	1.073	3.276	0.168537759	0.017074	10.90604886	41.58264451	587.0104
458.4	500.6	0.01513	0.085968	1.209	4.485	0.164811309	0.015301	7.83949179	49.4221363	574.8899
366.6	401.9	0.014741	0.100709	1.467	5.952	0.151887416	0.015368	6.339360147	55.76149644	553.6893
303.4	328.7	0.011867	0.112576	1.444	7.396	0.144408006	0.012174	4.07839629	59.83989273	531.5511
250.1	271.3	0.011239	0.123815	1.657	9.053	0.133954083	0.011678	3.231762501	63.07165523	509.4024
208.1	225	0.010285	0.1341	1.828	10.881	0.12881754	0.01049	2.403271581	65.47492681	488.2545
164.8	181.1	0.012008	0.146108	2.652	13.533	0.118521592	0.01253	2.336137646	67.81106446	464.116
129.4	142.5	0.011492	0.1576	3.226	16.759	0.109423722	0.01197	1.760749119	69.57181358	441.4455
103.7	113.4	0.009873	0.167473	3.482	20.241	0.102677413	0.010197	1.188500844	70.76031442	422.5177
80.9	89.1	0.010035	0.177508	4.503	24.744	0.093062952	0.010553	0.974075567	71.73438999	404.1192
60.7	67.5	0.010615	0.188123	6.287	31.031	0.085083476	0.011113	0.786783343	72.52117333	385.4987
46.5	51.4	0.009105	0.197228	7.091	38.122	0.0786706	0.009476	0.507918929	73.02909226	370.2775
37	40.4	0.007362	0.20459	7.282	45.404	0.074175404	0.007585	0.31667696	73.34576922	358.5012
30.3	32.8	0.006026	0.210616	7.352	52.756	0.069456695	0.006231	0.209662903	73.55543213	349.2395
24.9	26.9	0.005548	0.216164	8.251	61.007	0.065084308	0.005734	0.158268289	73.71370041	341.0082
19.5	21.3	0.006484	0.222648	12.168	73.175	0.061074894	0.006697	0.148669608	73.86237002	331.745

Table C-9 The BJH desorption pore distribution report for 1 mm crosslinked chitosan beads

ASAP 2000 V2.03										
SAMPLE DIRECTORY/NUMBER: DATA1 /42										
SAMPLE ID: 1 mm Bead										
SUBMITTER: HsienTY										
OPERATOR: HsienTY		SAMPLE WT: 0.1921 g								
UNIT NUMBER: 1		FREE SPACE: 55.1021 cc								
ANALYSIS GAS: Nitrogen		EQUIL INTRVL: 5 sec								
BJH DESORPTION PORE DISTRIBUTION REPORT										
PORE RANGE	AVERAGE	INCREMENTAL	CUMULATIVE	INCREMENTAL	CUMULATIVE	DIFFERENTIAL			INTEGRAL	
(A)	DIAMETER	PORE VOLUME	PORE VOLUME	PORE AREA	PORE AREA	PORE VOLUME f(D)	f(D)dlogD	D*f(D)dlogD	D*f(D)dlogD	D,av
	(A)	(cc/g)	(cc/g)	(sq. m/g)	(sq. m/g)	(cc/g)	(cc/g)	(cc/g)	(cc/g)	(A)
1766.5										
1242.8	1414.6	0.013597	0.013597	0.384	0.384	0.089036648				
1002.3	1096.5	0.01578	0.029377	0.576	0.96	0.168944393	0.0120482	13.5246709	13.5246709	460.3829834
845.1	910.1	0.017945	0.047322	0.789	1.749	0.24220664	0.015231	14.06888732	27.59355822	583.1021137
713.5	768	0.021181	0.068503	1.103	2.852	0.288121503	0.0194933	15.1911322	42.78469043	624.5666675
604.1	649.5	0.025044	0.093547	1.542	4.394	0.346461242	0.0229355	15.10987568	57.89456611	618.8821246
440	496	0.060915	0.154461	4.913	9.307	0.442508351	0.0543033	28.34901791	86.24358402	558.351843
361.5	392.8	0.040004	0.194465	4.074	13.381	0.468736224	0.0388848	15.58308331	101.8266673	523.6246488
285.7	314.4	0.042913	0.237379	5.459	18.841	0.419910118	0.045409	14.69434161	116.5210089	490.8648572
221.5	245.1	0.040257	0.277636	6.569	25.41	0.36419641	0.0433362	10.99006018	127.5110691	459.2742624
162	182.1	0.042211	0.319847	9.273	34.682	0.310697769	0.0458451	8.790803349	136.3018725	426.1471031
120.2	134.5	0.034571	0.354418	10.28	44.962	0.266729837	0.0374204	5.280011934	141.5818844	399.477127
94	103.6	0.025552	0.37997	9.862	54.824	0.239303336	0.0270163	2.893440848	144.4753253	380.2282424
72.7	80.4	0.025422	0.405392	12.654	67.478	0.227809084	0.0260633	2.172379521	146.6477048	361.7429668
56.3	62.1	0.023925	0.429318	15.4	82.877	0.215499041	0.0246094	1.587304205	148.235009	345.2802095
42.8	47.5	0.022891	0.452208	19.278	102.155	0.192248536	0.0242742	1.202784447	149.4377934	330.462516
33.7	37	0.01947	0.471678	21.05	123.205	0.187547197	0.019714	0.754061727	150.1918552	318.4203104
26.6	29.2	0.008396	0.480074	11.503	134.708	0.081714276	0.0138331	0.417067196	150.6089224	313.720223
21.5	23.4	0.005609	0.485683	9.591	144.299	0.060675111	0.0065815	0.1582842	150.7672066	310.4230672
17.1	18.7	0.00577	0.491453	12.359	156.658	0.058023569	0.0059018	0.113905469	150.881112	307.0102574

Table C-10 The BJH adsorption pore distribution report for 1 mm crosslinked chitosan beads

Sample: Crosslinked 1 mm Beads, Batch # CHI-B-X-1, 6/20/92

ASAP 2000 V2.03
SAMPLE DIRECTORY/NUMBER: DATA1 /42
SAMPLE ID: 1 mm Bead
SUBMITTER: HsienTY
OPERATOR: HsienTY SAMPLE WT: 0.1921 g
UNIT NUMBER: 1 FREE SPACE: 55.1021 cc
ANALYSIS GAS: Nitrogen EQUIL INTRVL: 5 sec

BJH ADSORPTION PORE DISTRIBUTION REPORT

PORE RANGE (A)	AVERAGE DIAMETER (A)	INCREMENTAL PORE VOLUME (cc/g)	CUMULATIVE PORE VOLUME (cc/g)	INCREMENTAL PORE AREA (sq. m/g)	CUMULATIVE PORE AREA (sq. m/g)
1142.5					
1011.9	1069.1	0.018758	0.018758	0.702	0.702
822.7	897.5	0.035867	0.054625	1.599	2.3
727.9	769.4	0.0186	0.073225	0.967	3.267
555.2	617.9	0.03715	0.110375	2.405	5.672
473.4	507.6	0.019338	0.129713	1.524	7.196
412.9	438.9	0.019034	0.148747	1.735	8.931
303.9	341.4	0.035522	0.184269	4.162	13.093
256.9	276.3	0.019613	0.203882	2.84	15.933
218.5	234.4	0.017866	0.221748	3.048	18.981
160	179.8	0.034405	0.256152	7.656	26.637
135	145.2	0.018337	0.274489	5.051	31.688
101.1	112.8	0.031387	0.305876	11.133	42.821
82.6	89.8	0.020577	0.326453	9.168	51.989
58.4	65.9	0.031023	0.357476	18.819	70.808
45.3	49.9	0.017811	0.375287	14.268	85.076
36.2	39.5	0.012577	0.387864	12.725	97.801
29.7	32.1	0.009348	0.397212	11.635	109.436
24.1	26.2	0.008713	0.405925	13.32	122.756
18.9	20.7	0.010147	0.416072	19.592	142.348

Table C-11 The control experiment of BJH desorption pore distribution report for 1 mm crosslinked chitosan beads

ASAP 2000 V2.03										
SAMPLE DIRECTORY/NUMBER: DATA1 /46										
SAMPLE ID: 1 mm Bead with water										
SUBMITTER: HsienTY										
OPERATOR: HsienTY		SAMPLE WT: 0.1710 g								
UNIT NUMBER: 1		FREE SPACE: 47.4929 cc								
ANALYSIS GAS: Nitrogen		EQUIL INTRVL: 5 sec								
BJH DESORPTION PORE DISTRIBUTION REPORT										
PORE RANGE	AVERAGE	INCREMENTAL	CUMULATIVE	INCREMENTAL	CUMULATIVE	DIFFERENTIAL			INTEGRAL	
(A)	DIAMETER	PORE VOLUME	PORE VOLUME	PORE AREA	PORE AREA	PORE VOLUME f(D	f(D)dlogD	D*f(D)dlogD	D*f(D)dlogD	D,av
	(A)	(cc/g)	(cc/g)	(sq. m/g)	(sq. m/g)	(cc/g)	(cc/g)	(cc/g)	(cc/g)	(A)
1415.3										
1057.5	1236.4	0.011176	0.011176	0.362	0.362	0.088300269				
856.9	935.8	0.013952	0.025127	0.596	0.958	0.152719917	0.011008625	10.53745594	10.53745594	419.3678488
703.7	764.9	0.01794	0.043068	0.938	1.896	0.209731779	0.015502529	12.09662318	22.63407911	525.5428419
581.1	630.4	0.022376	0.065444	1.42	3.316	0.269147158	0.019906201	12.78774382	35.42182293	541.2539412
479.4	520.2	0.029049	0.094493	2.234	5.549	0.34767218	0.025768506	13.66375005	49.08557298	519.4625314
324.5	371.9	0.064306	0.158798	6.916	12.465	0.379417849	0.061614819	24.76607655	73.85164953	465.0666225
258.5	283.7	0.032678	0.191476	4.607	17.072	0.330902537	0.035073544	10.22393816	84.07558769	439.0920412
205	225.3	0.034366	0.225842	6.102	23.174	0.341248444	0.033845049	7.843590107	91.9191778	407.0065701
158.4	175.4	0.032401	0.258242	7.388	30.562	0.289289114	0.035309688	6.415770359	98.33494816	380.7860385
120.7	134.1	0.030687	0.288929	9.151	39.714	0.259953783	0.032418487	4.523999893	102.858948	356.0007754
95.3	104.8	0.025118	0.314047	9.59	49.304	0.244780533	0.025896497	2.796821649	105.6557697	336.4329852
74.8	82.3	0.02446	0.338507	11.887	61.191	0.23252873	0.025104392	2.135128502	107.7908982	318.4303373
57.3	63.4	0.025771	0.364279	16.249	77.44	0.222658085	0.026343249	1.739971572	109.5308698	300.6785178
43.4	48.2	0.023778	0.388057	19.732	97.172	0.197058146	0.025322507	1.274988225	110.805858	285.5401603
34	37.3	0.020242	0.408299	21.679	118.85	0.190942787	0.020566147	0.795909892	111.6017679	273.3334343
26.9	29.5	0.008465	0.416765	11.487	130.337	0.08322304	0.013944984	0.424624757	112.0263926	268.7999056
21.8	23.7	0.005812	0.422577	9.819	140.156	0.063661207	0.006704956	0.16326569	112.1896583	265.4892678
17.1	18.7	0.006362	0.428938	13.591	153.747	0.060316489	0.006537368	0.127151801	112.3168101	261.8485892

Table C-12 The control experiment of BJH adsorption pore distribution report for 1 mm crosslinked chitosan beads

ASAP 2000 V2.03					
SAMPLE DIRECTORY/NUMBER: DATA1 /46					
SAMPLE ID: 1 mm Bead with water					
SUBMITTER: HsienTY					
OPERATOR: HsienTY		SAMPLE WT: 0.1710 g			
UNIT NUMBER: 1		FREE SPACE: 47.4929 cc			
ANALYSIS GAS: Nitrogen		EQUIL INTRVL: 5 sec			
BJH ADSORPTION PORE DISTRIBUTION REPORT					
PORE RANGE	AVERAGE	INCREMENTAL	CUMULATIVE	INCREMENTAL	CUMULATIVE
(A)	DIAMETER	PORE VOLUME	PORE VOLUME	PORE AREA	PORE AREA
	(A)	(cc/g)	(cc/g)	(sq. m/g)	(sq. m/g)
1249.5					
1115.1	1182.3	0.018284	0.018284	0.619	0.619
838.7	937.6	0.03534	0.053624	1.508	2.126
718.7	769.2	0.018657	0.072281	0.97	3.097
625.9	665.7	0.018082	0.090363	1.087	4.183
525.5	566.7	0.019028	0.10939	1.343	5.526
446.5	479.4	0.018519	0.127909	1.545	7.071
321.7	363.4	0.035344	0.163253	3.891	10.962
269.7	290.9	0.019119	0.182372	2.629	13.591
227.8	245	0.017254	0.199626	2.817	16.408
163.8	184.9	0.033678	0.233304	7.286	23.694
138.1	148.6	0.01814	0.251444	4.884	28.578
102.7	114.8	0.030985	0.282429	10.798	39.377
83.9	91.2	0.020215	0.302645	8.869	48.245
59.2	66.8	0.030807	0.333452	18.438	66.683
46	50.6	0.017729	0.351181	14.003	80.687
36.8	40.2	0.012629	0.36381	12.58	93.267
30.2	32.7	0.009408	0.373219	11.505	104.772
24.6	26.7	0.009039	0.382258	13.539	118.31
19.5	21.2	0.010161	0.392419	19.13	137.441

Table C-13 The BJH desorption pore distribution report for 1 mm cadmium -loaded crosslinked chitosan beads

ASAP 2000 V2.03										
SAMPLE DIRECTORY/NUMBER: DATA1 /41										
SAMPLE ID: 1 mm bead with Cd										
SUBMITTER: HsienTY										
UNIT NUMBER: 1		FREE SPACE: 48.2950 cc								
ANALYSIS GAS: Nitrogen		EQUIL INTRVL: 5 sec								
BJH DESORPTION PORE DISTRIBUTION REPORT										
PORE RANGE	AVERAGE	INCREMENTAL	CUMULATIVE	INCREMENTAL	CUMULATIVE	DIFFERENTIAL			INTEGRAL	
(A)	DIAMETER	PORE VOLUME	PORE VOLUME	PORE AREA	PORE AREA	PORE VOLUME f(D	f(D)dlogD	D*f(D)dlogD	D*f(D)dlogD	D,av
	(A)	(cc/g)	(cc/g)	(sq. m/g)	(sq. m/g)	(cc/g)	(cc/g)	(cc/g)	(cc/g)	(A)
1211.5										
975.4	1067.7	0.009664	0.009664	0.362	0.362	0.102654892				
835.2	894.2	0.011791	0.021455	0.527	0.89	0.17496073	0.009354573	8.468694814	8.468694814	394.718938
716.5	766.5	0.01572	0.037175	0.82	1.71	0.236127186	0.013683943	10.61668739	19.08538221	513.3929309
609.7	654.3	0.020199	0.057374	1.235	2.945	0.288145508	0.018375758	12.18496503	31.27034723	545.0264446
435	492.9	0.049573	0.106947	4.023	6.967	0.338089308	0.045911447	23.98184421	55.25219144	516.6315226
348.8	382.1	0.030731	0.137678	3.217	10.184	0.320405683	0.031579043	12.37582688	67.62801832	491.204247
269.4	298.6	0.030868	0.168545	4.135	14.32	0.275158735	0.033404876	10.32544721	77.95346553	462.5083244
207.8	230.3	0.025744	0.19429	4.471	18.791	0.228332881	0.028384855	6.772626509	84.72609204	436.0805602
152	170.9	0.02501	0.219299	5.855	24.645	0.184157879	0.028008526	5.0387338	89.76482584	409.3261977
115.6	128.5	0.017809	0.237108	5.542	30.188	0.149799277	0.019851374	2.656113857	92.42093969	389.7841477
91.9	100.8	0.012954	0.250062	5.14	35.328	0.130004998	0.013940174	1.446293048	93.86723274	375.3758378
73.6	80.6	0.010931	0.260993	5.427	40.755	0.113347792	0.011734191	0.971004332	94.83823708	363.3746387
56.3	62.4	0.011592	0.272585	7.427	48.182	0.099613799	0.012391108	0.804802488	95.64303956	350.8741844
42.7	47.4	0.0103	0.282885	8.694	56.876	0.085775778	0.011130838	0.550976501	96.19401606	340.0463654
33.3	36.7	0.009309	0.292194	10.157	67.033	0.086207502	0.00928569	0.352856236	96.5468723	330.4204477
26.4	28.9	0.005061	0.297255	6.999	74.032	0.050188265	0.006877095	0.2052813	96.7521536	325.4853698
21.1	23	0.00418	0.301435	7.256	81.288	0.04295044	0.004532198	0.1076397	96.8597933	321.3289542
14.7	17.9	0.005373	0.306807	12.039	93.327	0.034224164	0.00605686	0.108417803	96.9682111	316.0560584

Table C-14 The BJH adsorption pore distribution report for 1 mm cadmium -loaded crosslinked chitosan beads

Sample: Crosslinked 1 mm Beads, Batch # CHI-B-X-1, 6/20/92					
Adsorption with 1026 ppm Cd (0.1 g/100 mL) for 60 hrs, followed by freeze drying					
ASAP 2000 V2.03					
SAMPLE DIRECTORY/NUMBER: DATA1 /41					
SAMPLE ID: 1 mm bead with Cd					
SUBMITTER: HsienTY					
OPERATOR: HsienTY		SAMPLE WT: 0.2095 g			
UNIT NUMBER: 1		FREE SPACE: 48.2950 cc			
ANALYSIS GAS: Nitrogen		EQUIL INTRVL: 5 sec			
BJH ADSORPTION PORE DISTRIBUTION REPORT					
PORE RANGE	AVERAGE	INCREMENTAL	CUMULATIVE	INCREMENTAL	CUMULATIVE
(A)	DIAMETER	PORE VOLUME	PORE VOLUME	PORE AREA	PORE AREA
	(A)	(cc/g)	(cc/g)	(sq. m/g)	(sq. m/g)
1223.6					
1095.2	1152.1	0.016107	0.016107	0.559	0.559
825.3	922.1	0.030344	0.04645	1.316	1.875
717.5	763.7	0.016064	0.062514	0.841	2.717
616.6	659.2	0.015222	0.077736	0.924	3.64
533.1	568.6	0.014293	0.092029	1.005	4.646
381.1	431.5	0.029565	0.121594	2.74	7.386
311.3	338.9	0.015985	0.137579	1.887	9.273
253.9	276.5	0.015404	0.152983	2.228	11.501
204	223.3	0.015521	0.168505	2.781	14.282
161	177.1	0.015633	0.184137	3.53	17.812
128.1	140.5	0.013978	0.198115	3.978	21.791
102.2	112	0.01284	0.210955	4.585	26.376
78.7	87.1	0.013323	0.224278	6.119	32.495
58.6	65.4	0.012602	0.23688	7.709	40.204
44.8	49.6	0.009063	0.245943	7.309	47.513
35.4	38.8	0.006501	0.252444	6.702	54.215
28.6	31.2	0.005166	0.25761	6.628	60.843
23	25.1	0.005351	0.262961	8.522	69.365
16.2	19.6	0.006756	0.269717	13.771	83.136

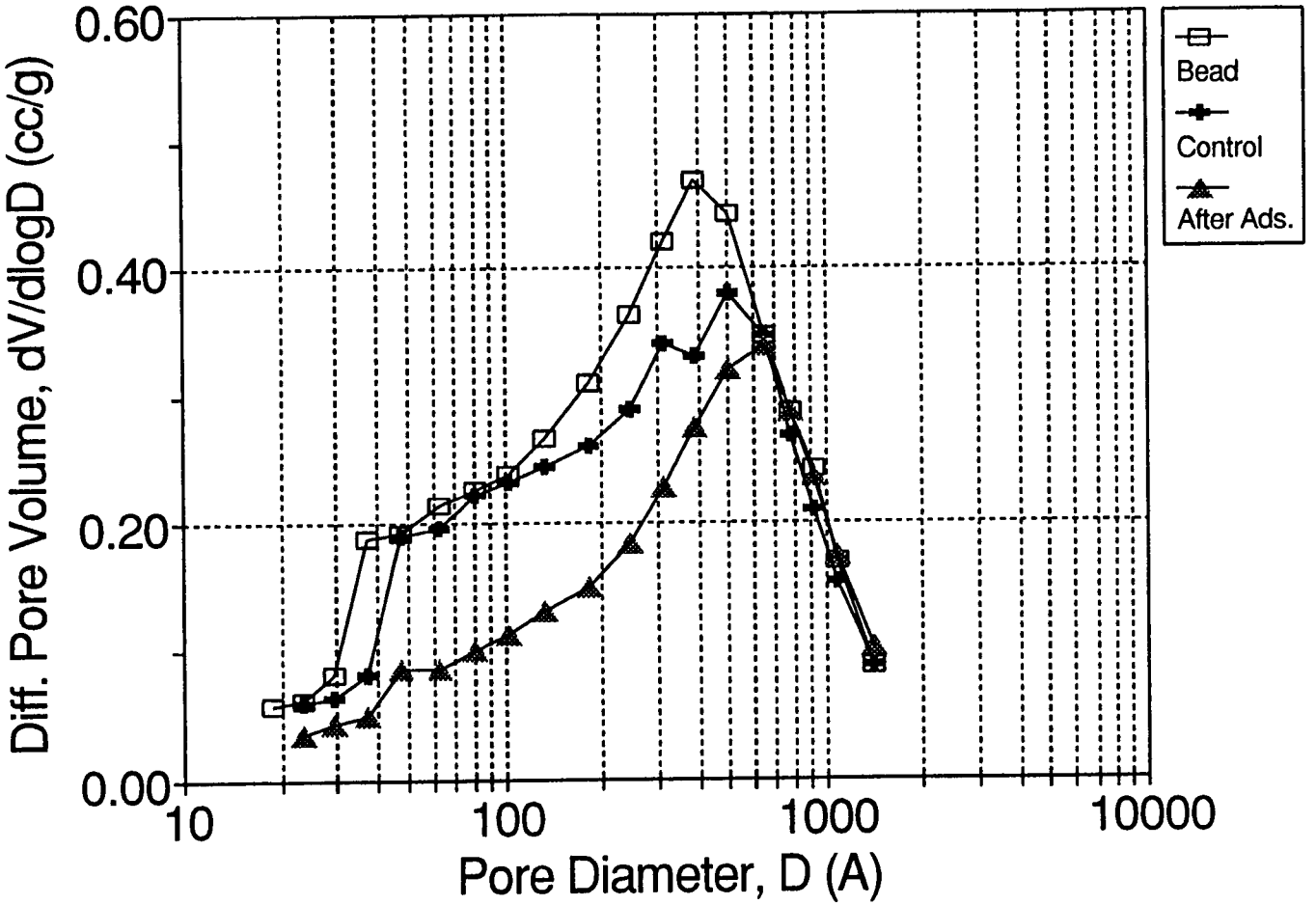

Figure C.1 The pore size distribution for 1 mm chitosan beads before and after cadmium adsorption

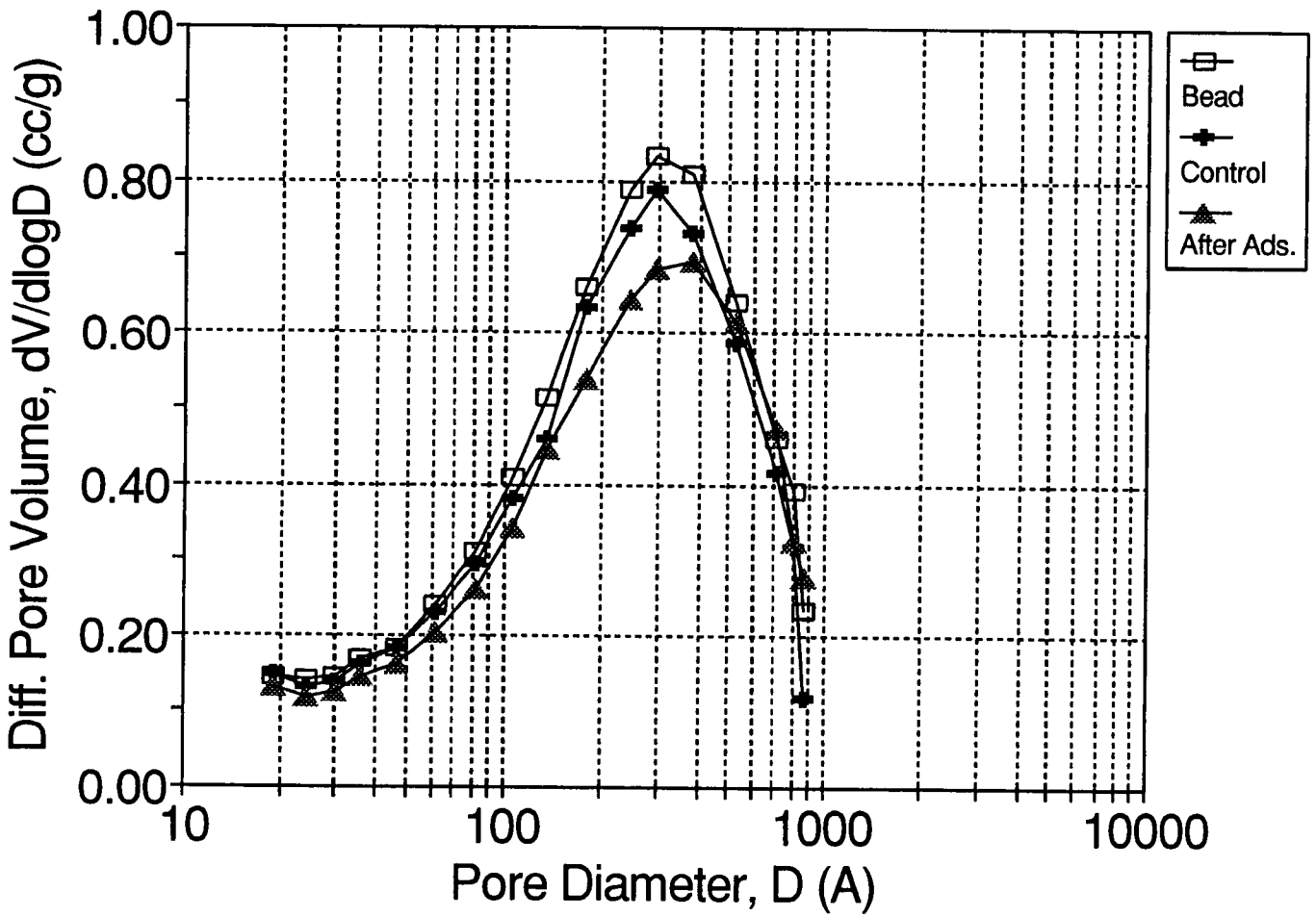

Figure C.2 The pore size distribution for 3 mm chitosan beads before and after cadmium adsorption

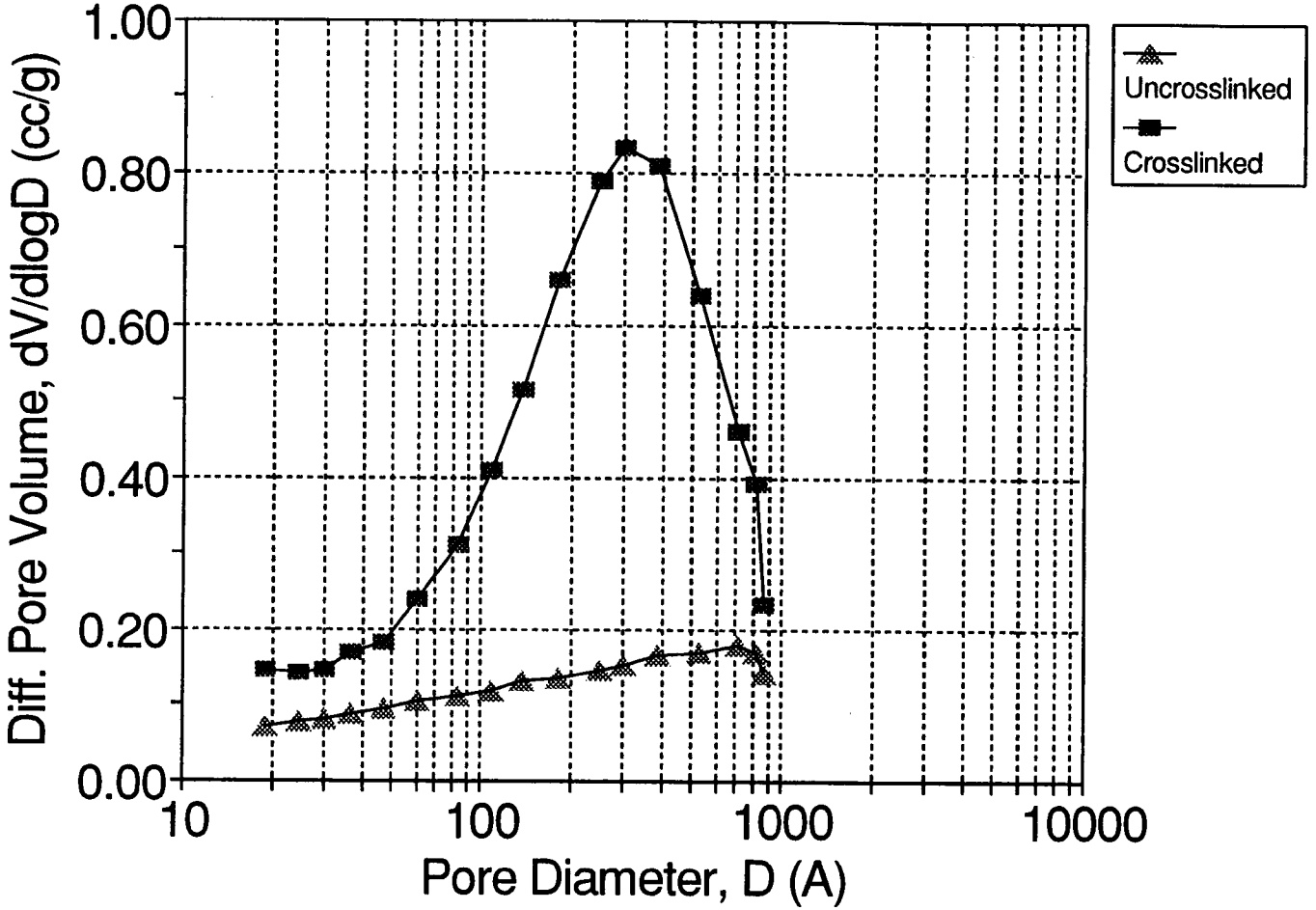

Figure C.3 The pore size distribution for crosslinked and uncrosslinked 3mm chitosan beads